

A LIFE PREDICTION MODEL FOR LAMINATED
COMPOSITE STRUCTURAL COMPONENTS

Final Technical Report

submitted by

David H. Allen

Aerospace Engineering Department
Texas A&M University
College Station, TX 77843

to

NASA Langley Research Center
Hampton, VA 23665

Contract No. NAG-1-979
May 1990



INTRODUCTION

This report details results of research performed during the period April 1, 1989 through March 31, 1990 under NASA contract no. NAG-1-979.

The general objective of this research has been to develop a life prediction methodology for laminated continuous fiber composites subjected to fatigue loading conditions.

SUMMARY OF COMPLETED RESEARCH

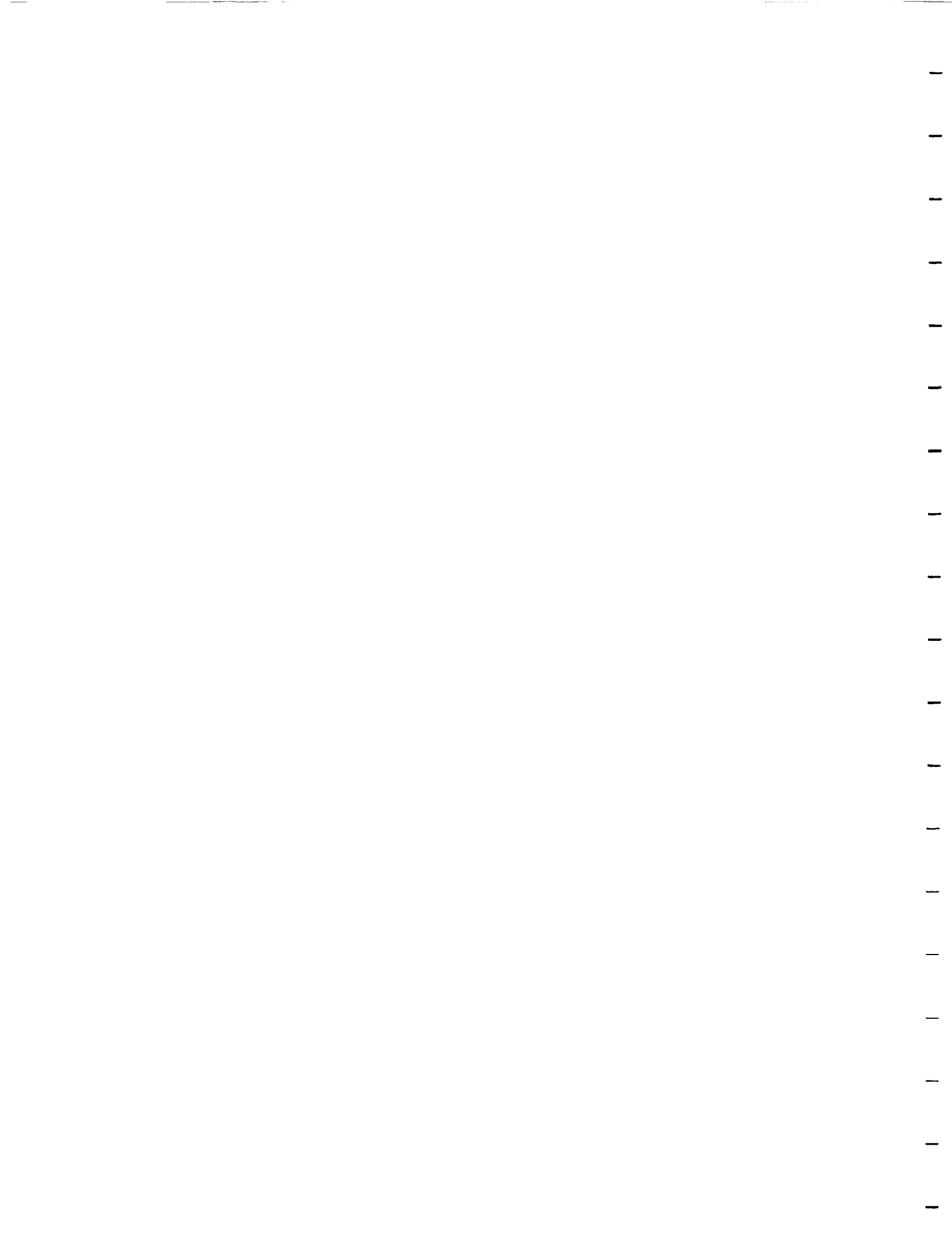
The following is a summary of research completed during the preceeding contract year:

- 1) a phenomenological damage evolution law has been formulated for matrix cracking which is independent of stacking sequence;
- 2) mechanistic and physical support has been developed for the phenomenological evolution law proposed in 1);
- 3) the damage evolution law proposed in 1) has been implemented to a finite element computer program; and
- 4) preliminary predictions have been obtained for a structural component undergoing fatigue loading induced damage.

The results reported above are covered in detail in the enclosed appendices.

PUBLICATIONS

1. Lo, D.C., Allen, D.H., and Harris, C.E., "A Continuum Model for Damage Evolution in Laminated Composites," Proc. IUTAM Symposium, Troy, New York, 1990 (Appendix A).
2. Allen, D.H., Lo, D.C., Georgiou, I.T., and Harris, C.E., "A Model for Predicting Damage Induced Fatigue Life of Laminated Composite Structural Components," Proc. 17th International Congress Aeronautical Sciences, Stockholm, 1990 (Appendix B).
3. Allen, D.H., "Life Prediction in Laminated Composites Using Continuum Damage Mechanics," Damage Mechanics of Composites, R. Talreja, Ed., Martinus-Nijhoff, 1990 (Appendix C).
4. Lo, D.C., Allen, D.H., and Buie, K.D., "Damage Prediction in Laminated Composites with Continuum Damage Mechanics," Proc. ASCE Materials Engineering Conference, Denver, 1990 (Appendix D).
5. Allen, D.H., "Continuum Damage Mechanics Model for Life Prediction of Laminated Composites," Proc. Durability 90, Brussels, 1990 (to appear).



APPENDIX A

A Continuum Model for Damage Evolution in Laminated Composites

D.C. Lo
D.H. Allen

Aerospace Engineering Department, Texas A&M University
College Station, Texas, USA 77843

and

C.E. Harris

Mechanics of Materials Branch, NASA Langley Research Center
Hampton, Virginia, USA 23665

Abstract

The accumulation of matrix cracking is examined using continuum damage mechanics lamination theory. A phenomenologically based damage evolutionary relationship is proposed for matrix cracking in continuous fiber reinforced laminated composites. The use of material dependent properties and damage dependent laminate averaged ply stresses in this evolutionary relationship permits its application independently of the laminate stacking sequence. Several load histories are applied to crossply laminates using this model and the results are compared to published experimental data. The stress redistribution among the plies during the accumulation of matrix damage is also examined. It is concluded that characteristics of the stress redistribution process could assist in the analysis of the progressive failure process in laminated composites.

Introduction

A unique property of composite materials is their evolutionary failure characteristic. The inhomogeneity of the microstructure provides numerous paths in which loads can be redistributed around the damaged region. Thus, the integrity and response of the component are affected more by the collective effects of the accumulated subcritical damage than by any single damage event. For laminated composites, this subcritical damage takes the form of matrix cracks, delaminations, debonding, and fiber fractures. Because the transfer of load away from the damaged area influences the damage evolution in the adjacent areas, the stresses at the ply level play an important role in the evolution of damage and the ultimate failure of the structure. Thus, this unique failure process that makes composites an attractive engineering material has also limited their efficient use in structures. The primary reason has been the shortage of analytical means to



model the complex events occurring within the laminate and the prediction of damage evolution.

A review of the current literature indicates that three approaches have been taken to solve this problem. The first approach is the phenomenological methodology. Empirical relationships are developed from a body of experimentally measured data. Statistical theory is frequently employed to correlate this data. Models of this type tend to be restricted to the stacking sequence utilized to construct them. The second approach, called the crack propagation method, identifies damage as dominant cracks and fracture mechanics is applied to predict crack growth. The physical significance of each damage mode is retained with this approach. Unfortunately, the damage state in composite materials contains a multitude of interacting defects. Analysis in this manner is complex and perhaps unmanageable. For example, if there are hundreds of cracks, then the finite element method would require tens of thousands of elements. The third and most recent approach is the use of internal state variables in a continuum damage mechanics framework to model the damage accumulation. The averaged effects of the damage are represented through the internal state variables. This theory provides a thermodynamically rigorous characterization of the continuum under examination. The continuum damage mechanics approach entails the formulation of constitutive relationships, damage variable descriptions, and the damage evolution laws. The damage evolution laws may either be phenomenological, mechanistic, or even some combination of both. Because this approach is capable of accounting for the stacking sequence, it differs considerably from the phenomenological approach. Furthermore, because the effects of each crack are treated in the constitutive equations rather than via fracture mechanics, the computational solution is simpler than the crack propagation approach.

In the current paper, the continuum damage mechanics lamination theory proposed by Allen, et al. (1987a,b) is reviewed. Also a matrix crack damage evolutionary law is developed and this phenomenologically based evolutionary relationship is used to examine the accumulation of damage and the accompanying stress redistribution among the plies in laminates subjected to fatigue loading conditions.

Review of the Damage Dependent Lamination Model

The continuum damage mechanics approach used herein is based on the thermodynamics of irreversible processes. It is postulated that the state of a material point in a system undergoing a dissipative process can be characterized by a set of observable and internal state variables if this process is sufficiently close to the equilibrium state. Through the application of constraints from the fundamental principles of thermodynamics as proposed by Coleman and Mizel (1966) and the assumption of interdependence among these state variables, Coleman and Gurtin (1967) showed that constitutive



equations for the material can be constructed in terms of the strain tensor, temperature, and internal state variables. The internal state variables may represent any dissipative process occurring in the medium. For the current application to distributed matrix cracks in laminated polymeric composites, Allen, et al. (1987a) selected a second order tensor valued internal state variable to represent the kinematics of the cracks. This tensor was first defined by Vakulenko and Kachanov (1971) to be

$$\alpha_{ij} = \frac{1}{V_L} \int_S u_i n_j dS, \quad (1)$$

where α_{ij} are the components of the internal state variable tensor, V_L is a local volume in which statistical homogeneity can be assumed, u_i and n_j are the crack face displacement and normals, respectively, and S is the crack surface area.

The thermomechanical response of an elastic material with damage was found to be related to the damage dependent Helmholtz free energy as follows,

$$\sigma_{Lij} = \frac{\partial h_L}{\partial \varepsilon_{Lij}} \quad (2)$$

where σ_{Lij} are the components of the locally averaged stress tensor, h_L is the volume averaged Helmholtz free energy and ε_{Lij} are components of the infinitesimal locally averaged strain tensor. The subscript L will be used herein to denote volume averaged quantities. The Helmholtz free energy, h_L , for an elastic material with distributed damage is defined by

$$h_L = h_{EL} + u_L^c, \quad (3)$$

where h_{EL} is the Helmholtz free energy of an equivalent undamaged elastic body and u_L^c is the energy associated with the damage effect on the material. These two energy quantities are expressed by second order Taylor series expansions of the corresponding state variables. If the higher ordered and residual effects are neglected and isothermal conditions are assumed, The ply level thermomechanical constitutive relationship of the damaged material is,

$$\sigma_{ij} = C_{Lijkl} \varepsilon_{kl} + I_{Lijkl} \alpha_{kl}, \quad (4)$$

where C_{Lijkl} is the undamaged material modulus tensor and I_{Lijkl} is denoted the damage modulus tensor. The components of this damage modulus tensor were shown by Allen, et al. (1987b) to be related to the modulus tensor as follows

$$I_{Lijkl} \approx -C_{Lijkl}. \quad (5)$$

Another result of the Coleman-Mizel formulation is the entropy production by the distributed damage in the absence of thermal gradients,

$$\int_{ij}^T \dot{\alpha}_{ij} \geq 0 \quad (6)$$



where the thermodynamic force, f_{ij}^T , associated with the evolution of a_{ij} is denoted by

$$f_{ij}^T = -\frac{\partial h}{\partial a_{ij}}. \quad (7)$$

inequality (6) will admit only those processes that yield non-negative rates of entropy production.

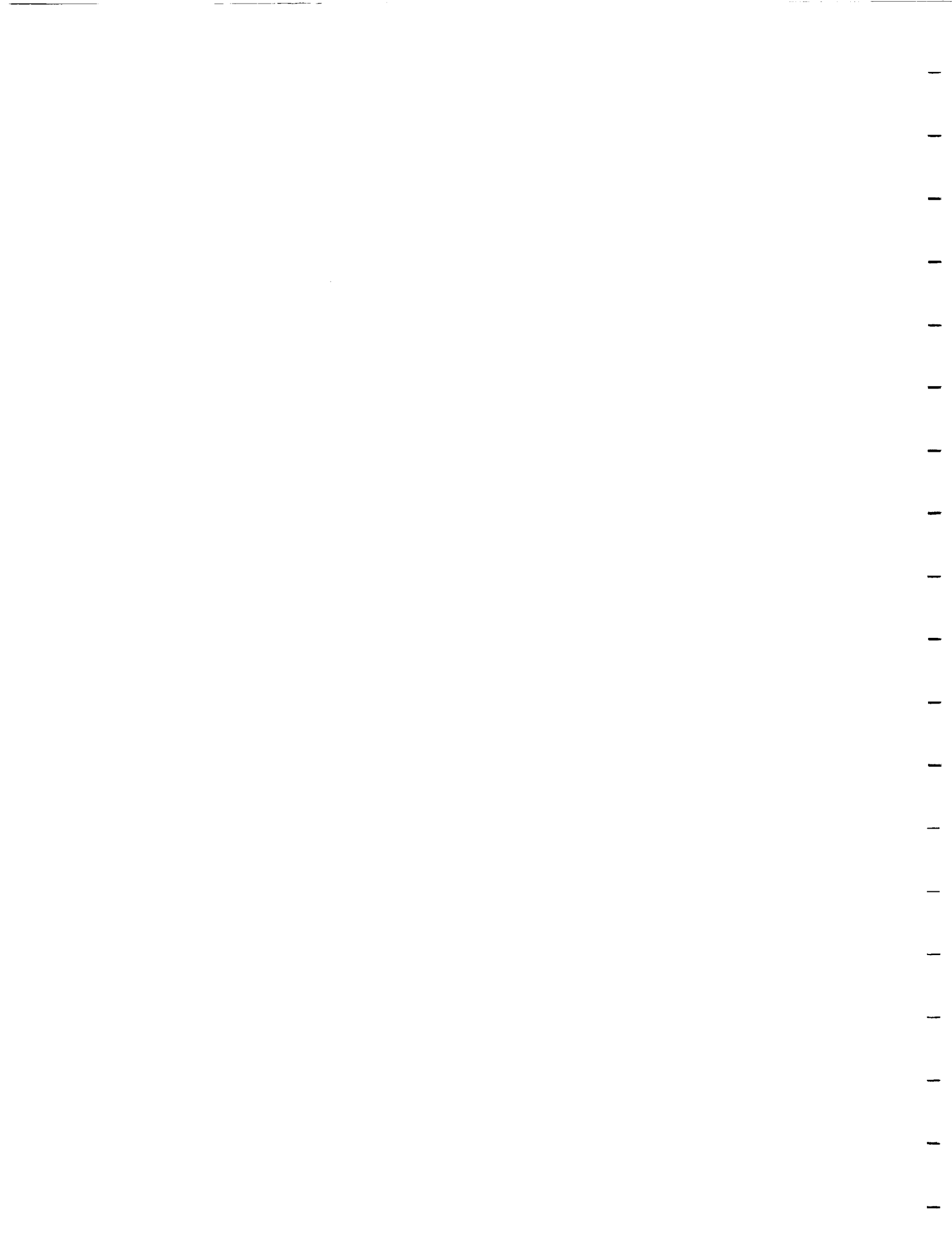
The response of a multilayered laminate with matrix damage is obtained by inplane averaging the ply level constitutive relationship shown in equation (4) and imposing the Kirchhoff hypothesis through the thickness to obtain the following modified set of laminate equations,

$$\begin{aligned} \{N\} = & \sum_{k=1}^n [Q]_{jk} (z_k - z_{k-1}) \{\varepsilon^o\} - \frac{1}{2} \sum_{k=1}^n [Q]_{jk} (z_k^2 - z_{k-1}^2) \{\kappa\} \\ & - \sum_{k=1}^n [Q]_{jk} (z_k - z_{k-1}) \{a^M\}_k, \end{aligned} \quad (8)$$

where $\{N\}$ is the resultant force per unit length vector, $[Q]_{jk}$ is the elastic modulus matrix for the k^{th} ply in laminate coordinates, z_k is the distance from the midplane to the k^{th} ply, ε^o and κ are the midplane strains and curvatures, respectively; and $\{a^M\}$ are the damage variables corresponding to the matrix cracks in the k^{th} ply. The effects of the matrix cracking on the resultant forces are contained in the last group of terms on the right hand side of equation (8). An expression for the resultant moments can be written in a similar form. The stiffness loss of composite crossply laminates with matrix cracks has been successfully predicted with this model by Allen, et al. (1987b, 1988) for specified damage states using equation (8). In addition, although it will not be discussed in this paper, the model has also been extended to include the effects of delamination by Harris, et al. (1987, 1988). A damage evolution relationship for this model will be introduced in the following section.

Evolutionary Equation for Internal State Variables

In order to characterize the development of the internal damage, the conditions for the initiation and progression of damage as well as a means to quantify changes in the damage state must be established. Concepts from linear elastic fracture mechanics can often be employed to assist in the development of the evolutionary equations for brittle damage. The thermodynamic force, f_{ij}^T , as defined by equation (7), represents the available free energy that can be delivered by the system for a small change in the internal state variable. However, this change will occur only if the energy delivered is equal to or greater than the energy required to produce this change in the internal state. Thus, the following initiation criterion based



on the relative magnitudes of the available and required thermodynamic forces, $(f_{ij}^T)_{req.}$ can be used for this model,

$$f_{ij}^T \geq (f_{ij}^T)_{req.} \quad (9)$$

The implementation of this criterion will require the determination of the required thermodynamic forces. The required thermodynamic forces are most likely to change with the damage state. This criterion is analogous to comparing the strain energy release rate to the critical value in fracture mechanics. Had the internal state variable been defined as the crack surface area, the thermodynamic force would be identical to the strain energy release rate.

One approach to the formulation of the internal state variable evolutionary relationships is through micromechanical considerations. However, this approach is dependent on the availability of micromechanical solutions that can model the essential physical characteristics of the damage state. For the problem of matrix cracks embedded in an orthotropic medium that is layered between two other orthotropic media, the solutions that are currently available are applicable only to very specific loading conditions and damage geometries. Therefore, the evolutionary equation proposed herein is phenomenological in nature. The form of the damage evolutionary relationship employed in this paper is based on the observation made by Wang, et al. (1984) that for some materials the rate of damage surface evolution per load step, $\frac{dS}{dN}$, follows the power law as shown below, in which the strain energy release rate, G , and a material parameter, n , serves as the basis and exponent, respectively.

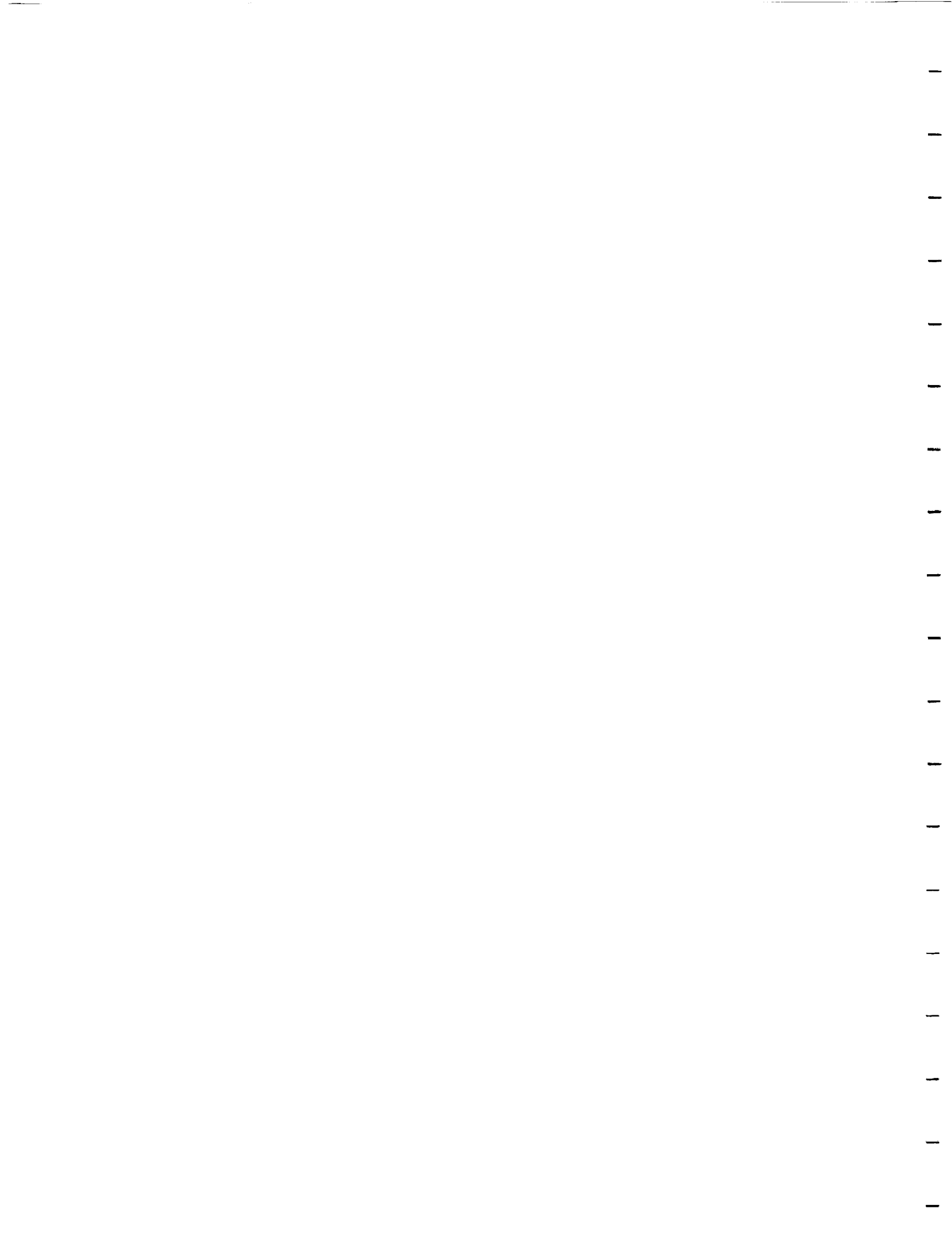
$$\frac{dS}{dN} = PG^n \quad (10)$$

where P is a material constant. To develop internal state variable evolutionary equations in the form of equation (10), α_{ij} has to be related to the damage surface area. Since α_{ij} , as defined by equation (1), represents the kinematics of the crack faces, the damage surface area alone will not be sufficient to describe the crack face displacements. Assuming that each crack in the material volume shares a common geometry and orientation, then the specification of the far field strains will complete this description. The rate of change of the internal state variable can therefore be expressed as follows,

$$\frac{d\alpha_{ij}}{dN} = \frac{d\alpha_{ij}}{dS} \frac{dS}{dN} \quad (11)$$

where the far field strains are reflected in the term $\frac{d\alpha_{ij}}{dS}$, which relates the changes in the internal state variable during the development of damage surfaces. Thus, using equations (10) and (11), the stable evolution of the internal state variable is defined by

$$d\alpha_{ij} = \frac{d\alpha_{ij}}{dS} k_1 G^n dN \quad (12)$$



where $\frac{da_{ij}}{dS}$ can be determined analytically for simplified damage geometries and loading conditions and k_1 is a material parameter.

It will now be shown that the strain energy release rate can be determined from the thermodynamic forces. The Helmholtz free energy for a body with distributed damage was defined earlier to be the sum of the Helmholtz free energy in an equivalent undamaged body, h_{EL} , and the energy of damage creation, u_L^c . Since h_{EL} is independent of the internal state variables, the thermodynamic force can be expressed in terms of u_L^c as

$$f_{ij}^T = -\frac{\partial u_L^c}{\partial a_{ij}}. \quad (13)$$

Allen, et al. (1987a) defined u_L^c as the mechanical energy of a continuum due to equivalent crack surface tractions acting on the crack faces. This energy encompasses the energy available for crack extension and the energy loss due to the apparent stiffness reduction caused by existing cracks. An association between the energy for crack extension and the strain energy release rate, G , is defined by

$$u_L^c = \frac{1}{V_L} \int_S G dS. \quad (14)$$

The strain energy release rate is obtained from equation (14) by differentiation with respect to the crack surface area. Thus,

$$G = V_L \frac{du_L^c}{dS}. \quad (15)$$

If the process is restricted to isothermal conditions, u_L^c depends only on the strain tensor, ε_{ij} , and the internal state variable, a_{ij} , so that equation (15) becomes

$$G = V_L \frac{\partial u_L^c}{\partial \varepsilon_{ij}} \frac{d\varepsilon_{ij}}{dS} + V_L \frac{\partial u_L^c}{\partial a_{ij}} \frac{da_{ij}}{dS}. \quad (16)$$

The relationship between the strain energy release rate and the available thermodynamic force is obtained by permitting crack extension under fixed grip conditions and using the definition of the thermodynamic force in equation (13).

$$G = -V_L \frac{da_{ij}}{dS} f_{ij}^T. \quad (17)$$

The internal state variable evolutionary equation shown in (12) can thus be expressed in terms of the available thermodynamic force as follows:

$$da_{ij} = \frac{da_{ij}}{dS} k_1 \left[-\frac{da_{mn}}{dS} f_{mn}^T \right]^n dN \quad \text{when} \quad f_{ij}^T \geq (f_{ij}^T)_{req}. \quad (18)$$

For crack propagation under a single fracture mode, the crack surface kinematics for a thin laminate can be characterized by a single component of

the internal state variable tensor. For example, consider the matrix crack damage state shown in Fig. 1, where all the crack planes are flat and oriented perpendicular to the plane formed by the lamina and parallel to the fibers, a pure opening mode (mode I) would correspond to the crack faces moving in a direction parallel to the crack face normals. Thus, in reference to the ply level cartesian coordinate system, the internal state variable tensor as defined by equation (1) will be zero except for α_{22} . Likewise, for the pure shearing mode (mode II), the only non-zero component of the internal state variable tensor would be α_{12} .

Matrix Crack Development in Multi-Ply Laminates

The evolutionary relationship shown in equation (18) provides a description of the damage development at the ply level. In laminates containing multiple plies of different orientation, the development of damage is influenced by the adjacent plies. This is attributed to the different stress states found in the neighboring plies and the redistribution of load among the plies that occurs during the accumulation of damage. The effects of this interaction on the damage development are included implicitly in the evolutionary equation through the thermodynamic forces and $\frac{d\alpha_{ij}}{dt}$ because laminate averaged damage dependent ply responses calculated from equation (8) are used to determine these quantities. Since the adjacent ply constraining effects are reflected through the laminate equations, the evolutionary equation can be applied independent of the laminate stacking sequence.

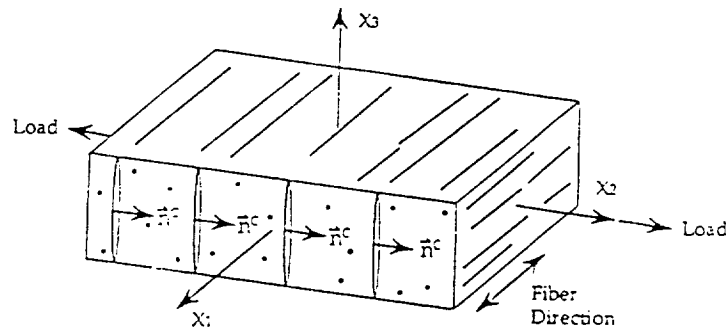
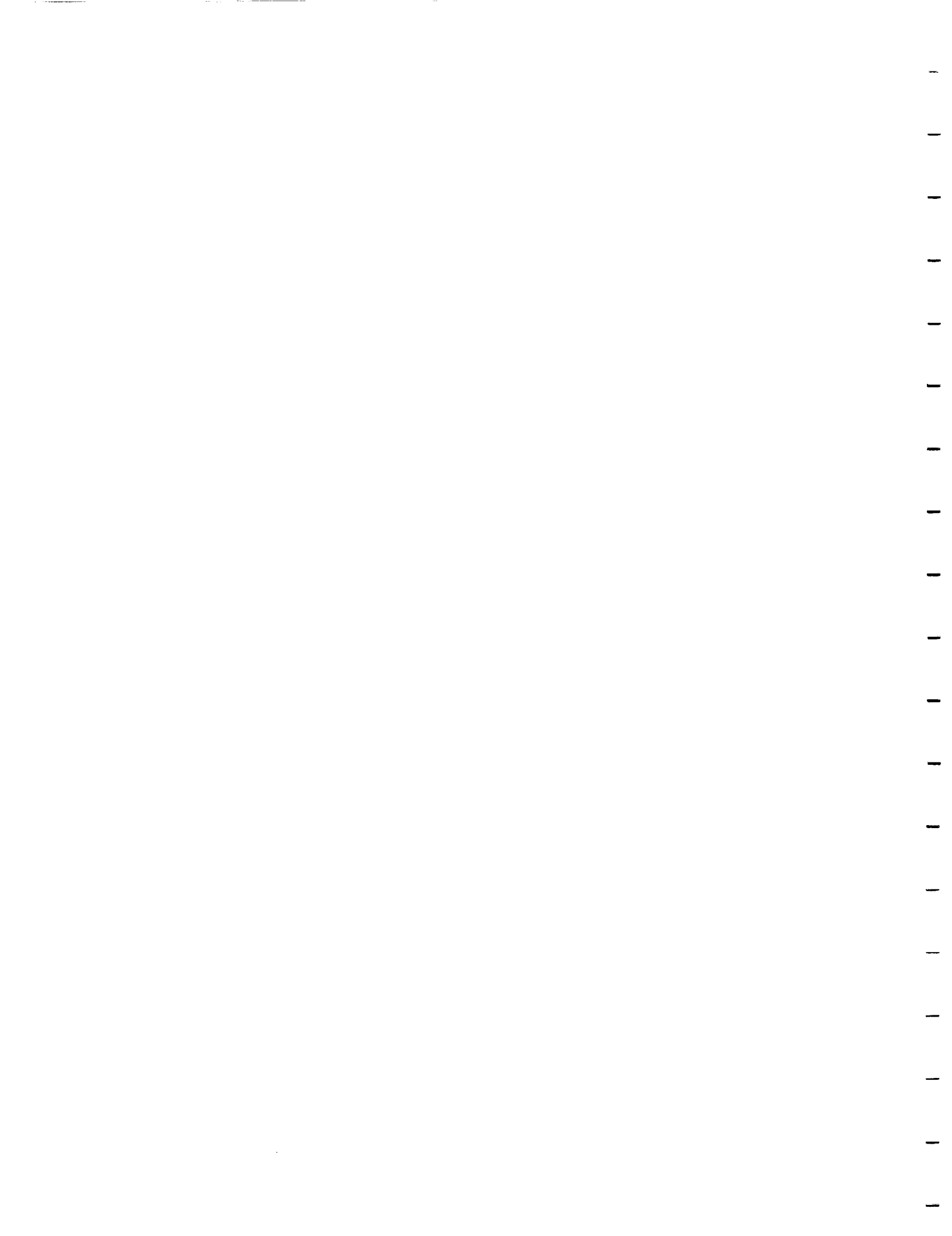


Figure 1. Idealized configuration of ply with matrix cracking.



The term $\frac{d\alpha_{22}}{dS}$, found in equation (18), reflects the changes to the internal state variable with respect to changes to the damage surfaces. $\frac{d\alpha_{22}}{dS}$ can be obtained analytically from relationships describing the kinematics of the crack surfaces for given damage states and loading conditions, should such solutions exist. For transverse matrix cracks in crossply laminates, the average crack face displacement in the pure opening mode can be approximated by a solution obtained by Lee, et al. (1989) for a medium containing an infinite number of alternating 0° and 90° plies. Thus $\frac{d\alpha_{22}}{dS}$ can be determined for crossply laminates subjected to uniaxial loading conditions. It has been found that for typical continuous fiber reinforced Graphite/Epoxy systems $\frac{d\alpha_{22}}{dS}$ can be assumed to be constant for a given applied load until the damage state has reached an advanced stage of development. This assumption has facilitated the determination of the material parameters k_1 and n . The damage state at any point in the loading history can now be determined by the integration of equation (18) using the laminate averaged ply responses. This integration is performed numerically because of the nonlinearity of the damage evolutionary equation. The fourth order Runge-Kutta method has been found to be suitable for this application.

The development of the matrix crack damage state in crossply laminates subjected to uniaxial fatigue loading is examined using the proposed damage evolution equation. To maintain the thermodynamic admissibility of the fatigue loading process, it is assumed that the values of the internal state variables remain constant during the unloading portion of the load cycle. It was further assumed that the required thermodynamic force is very small compared to the available thermodynamic force, thus α_{22} will change at the onset of load application. The material properties for AS4/3501-6 Graphite/Epoxy are used in the calculations to enable the comparison of model prediction to experimental measurements made by Chou, et al. (1982). The material parameters for this polymeric composite system have been found to be

$$k_1 = 4.42 \quad \text{and} \quad n = 6.39 \quad . \quad (19)$$

The damage histories for two crossply layups have been predicted using the model. One layup consists of four consecutive 90° plies laminated between 0° layers of two ply thickness. The other crossply laminate contains six consecutive 90° plies in the center. The model predictions of the damage state in the $[0_2/90_2]$ laminates fatigue loaded at a maximum stress amplitude of 38 ksi and 43 ksi are shown in Figs. 2 and 3, respectively. The lower stress amplitude is equivalent to eighty percent of the monotonic crack initiation stress, while the higher stress amplitude is equal to ninety percent of the initiation stress. The experimentally measured damage states were originally measured in terms of the crack density. However, the corresponding α_{22} for each damage level can be approximated by the relationship proposed by Lee, et al. (1989).



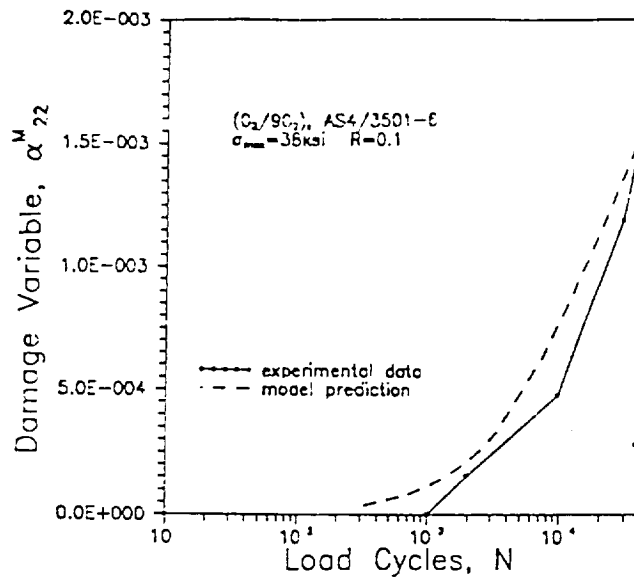


Figure 2. Matrix crack damage in the 90° plies of a $[0_2/90_2]_6$ AS4/3501-6 laminate loaded at a stress amplitude of 36ksi.

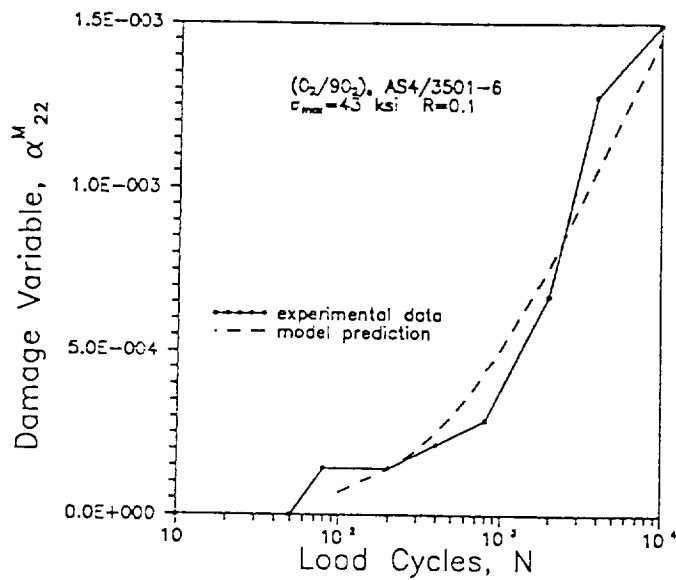


Figure 3. Matrix crack damage in the 90° plies of a $[0_2/90_2]_6$ AS4/3501-6 laminate loaded at a stress amplitude of 43ksi.

ORIGINAL PAGE IS
OF POOR QUALITY

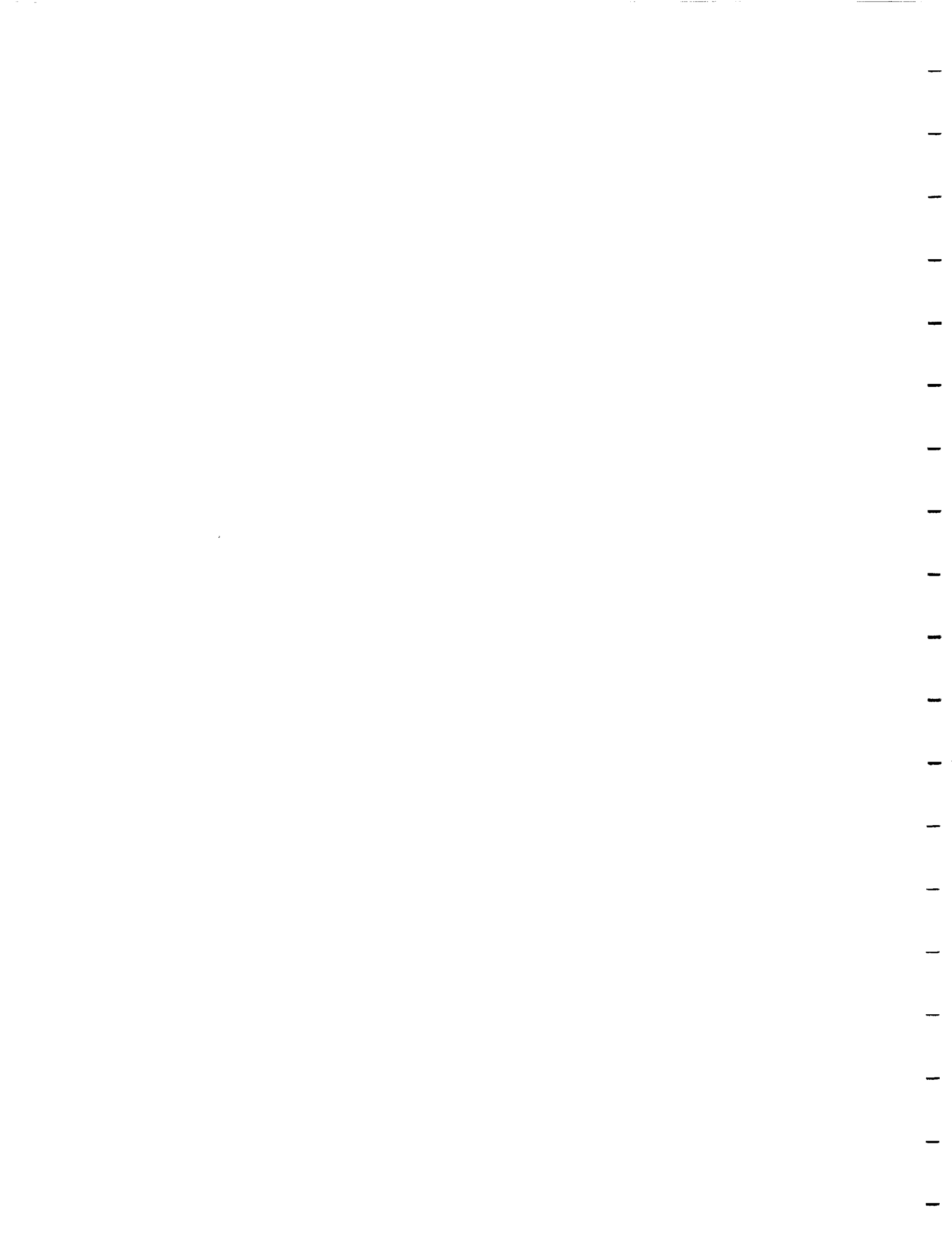


Good agreement is found between the model predictions and the experimental results. The damage evolution for the thicker $[0_2/90_3]$ laminate is shown in Fig. 4. This laminate was loaded at a maximum stress amplitude of 26 ksi. This amplitude corresponds to eighty percent of the quasi-static matrix crack initiation stress. The results for this load case indicated good agreement with the experimental data. The effect of the load redistribution on the damage evolution is apparent in this load case. A marked decrease in the rate of damage evolution after fifty thousand load cycles was indicated by the model. On the other hand, the experimental data showed this decrease to occur after only ten thousand load cycles. Since the evolution of delaminations were not included in the analysis, the predicted decrease in the rate of damage evolution is attributed only to the matrix crack induced transfer of load from the 90° plies to the adjacent 0° plies and the resulting decrease in the available thermodynamic force. The measured values of the damage state, however, may have been influenced by the formation of delaminations along the free edges and in the interior. Such occurrence can drastically affect the stress distribution among the plies and the available thermodynamic force for damage evolution.

To examine the amount of stress redistribution that occurs during the damage accumulation, the model was used to determine the axial stress in the 90° plies of the $[0_2/90_3]$ laminate fatigue loaded at three different stress amplitudes. Fig. 5 shows that for the stress amplitude of 38 ksi, the axial stress in the 90° plies after forty thousand cycles was less than fifty percent of the original stress level in the undamaged laminate. Therefore, the rate of damage evolution is expected to be relatively low during the latter stages of the loading history. This is observed in Fig. 6, which shows the corresponding values of the internal state variable, α_{22} , for the three load cases. The 26 ksi stress amplitude load case, on the other hand, produced only gradual changes in the axial stress and damage state as compared to the other two stress amplitudes. The percentage decrease from the original undamage stress level increased with the fatigue stress amplitude. These results demonstrate that the stress redistribution characteristics among the plies in the laminate are dependent on the loading conditions. These redistribution characteristics will affect the manner in which damage develops in the surrounding plies as well as eventual failure of the laminate.

Conclusion

A damage evolutionary relationship for the accumulation of matrix cracks has been presented. This phenomenologically based relationship operates as part of a continuum damage mechanics model developed to analyze the response of laminated composites. The utilization of material dependent quantities and damage dependent laminate averaged ply responses in the evolutionary relationship has enable it to function independent of the lam-



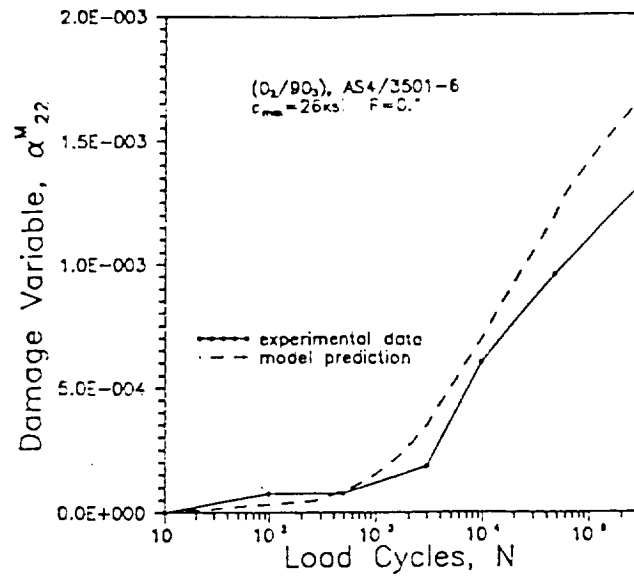


Figure 4. Matrix crack damage in the 90° plies of a $[0_2/90_3]_s$ AS4/3501-6 laminate loaded at a stress amplitude of 26ksi.

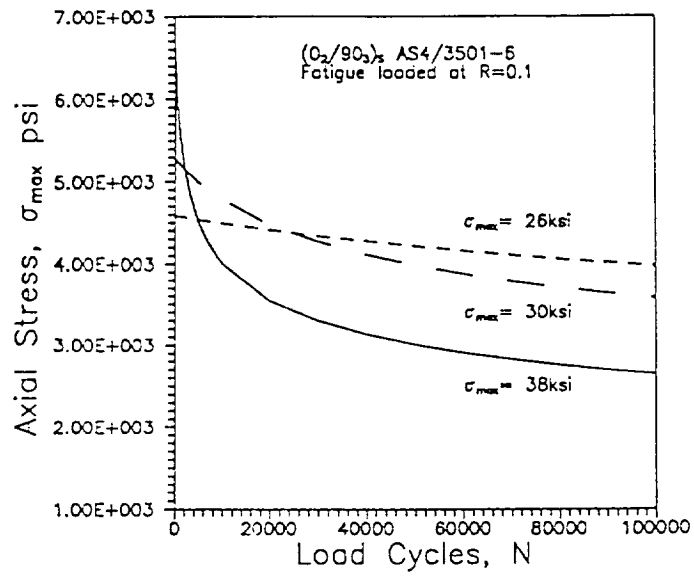
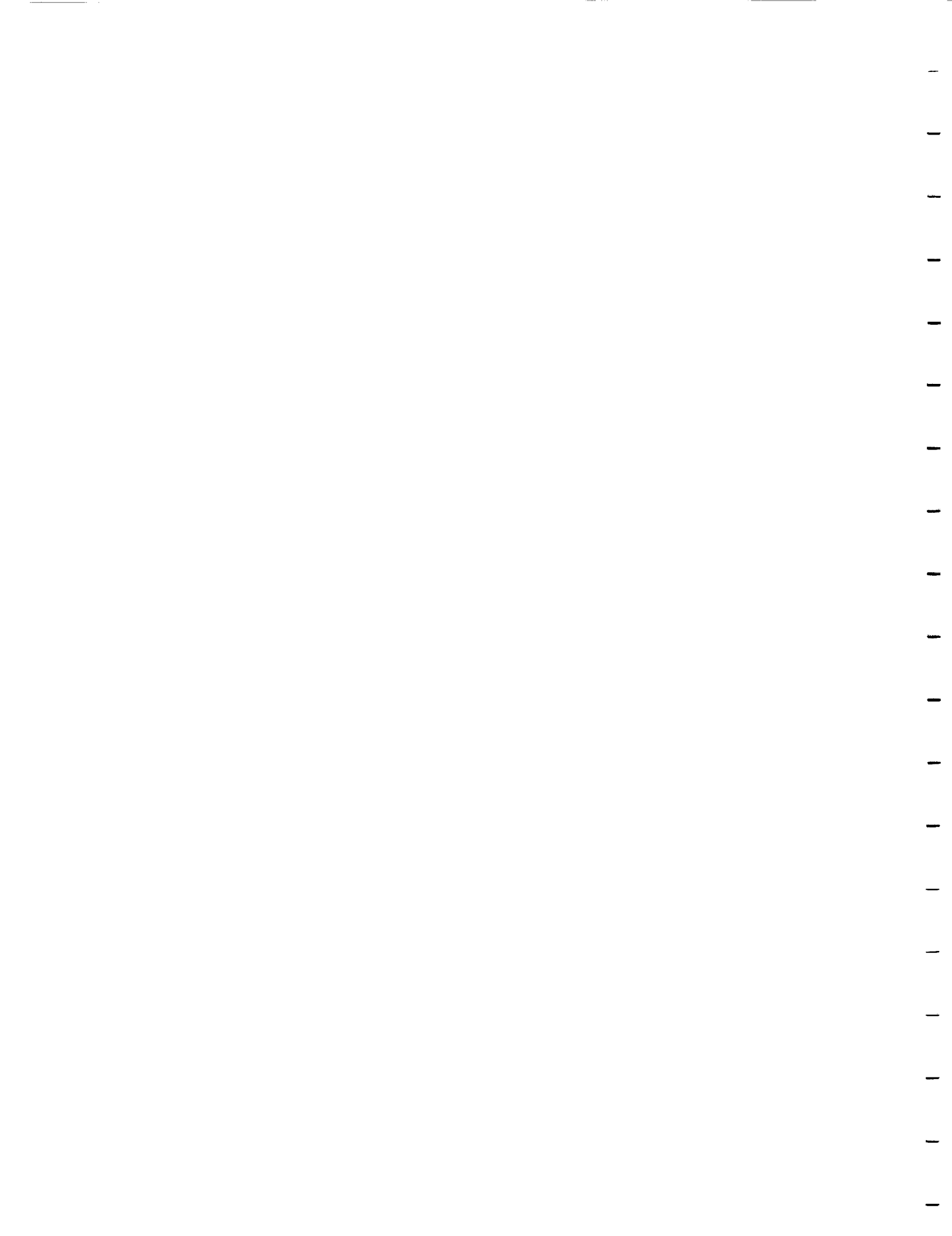


Figure 5. Damage induced stress redistribution in the 90° plies of $[0_2/90_3]_s$ laminates subjected to constant stress amplitude fatigue loading.



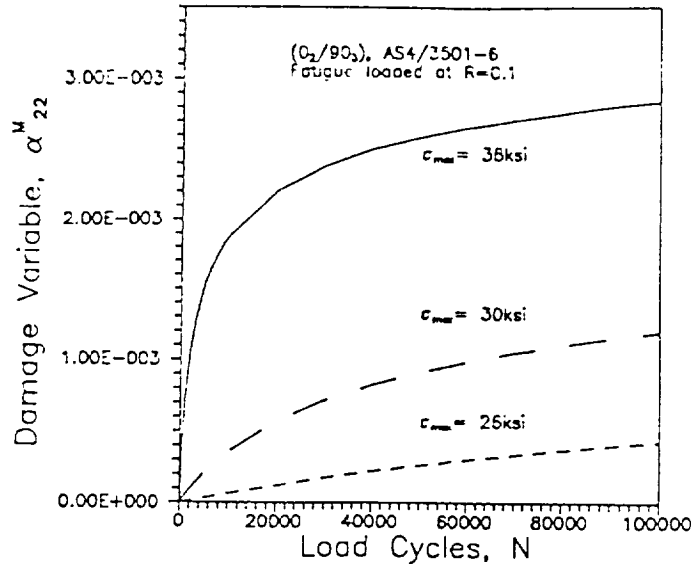


Figure 6. The accumulation of damage in the 90° plies of [0₂/90₃]_s laminates subjected to constant stress amplitude fatigue loading.

inate stacking sequence. The capability to predict the evolution of matrix cracks in crossply laminates subjected to fatigue loading conditions has been demonstrated. The evolutionary relationship has also been used to examine stress redistribution among the plies during the damage history of the laminate. It is found that the stress distribution behavior is dependent on the load amplitude. Higher applied loads result in rapid changes in the axial stress and damage state during the initial portion of the loading history. This is then followed by low rates of change for the remainder of the loading history. For lower load amplitudes, the stress redistribution process and damage accumulation proceed in a gradual manner.

The existence of other types of damage, such as delaminations, will alter the redistribution of stress among the plies and thus the evolution of the damage state. An evolutionary relationship for delamination is currently under development. The inclusion of this type of damage should provide better insight into the complex events occurring within the laminate. The information obtained from the stress redistribution histories could enhance the knowledge of failure characteristics in laminated composites and aid in the development of models for this progressive failure process.



Acknowledgments

This research was supported by NASA Langley Research Center under contract no. NAG-1-979 and NGT-50262.

References

- Allen, D.H., Harris, C.E., and Groves, S.E., 1987a, "A Thermomechanical Constitutive Theory for Elastic Composites With Distributed Damage-I. Theoretical Development," *Int. Journal of Solids and Structures*, Vol. 23, pp. 1301-1318.
- Allen, D.H., Harris, C.E., and Groves, S.E., 1987a, "A Thermomechanical Constitutive Theory for Elastic Composites With Distributed Damage-II. Application to Matrix Cracking in Laminated Composites," *Int. Journal of Solids and Structures*, Vol. 23, pp. 1319-1338.
- Allen, D.H., Harris, C.E., Groves, S.E., and Norvell, R.G., 1988, "Characteristics of Stiffness Loss in Crossply Laminates With Curved Matrix Cracks," *Journal of Composite Materials*, Vol. 22, pp. 71-80.
- Chou, P.C., Wang, A.S.D., and Miller, H., 1982, "Cumulative Damage Model for Advanced Composite Materials, AFWAL-TR-82-4083".
- Coleman, B.D., and Mizel, V.J., 1966, "Thermodynamics and Departures from Fourier's Law of Heat Conduction," *Arch. Rational Mech. Analysis*, 23, pp. 245-261.
- Coleman, B.D., and Gurtin, M.E., 1967, "Thermodynamics With Internal State Variables," *The Journal of Chemical Physics*, Vol. 47, pp. 597-613.
- Harris, C.E., Allen, D.H., and Nottorf, E.W., 1987, "Damage-Induced Changes in the Poisson's Ratio of Cross-Ply Laminates: An Application of a Continuum Damage Mechanics Model for Laminated Composites," *Damage Mechanics in Composites*, ASME, AD-Vol. 12, pp. 17-23.
- Harris, C.E., and Allen, D.H., 1988, "A Continuum Damage Model of Fatigue-Induced Damage in Laminated Composites," *SAMPE Journal*, Vol. 24, No. 4, pp. 43-51.
- Lee, J.W., Allen, D.H., and Harris, C.E., 1989, "Internal State Variable Approach for Predicting Stiffness Reductions in Fibrous Laminated Composites With Matrix Cracks," *Journal of Composite Materials*, Vol. 23, pp. 1273-1291.
- Vakulenko, A.A., and Kachanov, M.L., 1971, "Continuum Theory of Cracked Media," *Mekh. Tverdogo Tela*, 6, p.159.
- Wang, A.S.D., Chou, P.C., and Lei, S.C., 1984, "A Stochastic Model for the Growth of Matrix Cracks in Composite Laminates," *Journal of Composite Materials*, Vol. 18, pp.239-254.



APPENDIX B



A MODEL FOR PREDICTING DAMAGE INDUCED FATIGUE LIFE
OF LAMINATED COMPOSITE STRUCTURAL COMPONENTS

by

David H. Allen*

David C. Lo**

Ioannis I. Georgiou**

Aerospace Engineering Department
Texas A&M University
College Station, TX. 77843-3141

and

Charles E. Harris***

Mechanics & Materials Branch
NASA Langley Research Center
Hampton, VA. 23665

Introduction

Abstract

This paper presents a model for predicting the life of laminated composite structural components subjected to fatigue induced microstructural damage. The model uses the concept of continuum damage mechanics, wherein the effects of microcracks are incorporated into a damage dependent lamination theory instead of treating each crack as an internal boundary. Internal variables are formulated to account for the effects of both matrix cracks and internal delaminations. Evolution laws for determining the damage variables as functions of ply stresses are proposed, and comparisons of predicted damage evolution are made to experiment. In addition, predicted stiffness losses, as well as ply stresses are shown as functions of damage state for a variety of stacking sequences.

Structural applications using composite materials continue to increase in the aerospace engineering community. This is primarily due to the fact that aerospace applications are driven by high specific strength accompanied by low mass. Although composites are expensive when compared to monolithic materials, their improved properties can make them cost effective alternatives in such applications as space structures, wherein the cost of launching a pound of mass is exorbitant.

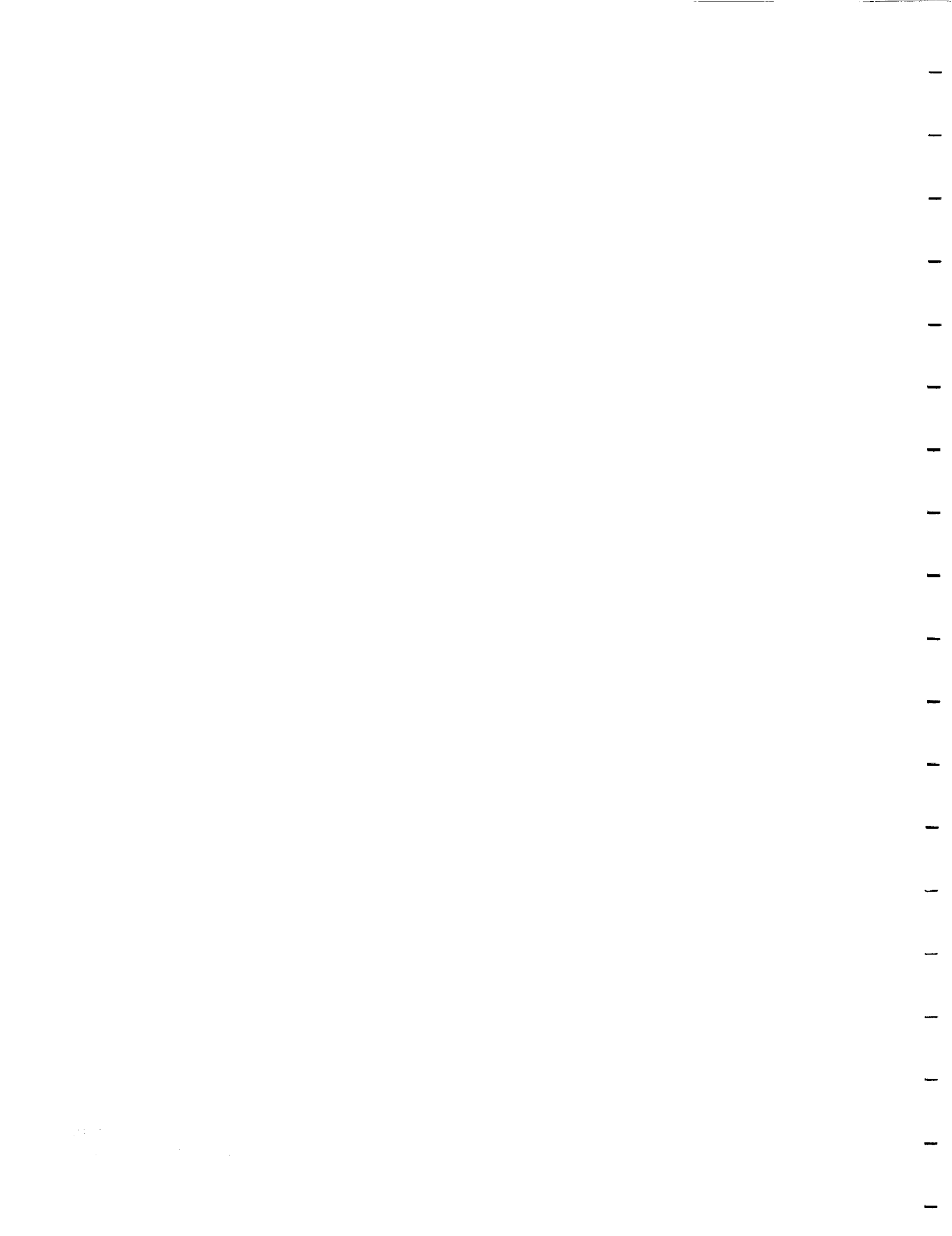
Although composites possess many inviting material characteristics, there are nevertheless some shortcomings. Possibly the most significant one is the fact that most composites develop microstructural damage when subjected to long term fatigue conditions. This is due to the fact that combining two materials with dissimilar mechanical properties results in a multitude of stress singularities when external loads are applied. These tremendous gradients contribute to stable microcracking which continues to evolve throughout the life of the structural component, and, in many circumstances, the damage leads to ultimate fracture of the part and subsequent failure of the structure.

Experimentally, this evolution of damage is illustrated by the x-ray micrographs shown in

* Professor, Associate Fellow AIAA

** Graduate Research Assistant

*** Branch Manager, Member AIAA



Figs. 1-4 [1]), wherein successive damage states are shown for a coupon of graphite/epoxy $(0/90_2)_s$ composite subjected to fatigue loading. In the photos the coupons have been subjected to uniaxial loading in the vertical direction, leading to transverse matrix cracks in the 90° plies (horizontal lines), longitudinal splits in the 0° plies (vertical lines) and interply delaminations between the 0° and 90° plies (shaded grey areas). Typically, the matrix cracks induce stress concentrations which precede the growth of delaminations, as shown in Fig. 5. Furthermore, this damage is accompanied by a small loss in component axial stiffness, as shown in Fig. 6. It has been conclusively determined that the damage is stress induced, so that the damage state and resulting stiffness are strongly affected by load history. In addition, the growth of damage is dependent on stacking sequence, as illustrated in Fig. 7. Note that the delaminations tend to propagate normal to the loading direction in a $(0/90_3)_s$ laminate, as opposed to vertically in a $(0/90_2)_s$ laminate. It is hypothesized that these variations are due to differences in ply level stresses caused by changing the ply stacking sequence. In fact,

this process can be considered to be in some sense beneficial because the integration of two separate brittle materials results in damage, which is a ductile-like phenomenon, thus causing load transference not unlike that which occurs in metals.

The current procedure for predicting life in composites seems to be largely phenomenological in nature; that is, the method of analysis is in most cases dependent on component geometry, load history, and even stacking sequence and environmental conditions. Probably the most direct procedure utilized is nod failure laws not unlike Miner's rule [2,3]. As a result, they apply only to a predetermined geometry and stacking sequence. Perhaps the most ambitious approach uses linear elastic finite elements and treats each crack as an internal boundary subject to growth determined by fracture mechanics criteria [4,5]. While this is desirable and probably the most accurate approach, it would require supercomputing capability for a typically complicated damage state.

For the past several years the authors have been developing an alternative model for predicting damage development in laminated composites. The model can be used for any

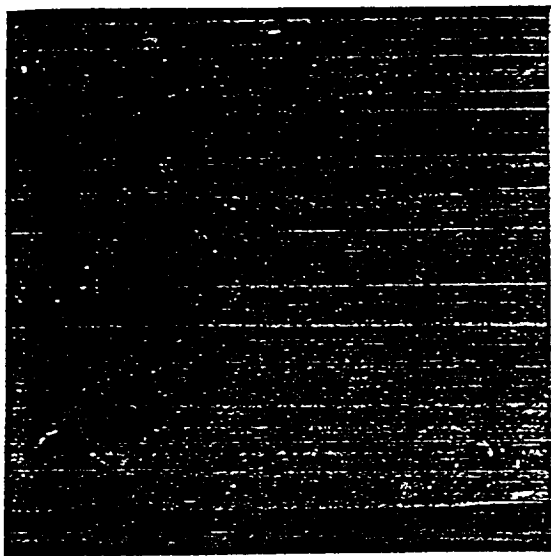


Fig. 1. Enlarge X-ray radiograph of #1 $(0/90_2)_s$ LVE, $C=260,000$, $(f=2.0 \text{ Hz, } R=0.1, F_{max}=10,230 \text{ KN})$

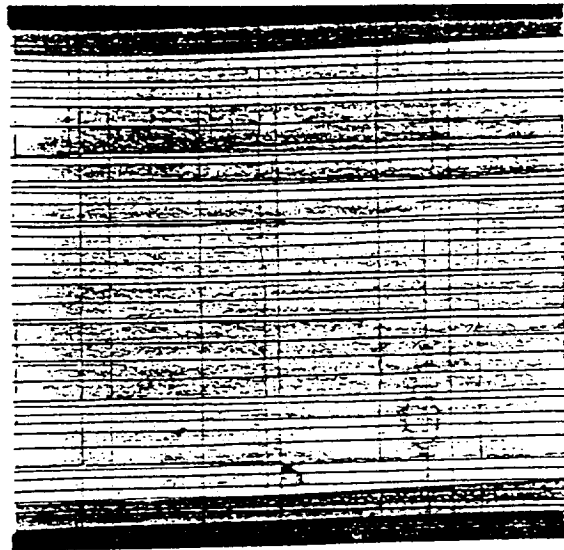


Fig. 2. Enlarged X-ray radiograph of #1 $(0/90_2)_s$ LVE, $C=588,000$, $(f=2.0 \text{ Hz, } R=0.1, F_{max}=10,230 \text{ KN})$

ORIGINAL PAGE IS
OF POOR QUALITY



stacking sequence, using only initial linear elastic orthotropic ply properties. It has the capability to predict the effects of matrix cracks and delaminations on ply stresses. Therefore, it can be used to predict damage evolution as a function of load history such as that shown in Figs. 1-4. Furthermore, the model may be used to model the responses of beams and plates with stress gradients, so that it is not component specific. At the time of this writing the model had reached a fairly advanced state, although it would be premature to call the model mature at this point. This paper gives a brief review of the current state of development of the model. Although we do not pretend to suggest that the model is a usable design tool at this time, we are hopeful that the methodology suggested herein is moving in the right direction.

The structure is modelled as a simply connected domain, with the effects of microcracking reflected by a set of internal state variables (ISV's) which enter the problem description via the constitutive equations. Thus, the necessity to model each crack with tens (or hundreds) of finite elements is avoided with little loss of accuracy and considerable computational savings. To this end, the approach is similar to self-consistent schemes [6] and global/local methods [7] utilized in other applications.

The necessary parts of the model are as follows: 1) a kinematic description of the damage state; 2) a damage dependent set of ply level stress-strain relations which account for matrix cracking; 3) a damage dependent lamination theory which models the effects of interply delamination; 4) a set of damage evolution laws for predicting the load history dependence of the damage state at each material point; 5) a structural algorithm for modelling the response

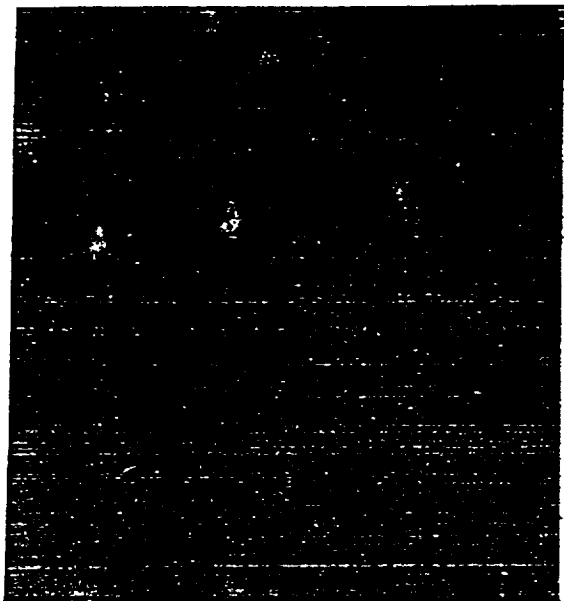


Fig. 3. Enlarged X-ray radiograph of #1 $(0/90_2)_s$ LVI, $C=588,000$, $(f=2.0 \text{ Hz, } R=0.1, F_{max}=10.230 \text{ kN})$

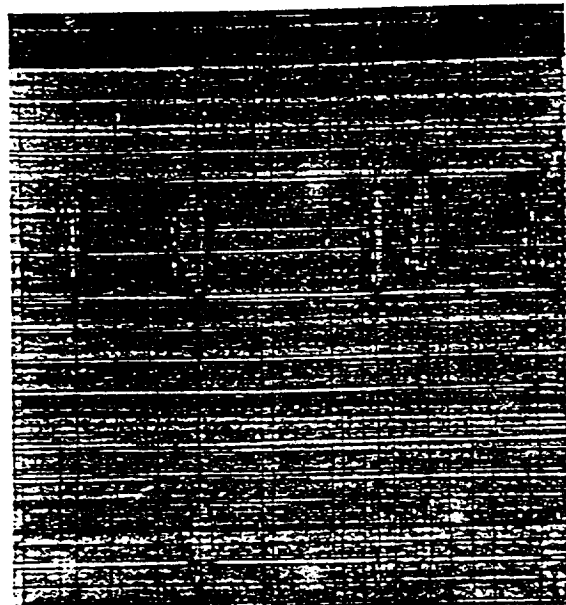


Fig. 4. The state of a delamination group in specimen #1 of $(0/90_2)_s$ laminate, $C=1,130,000$, $(f=2.0 \text{ Hz, } R=0.1, F_{max}=10.230 \text{ kN})$



of components with spatially variable and load history dependent stresses and damage; and 6) a failure function for predicting unstable crack growth leading to loss of component structural integrity. These parts are described briefly in the following subsections.

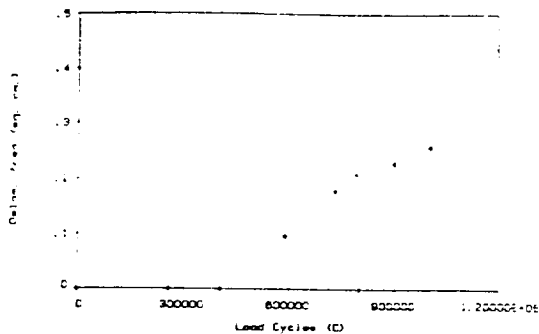


Fig. 5. Delamination Area vs Load Cycles Graph: $(0/90_2)_5$ Specimen

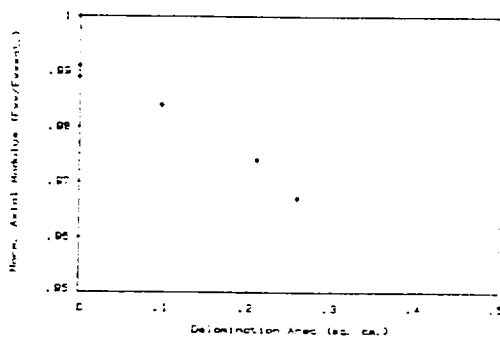


Fig. 6. Normalized axial Modulus vs Delamination Area Graph: $(0/90_2)_5$ Specimen

Kinematic Description of the Matrix Cracking

Since matrix cracks appear to be the first mode of damage to occur in all cases, it would seem that they should be modelled first. Typically, these are of a scale which is very small compared to the geometry of a structural component. Thus, it is hypothesized that a local volume element may be selected which is small compared to the boundary value problem of interest and, at least for the case of matrix cracking, the damage can be assumed to be statistically, spatially homogeneous in this

element. Modelling the effects of matrix cracks would then appear to be ideally suited to the approach taken in continuum damage mechanics. In this approach, first proposed by L.M. Kachanov in 1958 [8], it is hypothesized that the effect of microcracks may be locally averaged on a scale which is small compared to the scale of the structural component. Although the procedure has been extensively utilized in the literature, until recently, it has not been applied to laminated anisotropic media [9-13].

A straightforward and direct approach to averaging the kinematic effects of cracks within the local volume element was taken by Vavrikov and M.L. Kachanov in 1971 [14]. This average is given by the following second order tensor:

$$\bar{\epsilon}_{ij} = \frac{1}{V} \sum_{k=1}^N \epsilon_{ij}^k \quad (1)$$

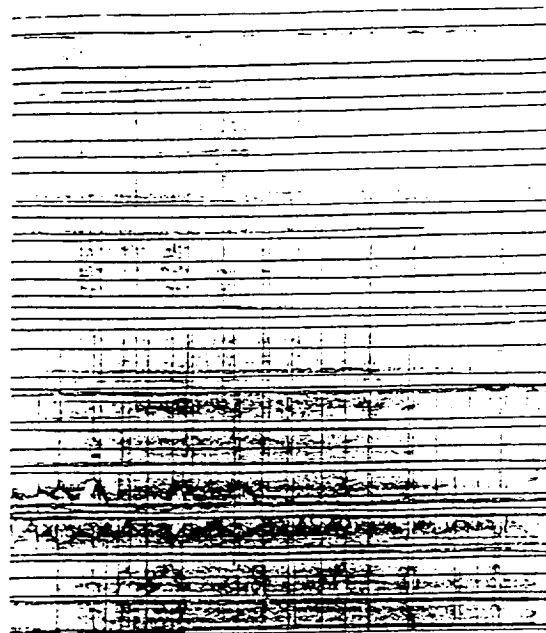


Fig. 7. State of grouping of delaminations, shown in Fig. 5, in #1 $(0/90_2)_5$ laminate, $c=200,000$ ($f=2.0$ Hz., $P=0.1$, $F_{max}=10,230$ KN)



where u_{ij}^M is the ISV for matrix cracking in each ply, V_L is an arbitrarily chosen local volume element or ply thickness which is sufficiently large that u_{ij}^M does not depend on the size of V_L , u_i^C are crack opening displacements in V_L , u_i^C are the components of a unit normal to the crack faces, and S_C is the surface area of matrix cracks in V_L , as shown in Fig. 8.

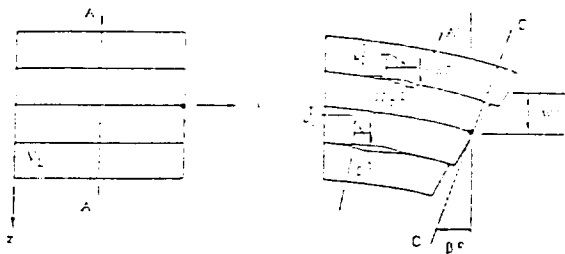


Fig. 8. Deformation Geometry for Region A_L .

Ply Level Stress-Strain Relations

For the case where all matrix cracks are normal to the laminate plane the local volume averaging process can be shown to result in the following ply level stress-strain relations [15,16]:

$$\begin{Bmatrix} c_{Lx} \\ c_{Ly} \\ c_{Lz} \\ c_{Lyz} \\ c_{Lxz} \\ c_{Lxy} \end{Bmatrix} = \begin{bmatrix} Q_{11} & Q_{12} & Q_{13} & Q_{14} & Q_{15} & Q_{16} \\ Q_{12} & Q_{22} & Q_{23} & Q_{24} & Q_{25} & Q_{26} \\ Q_{13} & Q_{23} & Q_{33} & Q_{34} & Q_{35} & Q_{36} \\ Q_{14} & Q_{24} & Q_{34} & Q_{44} & Q_{45} & Q_{46} \\ Q_{15} & Q_{25} & Q_{35} & Q_{45} & Q_{55} & Q_{56} \\ Q_{16} & Q_{26} & Q_{36} & Q_{46} & Q_{56} & Q_{66} \end{bmatrix} \begin{Bmatrix} c_{Lx}^M - u_{xx}^M \\ c_{Ly}^M - u_{yy}^M \\ c_{Lz}^M - u_{zz}^M \\ \gamma_{Lyz}^M - 0 \\ \gamma_{Lxz}^M - 0 \\ \gamma_{Lxy}^M - u_{xy}^M \end{Bmatrix} \quad (2)$$

where Q_{ij} are components of the elastic (undamaged) modulus tensor in ply coordinates, and the subscripts L imply that the components of the stress and strain tensor are locally averaged [15].

Damage Dependent Lamination Theory

Unlike the ply level model for matrix cracking, statistical homogeneity cannot be assumed for delaminations. Although statistical homogeneity appears to hold in the plane of the laminate, the same cannot be said for the through-thickness direction. Thus, damage is accounted for via area averaging in the laminate plane, accompanied by a kinematic assumption through the thickness. Accordingly, the laminate equations are constructed by assuming that the Kirchhoff-Love hypothesis may be modified to include the effects of jump displacements u_i^D , v_i^D , and w_i^D , as well as jump rotations θ_i^D and ψ_i^D for the i th delaminated ply interface, as shown in Fig. 9. Mathematically, then [17]

$$u(x,y,z) = u^0(x,y) + z(\theta^0 + H(z-z_i)\theta_i^D) + H(z-z_i)u_i^D \quad (3)$$

$$v(x,y,z) = v^0(x,y) + z(\psi^0 + H(z-z_i)\psi_i^D) + H(z-z_i)v_i^D \quad (4)$$

and

$$w(x,y,z) = w^0(x,y) + H(z-z_i)w_i^D \quad (5)$$

where the superscripts 0 imply undamaged midsurface quantities, and $H(z-z_i)$ is the heavyside step function. Also, a repeated index i in a product is intended to imply summation, and the superscripts D imply displacement components across the delamination.

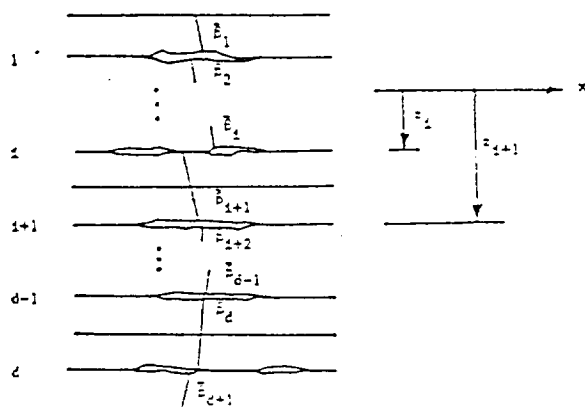


Fig. 9. Schematic of Delaminated Region in a Composite Layup.



The displacement equations are averaged over the local area in order to produce locally averaged displacements to be utilized in the laminate formulation. Thus,

$$u_L(x, y, z) = \frac{1}{h_L} \int_{h_L} [v^C - z_1 v^C + H(z - z_1)(u_1^D) + H(z - z_1) u_1^D] dx dy \quad (6)$$

$$v_L(x, y, z) = \frac{1}{h_L} \int_{h_L} [v^C - z_1 v^C + H(z - z_1)(v_1^D) + H(z - z_1) v_1^D] dx dy \quad (7)$$

and

$$w_L(x, y, z) = \frac{1}{h_L} \int_{h_L} [w^C - z_1 w^C + H(z - z_1) w_1^D] dx dy \quad (8)$$

by averaging the displacements, the delamination jump discontinuities are also averaged over h_L .

The resultant laminate equations may be obtained by substituting equations (6) through (8) into the strain-displacement equations, and this result into equation (2). This result is then integrated through the laminate thickness and the divergence theorem is employed to obtain the following laminate equations [17]:

$$\begin{aligned} (N)_k &= \sum_{k=1}^n [Q]_k (z_k - z_{k-1}) (u_L^C) - \frac{1}{2} \sum_{k=1}^n [Q]_k (z_k^2 - z_{k-1}^2) (u_L^C) \\ &+ \frac{C}{h_L} [\bar{Q}]_1 z_1 \begin{Bmatrix} 0 \\ 0 \\ 0 \\ 0 \\ 0 \\ 0 \\ 0 \\ 0 \\ 0 \\ 0 \end{Bmatrix} + \frac{d+1}{h_L} (z_1 - z_{1-1}) [\bar{Q}]_1 \begin{Bmatrix} 0 \\ 0 \\ 0 \\ 0 \\ 0 \\ 0 \\ 0 \\ 0 \\ 0 \\ 0 \end{Bmatrix} \\ &- \frac{1}{h_L} \sum_{k=1}^n [Q]_k (z_k - z_{k-1}) (u_M)_k \quad (9) \end{aligned}$$

$$\begin{aligned} (M)_k &= \frac{1}{2} \sum_{k=1}^n [Q]_k (z_k^2 - z_{k-1}^2) (u_L^C) - \frac{1}{3} \sum_{k=1}^n [Q]_k (z_k^3 - z_{k-1}^3) (u_L^C) \\ &+ \frac{C}{h_L} [\bar{Q}]_1 z_1^2 \begin{Bmatrix} 0 \\ 0 \\ 0 \\ 0 \\ 0 \\ 0 \\ 0 \\ 0 \\ 0 \\ 0 \end{Bmatrix} + \frac{d+1}{h_L} [\bar{Q}]_1 (z_1^2 - z_{1-1}^2) \begin{Bmatrix} 0 \\ 0 \\ 0 \\ 0 \\ 0 \\ 0 \\ 0 \\ 0 \\ 0 \\ 0 \end{Bmatrix} \\ &- \frac{1}{h_L} \sum_{k=1}^n [Q]_k (z_k^2 - z_{k-1}^2) (u_M)_k \quad (10) \end{aligned}$$

where $[N]$ and $[M]$ are the resultant forces and moments per unit length, respectively, and $(u_M)_k$ and $(v_M)_k$ represent the damage due to matrix cracking and interply delamination, respectively. Furthermore, n is the number of plies, and d is the number of delaminated ply interfaces.

The internal state variable for delamination, (u_1^D) , is obtained by employing the divergence theorem on a local volume element of the laminate.

The resulting procedure gives [17]:

$$u_{11}^D = \frac{1}{h_L} \int_{h_L} u_1^D n_2 ds \quad (11a)$$

$$u_{21}^D = \frac{1}{h_L} \int_{h_L} v_1^D n_2 ds \quad (11b)$$

$$u_{31}^D = \frac{1}{h_L} \int_{h_L} u_1^D n_2 ds \quad (11c)$$

$$u_{41}^D = \frac{1}{h_L} \int_{h_L} v_1^D n_2 ds \quad (11d)$$

$$u_{51}^D = \frac{1}{h_L} \int_{h_L} u_1^D n_2 ds \quad (11e)$$

where the subscript i is associated with the i th delaminated ply interface. Furthermore, v_{L1} is equivalent to $t_1 h_L$, where t_1 is the thickness of the two plies above and below the delamination [17]. By definition, the z component of the unit normal, n_2 , is equivalent to unity. The matrices $[Q]$ with subscripts k are the standard elastic property matrices for the undamaged plies. The matrices $[\bar{Q}]$ with subscripts i apply to the i th delaminated ply interface. They represent average properties of the plies above and below the delamination [17].

While the damage-dependent laminate analysis model may be used to predict any of the effective engineering moduli for a laminate, experimental results are only available for the axial modulus and Poisson's ratio. Therefore, the general utility of the model is demonstrated by comparing model predictions to experimental results for E_x and ν_{xy} [18].

Model predictions have been made for a



typical graphite/epoxy system. The bar chart shown in Fig. 10 compares the model predictions to the experimental values for the engineering modulus, E_x , for combined matrix cracking and delamination. The delamination interface

location and percent of delamination area are listed in the figure underneath the laminate stacking sequence. As can be seen, the comparison between model results and the experimental results is quite good. Some limited results for Poisson's ratio are given in Fig. 11 using the same bar chart format. With the exception of the $[0/90]_s$ laminate, these results are also quite good. Note that these results have been obtained for a single set of input data which do not depend on stacking sequence.

Evaluation of Ply Stresses

In order to evaluate the stress state in each ply, it is first necessary to substitute

displacement equations (6) through (8) into the locally averaged strain-displacement equations. Utilizing the divergence theorem on this result will then give the following equations for the strains in each ply [19]:

$$\epsilon_{L_x}^D = \epsilon_{L_x}^0 - z [k_{L_x} + H(z-z_i) a_{51}^D] + H(z-z_i) a_{31}^D \quad (12)$$

$$\epsilon_{L_y}^D = \epsilon_{L_y}^0 - z [k_{L_y} + H(z-z_i) a_{21}^D] + H(z-z_i) a_{22}^D \quad (13)$$

$$\epsilon_{L_z}^D = \epsilon_{L_z}^0 + H(z-z_i) a_{11}^D \quad (14)$$

$$\epsilon_{L_{yz}}^D = \epsilon_{L_{yz}}^0 [k_{L_{yz}} + H(z-z_i) a_{41}^D] \quad (15)$$

$$\epsilon_{L_{xz}}^D = \epsilon_{L_{xz}}^0 [k_{L_{xz}} + H(z-z_i) a_{51}^D] \quad (16)$$

$$\epsilon_{L_{xy}}^D = \epsilon_{L_{xy}}^0 - \epsilon_{L_{xy}}^0 \quad (17)$$

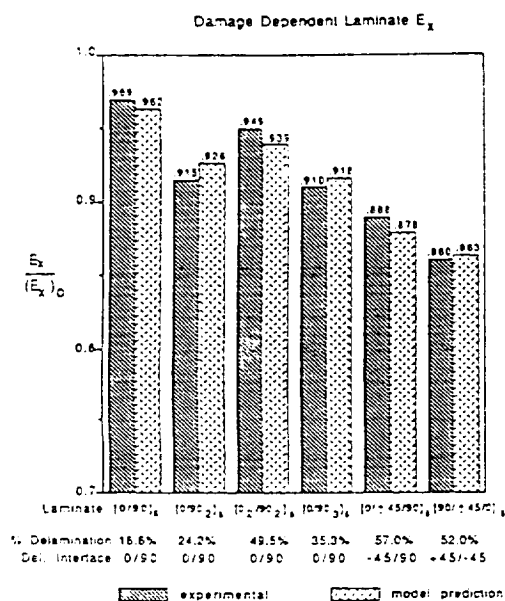


Fig. 10. Comparison of Experimental Results and Model Predictions of the Laminate Engineering Modulus, E_x , Degraded by both Matrix Cracking and Delamination Damage.

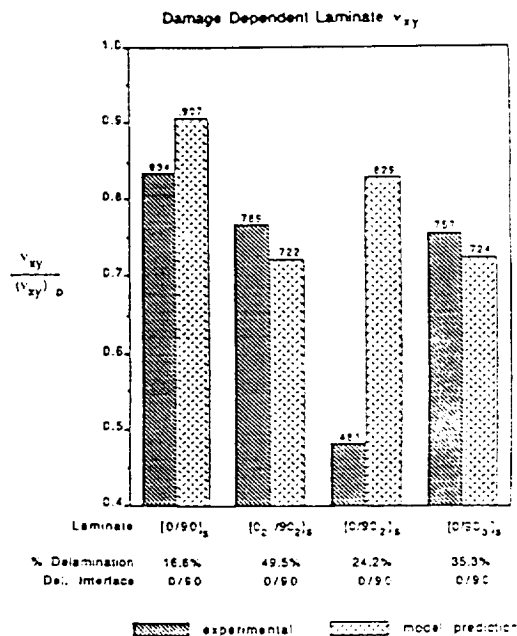


Fig. 11. Comparison of Experimental Results and Model Predictions of the Laminate Engineering Poisson's Ratio, ν_{xy} , Degraded by both Matrix Cracking and Delamination Damage.



The above equations may be utilized to obtain the ply strains, and these results may be substituted into equation (2) to obtain the stresses in each ply [19]. Since the ply stresses determined by this procedure represent locally averaged values, they must be considered to be far-field stresses, so that stress intensity factors would be needed in order to determine matrix crack-tip stresses. This point will be discussed further in the section on damage evolution laws.

A computer code has been constructed to determine the effect of damage on the "far-field" ply stresses in composite laminates [19].

Predicted stresses are shown in Figs. 12 and 13 for a typical crossply laminate and a candidate quasi-isotropic layup with representative damage states. As evidenced from the results, the damage significantly affects the far-field ply stresses. Matrix cracks had a significant effect on ply stresses in the 90° plies in the cross-ply laminate. The quasi-isotropic laminate exhibited a small stress reduction in the ±45° plies, but showed a substantial stress reduction (fifteen percent versus one percent) in the 90° plies.

Damage Evolution Laws

Since the ply stresses determined by this procedure represent locally averaged values, they

must be considered to be far-field stresses, so that ISV evolution laws are generally of the form [19]:

$$\dot{\sigma}_{ij}^M = \dot{\sigma}_{ij}^M (\epsilon_{kk}, T, \sigma_{kk}^M, \sigma_{kk}^D, K_I, K_{II}, K_{III}) \quad (18)$$

and

$$\dot{\sigma}_{ij}^D = \dot{\sigma}_{ij}^D (\epsilon_{kk}, T, \sigma_{kk}^M, \sigma_{kk}^D, K_I, K_{II}, K_{III}) \quad (19)$$

where K_I , K_{II} , and K_{III} are the stress intensity factors, which relate the far-field stresses to the crack tip stresses for a given crack geometry. However, it is assumed that the geometry of both matrix cracking and delaminations is sufficiently independent of stacking sequence that the stress intensity factors may be treated as "material properties" and thus possess the same stress intensity factor dependence for all stacking sequences. Thus, they are encompassed implicitly in the material constants required to characterize damage evolution laws (18) and (19).

One approach to the formulation of the internal state variable evolutionary relationships is through micromechanical considerations. However, this approach is dependent on the availability of micromechanical solutions that can model the essential physical characteristics of the damage state. For the

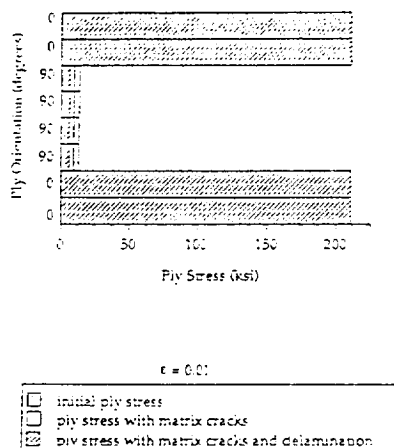


Fig. 12. Far Field Stresses in a $[0_2/90_2]_s$ Laminate

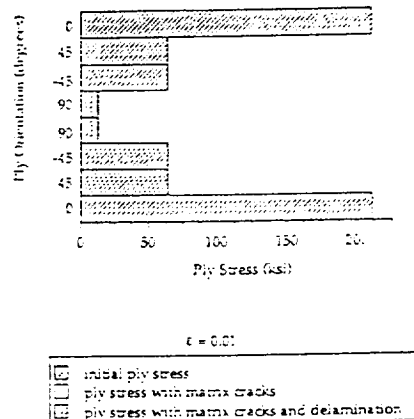


Fig. 13. Far Field Ply Stresses in a $[0/\pm 45/90]_s$ Laminate.



problem of matrix cracks embedded in an orthotropic medium that is layered between two other orthotropic media, the solutions that are currently available are applicable only to very specific loading conditions and damage geometries. Therefore, the evolutionary equation proposed herein is phenomenological in nature. The form of the damage evolutionary relationship employed in this paper is based on the observation made by Wang, et al. [20] that for some materials the rate of damage surface evolution per load step, $\frac{dS}{dN}$, follows a power law in the energy release rate, G . Thus [21],

$$\frac{dM_{ij}}{dS} = \frac{dM_{ij}}{dS} k_1 G^{1/n} \quad (20)$$

The term dM_{ij}/dS reflects the changes to the internal state variable with respect to changes to the damage surfaces. dM_{ij}/dS can be obtained analytically from relationships describing the kinematics of the crack surfaces for given damage states and loading conditions, should such solutions exist. For transverse matrix cracks in crossply laminates, the average crack face displacement in the pure opening mode can be approximated by a solution obtained by Lee, et al. [22] for a medium containing an infinite number of alternating 0° and 90° plies. Thus, dM_{ij}/dS can be determined for crossply laminates subjected to uniaxial loading conditions. It has been found that for typical continuous fiber reinforced graphite/epoxy systems dM_{ij}/dS can be assumed to be constant for a given applied load until the damage state has reached an advanced stage of development. This assumption has facilitated the determination of the material parameters k_1 and n . The material properties for AS4/3501-6 graphite/epoxy are used in the calculations to enable the comparison of model prediction to experimental measurements made by Chou, et al. [24]. The material parameters for this polymeric composite system have been found to be

$$k_1 = 4.42 \quad \text{and} \quad n = 6.39 \quad (21)$$

The damage history for a typical crossply layup has been predicted using the model. The model prediction for the damage state in the $[0_2/90_3]_s$ laminate fatigue loaded at a maximum stress

amplitude of 26 ksi is shown in Fig. 14.

Good agreement is found between the model predictions and the experimental results.

To examine the amount of stress redistribution that occurs during the damage accumulation, the model was used to determine the axial stress in the 90° plies of the $[0_2/90_3]_s$ laminate fatigue loaded at three different stress amplitudes. Fig. 15 shows that for the stress amplitude of 26 ksi, the axial stress in the 90° plies after forty thousand cycles was less than half that of the original stress level in the

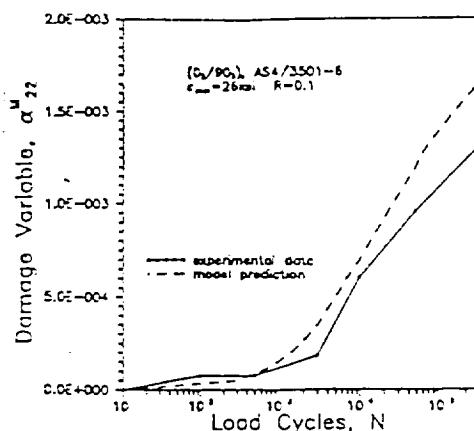


Fig. 14. Matrix crack damage in the 90° plies of a $[0_2/90_3]_s$ AS4/3501-6 laminate loaded at a stress amplitude of 26 ksi.

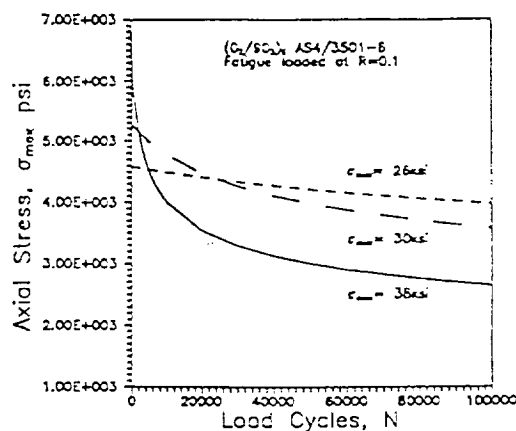


Fig. 15. Damage induced stress redistribution in the 90° plies of $[0_2/90_3]_s$ laminates subjected to constant stress amplitude fatigue loading.



undamaged laminate. These results demonstrate that the stress redistribution characteristics among the plies in the laminate are dependent on the loading conditions. These redistribution characteristics will affect the manner in which damage develops in the surrounding plies as well as eventual failure of the laminate.

Life Prediction

Usually, ultimate failure of laminated composites is caused by large scale fracture which is induced by fiber fracture at delamination sites. Therefore, there is not only a synergistic effect between matrix cracking and delamination, but also between delamination and the ultimate failure event. Since fiber fracture occurs very near the end of the component life, rather than model it with an additional internal variable, it is preferable to simply treat it as the ultimate failure event and model it with a failure function. Typically, one of two approaches could be taken. A phenomenological approach would entail the modification of an existing failure function such as the Tsai-Wu failure function to account for the existing damage state. Alternatively, a fracture criterion could also be modified to account for the damage induced stress redistribution. The authors are pursuing this subject further at this time.

Conclusion

The authors have shown that by constructing local averages of the kinematic effects of microcracking it is possible to construct continuous internal variables which appear explicitly in a modified laminations theory for layered composites with damage. Comparisons of predicted stiffness loss as a function of damage state to experimental results lend credence to the model.

Because the lamination theory is damage dependent, it produces predicted stress

redistribution as damage develops for a given fatigue load history. This predicted stress redistribution in turn affects the evolution of damage, thus producing a life prediction model which can be used for any stacking sequence regardless of the load history applied to the component. However, while initial model comparisons to experiment are favorable, further research is suggested before the model is utilized in a design setting.

Acknowledgement

Partial funding for this research was supplied by NASA Langley Research Center under grant no. NAG-1-979.

References

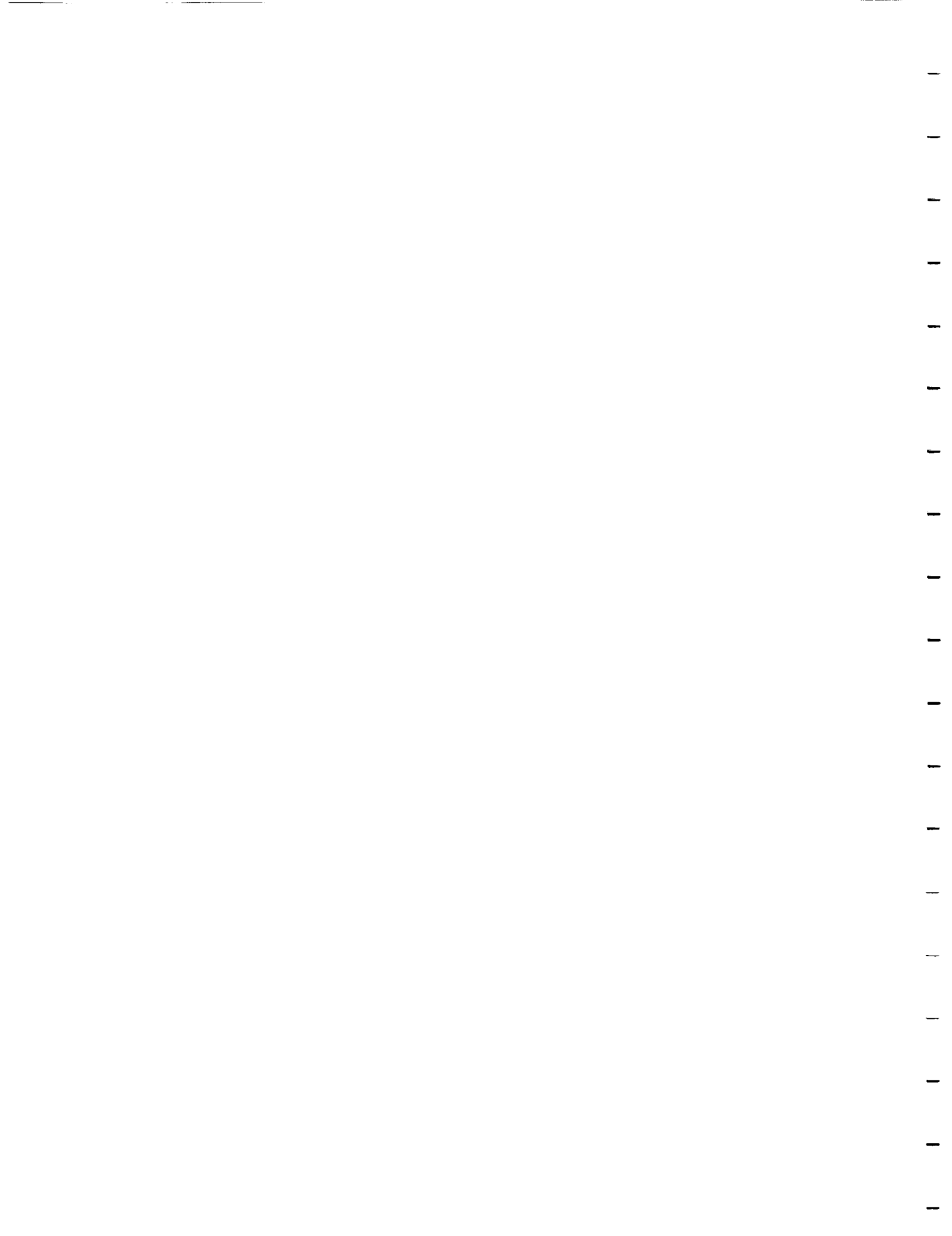
1. Georgiadis, I.T., "Initiation Mechanisms and Fatigue Growth of Internal Delamination in Graphite/Epoxy Cross-Ply Laminates, Texas A&M University, Thesis, December, 1986.
2. Miner, M.A., "Cumulative Damage in Fatigue," Journal of Applied Mechanics, Vol. 12, p. 159, 1945.
3. Hahn, H.T., "Fatigue Behavior and Life Prediction of Composite Laminates", Composite Materials: Testing and Design (Fifth Conf.), ASTM STP 674, pp. 383-417, 1979.
4. Caruso, J.J. and Chamis, C.C., "Assessment of Simplified Composite Micromechanics Using Three-Dimensional Finite-Element Analysis," J. Composites Technology & Research, Vol. 6, No. 3, pp. 77-83, 1984.
5. Chamis, C.C. and Smith, G.T., "CODSTRAN: Composite Durability and Damage Tolerance: Simplified Predictive Methods," NASA Report TM-100179, NASA, Washington, 1978.
6. Mura, T., "Micromechanics of Defects in Solids," Mechanics of Elastic and Inelastic Solids, 2, Martinus Nijhoff Publishers, Netherlands, 1982.
7. Noor, A.H., "Micropolar Beam Models for Lattice Grids with Rigid Joints," Computer Methods in Applied Mechanics and Engineering, Vol. 21, pp. 249-263, 1980.
8. Kachanov, L.M., "On the Creep Fracture Time," Izv. Ak. SSR, Otd. Tekhn. Nauk, No. 8, pp. 26-31, 1958.
9. Talreja, R., "A Continuum Mechanics Characterization of Damage in Composite Materials," Proc. R. Soc. London, Vol. 399A, pp. 195-216, 1985.



11. Talreja, R., "Transverse Cracking and Stiffness Reduction in Composite Laminates," Journal of Composite Materials, Vol. 21, pp. 355-375, 1985.
12. Talreja, R., "Stiffness Properties of Composite Laminates with Matrix Cracking and Interior Delamination," Danish Center for Applied Mathematics and Mechanics, The Technical University of Denmark, No. 321, March, 1986.
13. Weitsman, Y., "Environmentally Induced Damage in Composites," Proceedings of the 5th Symposium on Continuum Modeling of Discrete Structures, A.S.M. Spencer, Ed., Nottingham, U.K., 1985.
14. Vekilenko, A.A., and Kachanov, M.L., "Continuum Theory of Cracked Media," Izv. AN SSSR, Mekhanika Tverdogo Tela, Vol. 6, p. 159, 1971.
15. Allen, D.H., Harris, C.E., and Groves, S.E., "A Thermomechanical Constitutive Theory for Elastic Composites with Distributed Damage - Part I: Theoretical Development," Int. Journal Solids & Structures, Vol. 23, No. 9, pp. 1301-1318, 1987.
16. Allen, D.H., Harris, C.E., and Groves, S.E., "A Thermomechanical Constitutive Theory for Elastic Composites with Distributed Damage - Part II: Application to Matrix Cracking in Laminated Composites," Int. Journal Solids & Structures, Vol. 23, No. 9, pp. 1319-1338, 1987.
17. Allen, D.H., Groves, S.E., and Harris, C.E., "A Cumulative Damage Model for Continuous Fiber Composite Laminates with Matrix Cracking and Interply Delaminations," Composite Materials: Testing and Design (8th Conference), ASTM STP, American Society for Testing and Materials, 1987.
18. Harris, C.E., Allen, D.H., and Nottorf, E.W., "Damage Induced Changes in the Poisson's Ratio of Cross-Ply Laminates: An Application of a Continuum Damage Mechanics Model for Laminated Composites," Proceedings ASME Winter Annual Meeting, American Society of Mechanical Engineers, 1987.
19. Allen, D.H., Nottorf, E.W., and Harris, C.E., "Effect of Microstructural Damage on Ply Stresses in Laminated Composites," Recent Advances in the Macro- and Micro-Mechanics of Composite Materials Structures, AD-Vol. 13, ASME, pp. 135-146, 1986.
20. Wang, A.S.D., Chou, P.C., and Lei, S.C., "A Stochastic Model for the Growth of Matrix Cracks in Composite Laminates," Journal of Composite Materials, Vol. 18, pp. 239-254, 1984.
21. Lo, D.C., Allen, D.H., and Harris, C.E., "A Continuum Model for Damage Evolution in Laminated Composites," Proceedings IUTAM Symposium, Troy, N.Y., 1990 (to appear).
22. Lee, J.W., Allen, D.H., and Harris, C.E., "Internal State Variable Approach for Predicting Stiffness Reductions in Fibrous Laminated Composites With Matrix Cracks," Journal of Composite Materials, Vol. 23, pp. 1273-1291, 1989.
23. Chou, P.C., Wang, A.S.D., and Miller, H., "Cumulative Damage Model for Advanced Composite Materials," AFWAL-TR-82-4083, 1982.



APPENDIX C



LIFE PREDICTION IN LAMINATED COMPOSITES USING CONTINUUM DAMAGE MECHANICS

by

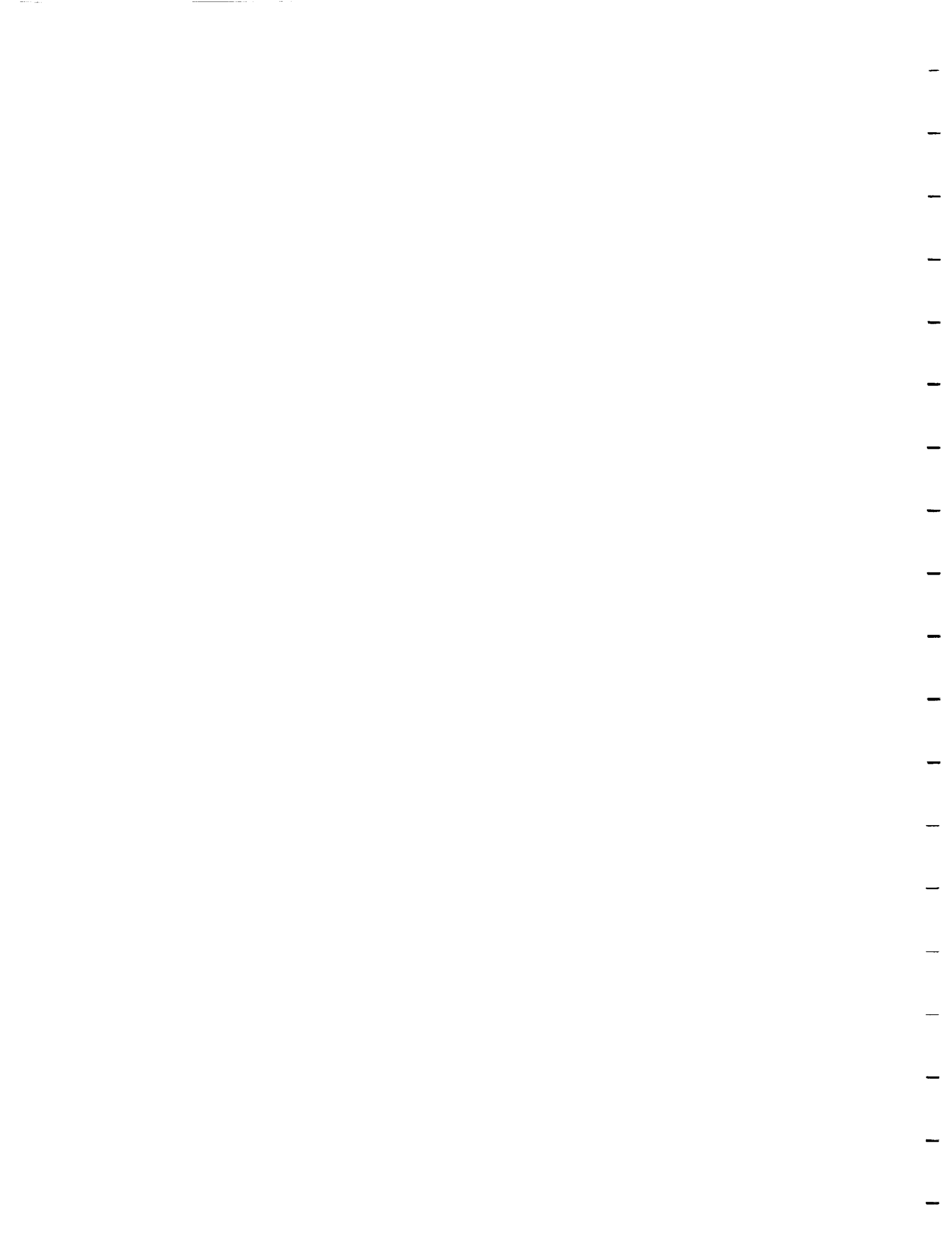
David H. Allen
Aerospace Engineering Department
Texas A&M University
College Station, TX. 77843-3141

INTRODUCTION

Laminated continuous fiber composite structural components are observed to develop substantial load induced noncatastrophic microstructural damage. Since this damage quite often leads to very small changes in linear elastic material properties, analysts are sometimes lead to the fallacious assumption that linear elastic analysis need only be supplemented by a knock-down safety factor in order to design away from failure. This supposition is erroneous. Although substantial globally stable microcracking can be accepted without component failure, the progression of this damage ultimately determines the life of the structure. Furthermore, the damage is spatially variable, tending to congregate in regions of high stress, and since stress concentrations are unavoidable in heterogeneous media, the development of damage is inescapable. In fact, this process can be considered to be in some sense beneficial because the integration of two separate brittle materials results in this damage, which is a ductile-like phenomenon, thus causing load transferral not unlike that which occurs in metals.

A complicating feature of life prediction is the fact that the mode of failure in a component of given structural shape is observed to be dependent on the load history involved. In the same way that monotonic tension and compression in composites is observed to result in differing failure characteristics, varying the fatigue spectrum applied to a particular component can result in gross changes in the observed failure characteristics.

**ORIGINAL PAGE IS
OF POOR QUALITY**

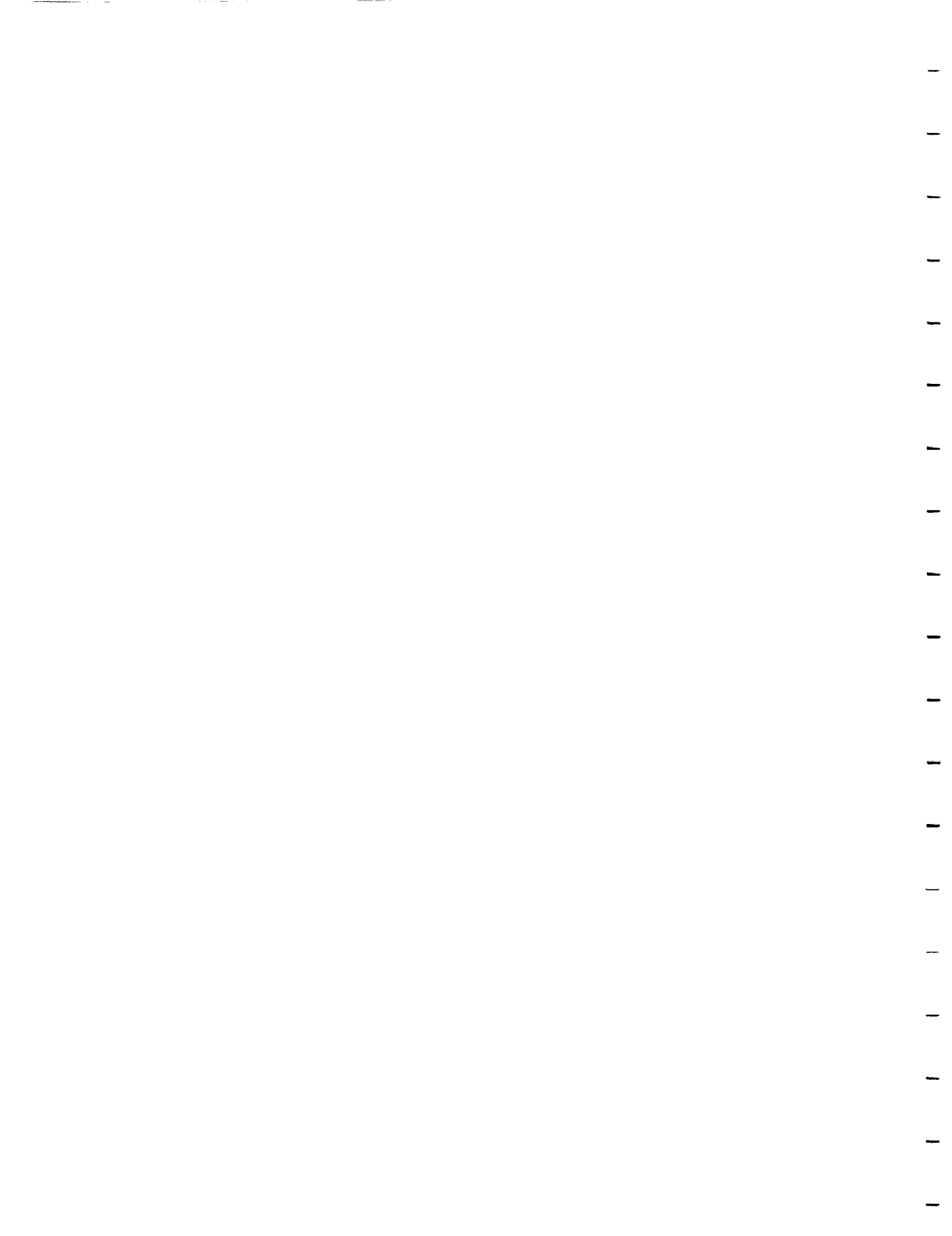


Most current methodologies for life prediction in composites seem to be extremely limited in nature in that they are largely ad hoc in nature; that is, the methods of analysis are in most cases dependent on component geometry, load history, and even stacking sequence and environmental conditions. Probably the most direct procedures utilize phenomenological failure laws not unlike Miner's rule [1,2]. As a result, they apply only to predetermined geometry and stacking sequences.

Perhaps the most ambitious approach attempts to bring all of the details of the mechanics into focus by using linear elastic finite elements and treating each crack as an internal boundary subject to growth determined by fracture mechanics criteria [3,4]. While this is desirable and probably the most accurate approach, it would require supercomputing capability for a typically complicated damage state such as that found in the circular cutout shown in Fig. 1.

The current chapter of this text reviews an approach to this problem which, although not complete at the time of this writing, has the potential to model the life of a laminated structural component, no matter what the geometric shape, and for any loading history, given only a set of input data which do not depend on the stacking sequence. Furthermore, the structure is modelled as a simply connected domain, with the effects of microcracking reflected by a set of internal state variables (ISV's) which enter the problem description via the constitutive equations. Thus, the necessity to model each crack with tens (or hundreds) of finite elements is obviated with little loss of accuracy and considerable computational savings. To this end, the approach is similar to self-consistent schemes [5] and global-local methods [6] utilized in other applications.

Although the author is not so bold as to suggest that the methodology proposed herein represents a panacea, it is hoped that this approach is at least moving towards a generalized analysis tool applicable to laminated composite structural component life prediction. In the same way that classical plasticity theory developed in the early part of this century for isotropic and homogeneous media, the model possesses some features which are already grounded in fundamental mechanics, and some parts which are phenomenological at this time and will thus require future refinement. Therefore, the model should be treated as in a transitory state, and each user

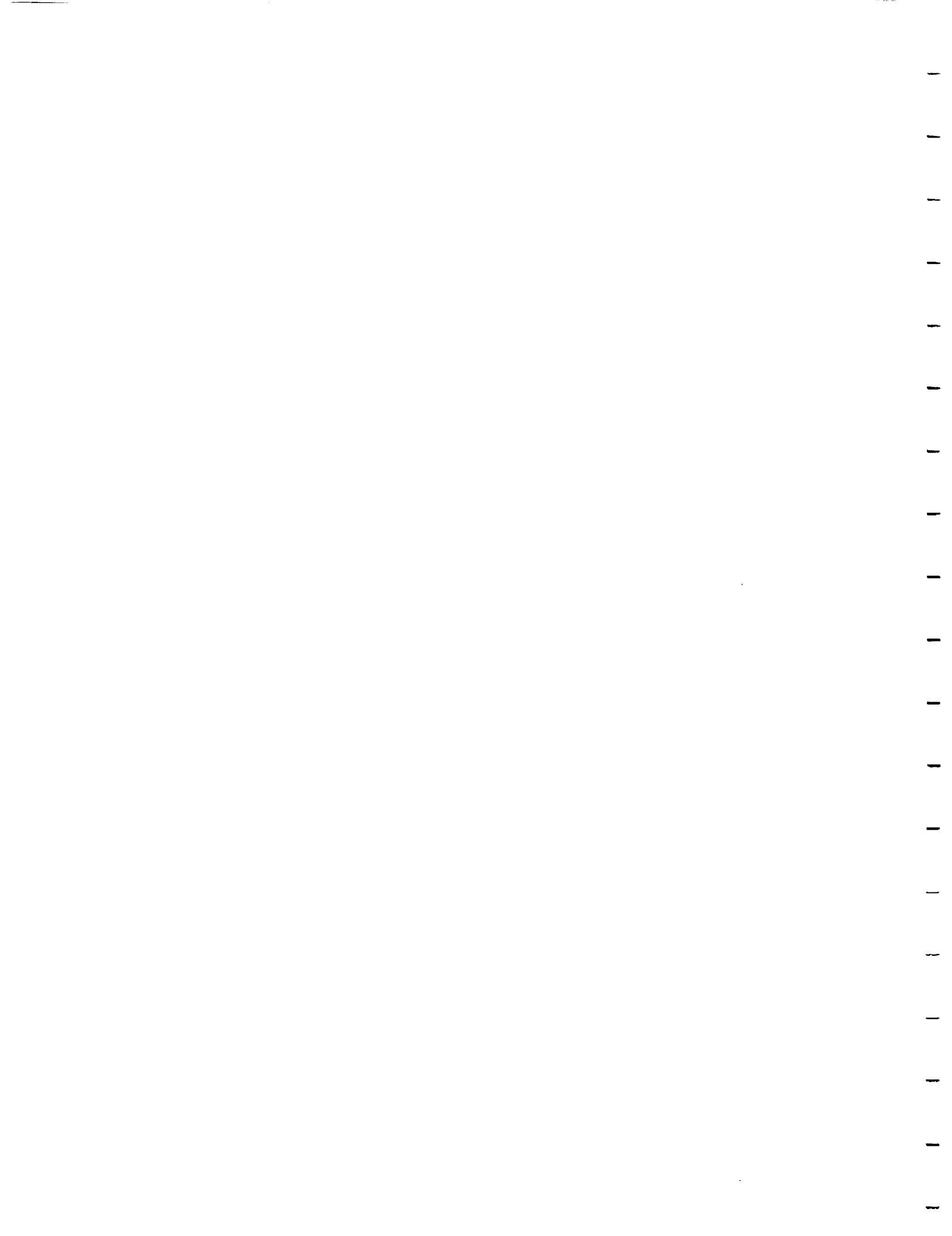


will want to supplement model predictions with a liberal experimental verification program. The usefulness of the model will thus vary from one application to another, and will be measured by the number of experiments which can be avoided with model usage.

The primary objective of the damage model is to develop the capability to predict the fatigue life of laminated structural components. Accordingly, it is essential that the constitutive inputs to the model be independent of the geometry and stacking sequence for the particular application at hand. The approach taken to this objective is to construct a nonlinear damage dependent lamination theory which can be implemented to any computational structural algorithm such as a finite element code. This then allows for modification of linear elastic codes via a time stepping scheme to account for load history dependent damage and an iterative algorithm to account for nonlinearity on each time step. The necessary parts of the model are as follows: 1) a kinematic description of the damage state; 2) a damage dependent set of ply level stress-strain relations which account for matrix cracking; 3) a damage dependent lamination theory which models the effects of interply delaminations; 4) a set of damage evolution laws for predicting the load history dependence of the damage state at each material point; 5) a structural algorithm for modelling the response of components with spatially variable and load history dependent stresses and damage; and 6) a failure function for predicting unstable crack growth leading to loss of component structural integrity. The chapter will review recent developments in each of the above areas, and support for the model will be demonstrated via experimental results.

MODEL DEVELOPMENT

As shown in Fig. 1, a typical laminated continuous fiber composite with brittle matrix usually undergoes three significant and physically different modes of damage: matrix cracking; interply delamination; and fiber breakage. Normally, a substantial distribution of matrix cracks occurs before delamination initiation, and the culmination of this phase of damage is accordingly termed the characteristic damage state [7] because it appears to reach this configuration independently of the load history. Delaminations then begin to appear as a result of stress concentrations at the intersections



of matrix cracks in adjacent plies, as shown in Fig. 2. Finally, the development of large scale delaminations causes stresses sufficient to induce fiber breakage, and this usually leads to component failure via unstable fracture. A significant literature exists detailing the experimental observation of these events [8-12].

Since matrix cracks appear to be the first mode of damage to occur in all cases, it would seem that they should be modelled first. Typically, these are of a scale which is very small compared to the geometry of a structural component. For example, a typical saturation crack spacing in graphite/epoxy is about thirty cracks per inch (for a ply thickness of 0.0055 in). Thus, it is hypothesized that a local volume element may be selected which is small compared to the boundary value problem of interest and, at least for the case of matrix cracking, the damage can be assumed to be statistically spatially homogeneous in this element, as shown in Fig. 3. Modelling the effects of matrix cracks would then appear to be ideally suited to the approach taken in continuum damage mechanics. In this approach, first proposed by L.M. Kachanov in 1958 [13], it is hypothesized that the effect of microcracks may be locally averaged on a scale which is small compared to the scale of the structural component. Although the procedure has been extensively utilized in the literature, until recently it has not been applied to laminated orthotropic media [14-18].

Kinematic Description of the Damage State

A straightforward and direct approach to averaging the kinematic effects of cracks within the local volume element was taken by Vakulenko and M.L. Kachanov in 1971 [19]. This average is given by the following second order tensor:

$$u_{ij}^M = \frac{1}{V_L} \int_{S_C} u_{ij}^C n_j^C ds \quad (1)$$

where u_{ij}^M is the ISV for matrix cracking in each ply, V_L is an arbitrarily chosen local volume element of ply thickness which is sufficiently large that u_{ij}^M does not depend on the size of V_L , u_i^C are crack opening



displacements in V_L , n_j^C are the components of a unit normal to the crack faces, and S_L is the surface area of matrix cracks in V_L , as shown in Fig. 4. It will be shown in the next section that definition (1) is thermodynamically consistent with the constitutive equations developed herein.

Ply Level Stress-Strain Relations

Consider the local volume element shown in Fig. 5 with traction boundary conditions on the external surface S_1 . In addition, the interior V_L is assumed to be composed entirely of linear elastic material and cracks (which may include thin surface layers of damage). Integrating the pointwise Helmholtz free energy over the local volume will result in [20]

$$h_{EL} = A_L + B_{Lij} \epsilon_{Lij} + \frac{1}{2} C_{Lijkl} \epsilon_{Lij} \epsilon_{Lkl} + D_L \Delta T_L + E_{Lij} \epsilon_{Lij} \Delta T_L + \frac{1}{2} F_L \Delta T_L^2 \quad (2)$$

where A_L , B_{Lij} , C_{Lijkl} , D_L , E_{Lij} , and F_L are locally averaged undamaged material constants. Furthermore, the locally averaged stress is defined by

$$\sigma_{Lij} = \frac{1}{V_L} \int_{V_L} \sigma_{ij} dV \quad (3)$$

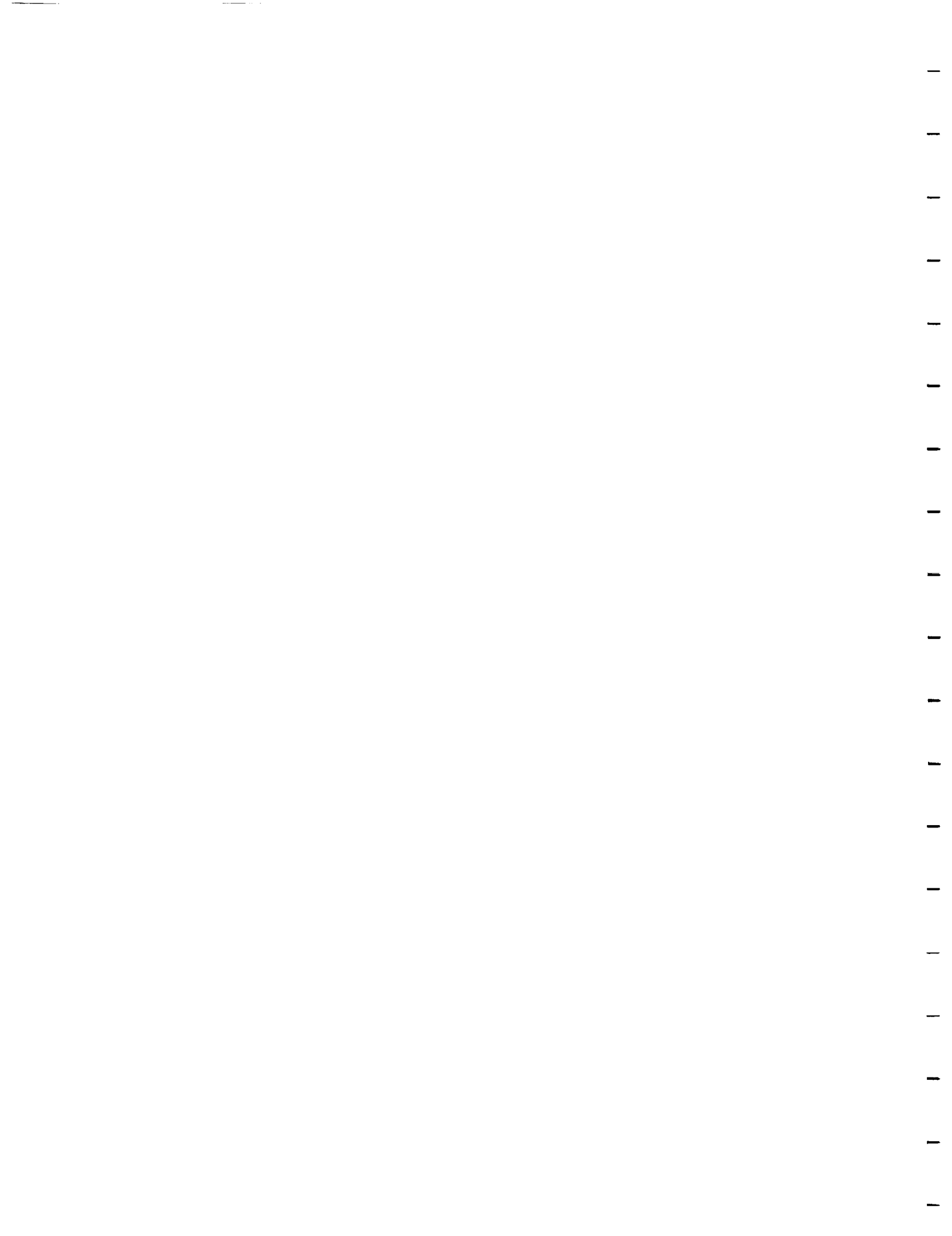
and the locally averaged strain is defined by

$$\epsilon_{Lij} = \frac{1}{V_L} \int_{S_1} \frac{1}{2} (u_i n_j + u_j n_i) dS \quad (4)$$

where n_j are components of the unit outer normal vector to the surface S_1 . It follows that the governing field equations may be integrated over the local volume to obtain

1) conservation of linear momentum:

$$\sigma_{Lji,j} = 0 \quad (5)$$



2) conservation of angular momentum:

$$\rho_L \dot{L}_{ij} = L_{ji} \quad (6)$$

3) conservation of energy,:

$$\dot{u}_L' = \rho_L \dot{L}_{ij} L_{ij} + q_{Lj,j} - r_L \quad (7)$$

where u_L' is as defined below, q_{Lj} is the locally averaged heat flux vector, r_L is the locally averaged heat supply; and

4) the entropy production inequality:

$$\dot{s}_L = \frac{r_L}{T_L} + \left(\frac{q_{Lj}}{T_L} \right)_{,j} \geq 0 \quad (8)$$

where s_L is the locally averaged entropy, and T_L is the locally averaged temperature. The effective locally averaged internal energy, u_L' , is given by

$$\dot{u}_L' = \dot{u}_{EL} + \dot{u}_L^C \quad (9)$$

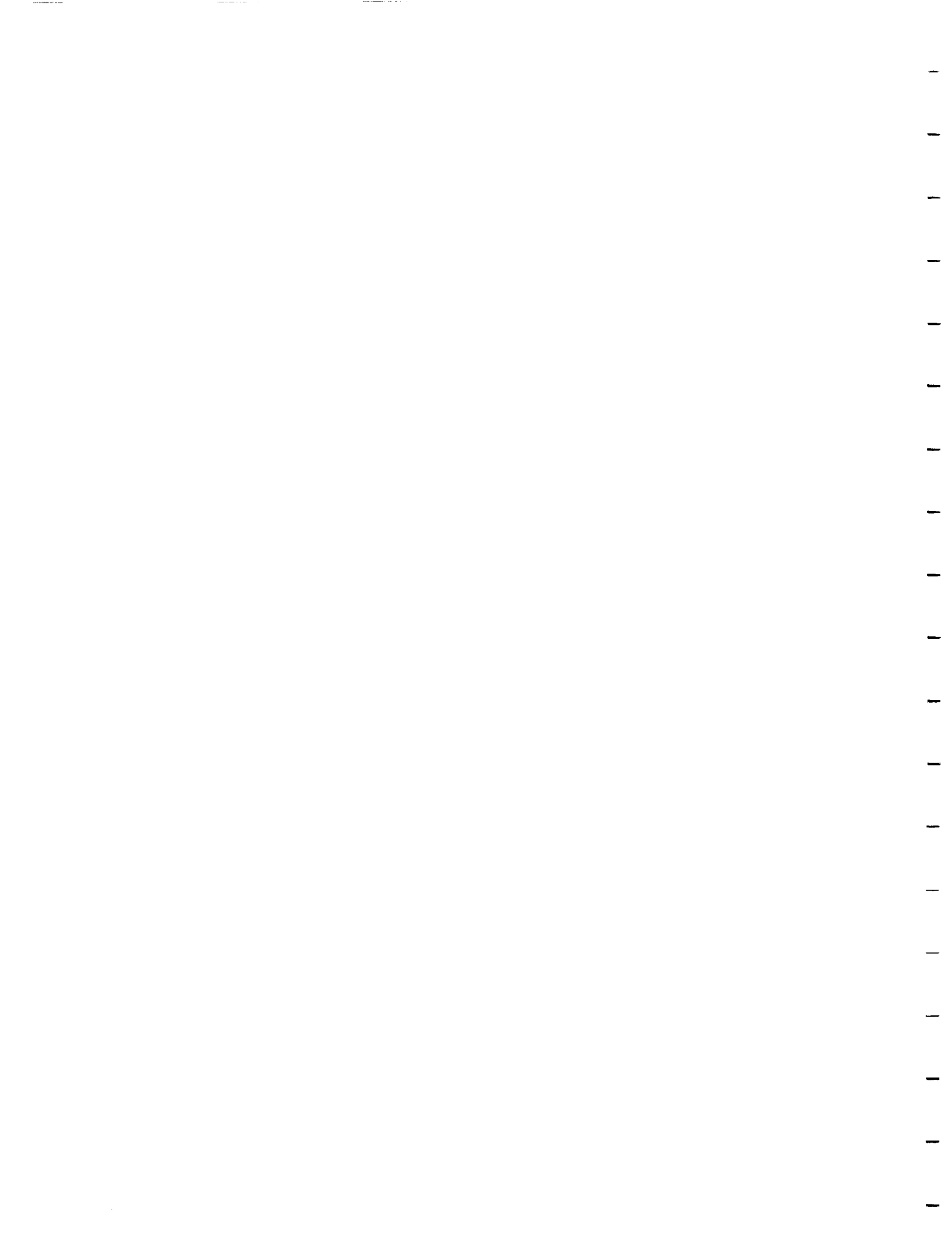
where u_{EL} represents the locally averaged internal energy of the equivalent uncracked body, given by

$$\dot{u}_{EL}^C = - \frac{1}{V_L} \int_{V_L} \dot{u} dV - \frac{1}{V_L} \int_{S_2} T_i^E \dot{u}_i dS \quad (10)$$

where T_i^E are called equivalent tractions, representing tractions in the uncracked pl. acting along fictitious crack faces [20], and u_L^C is the mechanical power output due to cracking, given by

$$\dot{u}_L^C = - \frac{1}{V_L} \int_{S_2} T_i^C \dot{u}_i dS \quad (11)$$

where T_i^C are fictitious tractions applied to the crack faces which represent the difference between the actual crack face tractions and T_i^E . Equations (5)



through (8) are identical in form to pointwise field equations in a continuum [20].

On the basis of this similarity the locally averaged Helmholtz free energy is now defined to be [20]:

$$h_L = u_L - I_L s_L = u_{EL} - I_L s_L + u_L^C = h_{EL} + u_L^C \quad (12)$$

where it can be seen from equation (2) that h_{EL} is the locally averaged undamaged elastic Helmholtz free energy.

The similarity between the pointwise and local field equations leads to the conclusion that [21]

$$\sigma_{Lij}^C = \frac{\partial h_L}{\partial \epsilon_{Lij}} = \frac{\partial h_{EL}}{\partial \epsilon_{Lij}} + \frac{\partial u_L^C}{\partial \epsilon_{Lij}} \quad (13)$$

Using equations (1) and (11), along with Cauchy's boundary conditions gives

$$\dot{u}_L^C = - \sigma_{Lij}^C \dot{u}_{Lij}^M \quad (14)$$

where σ_{Lij}^C are locally averaged equivalent crack face stresses [20]. Thus, the thermodynamic significance of definition (1) is established.

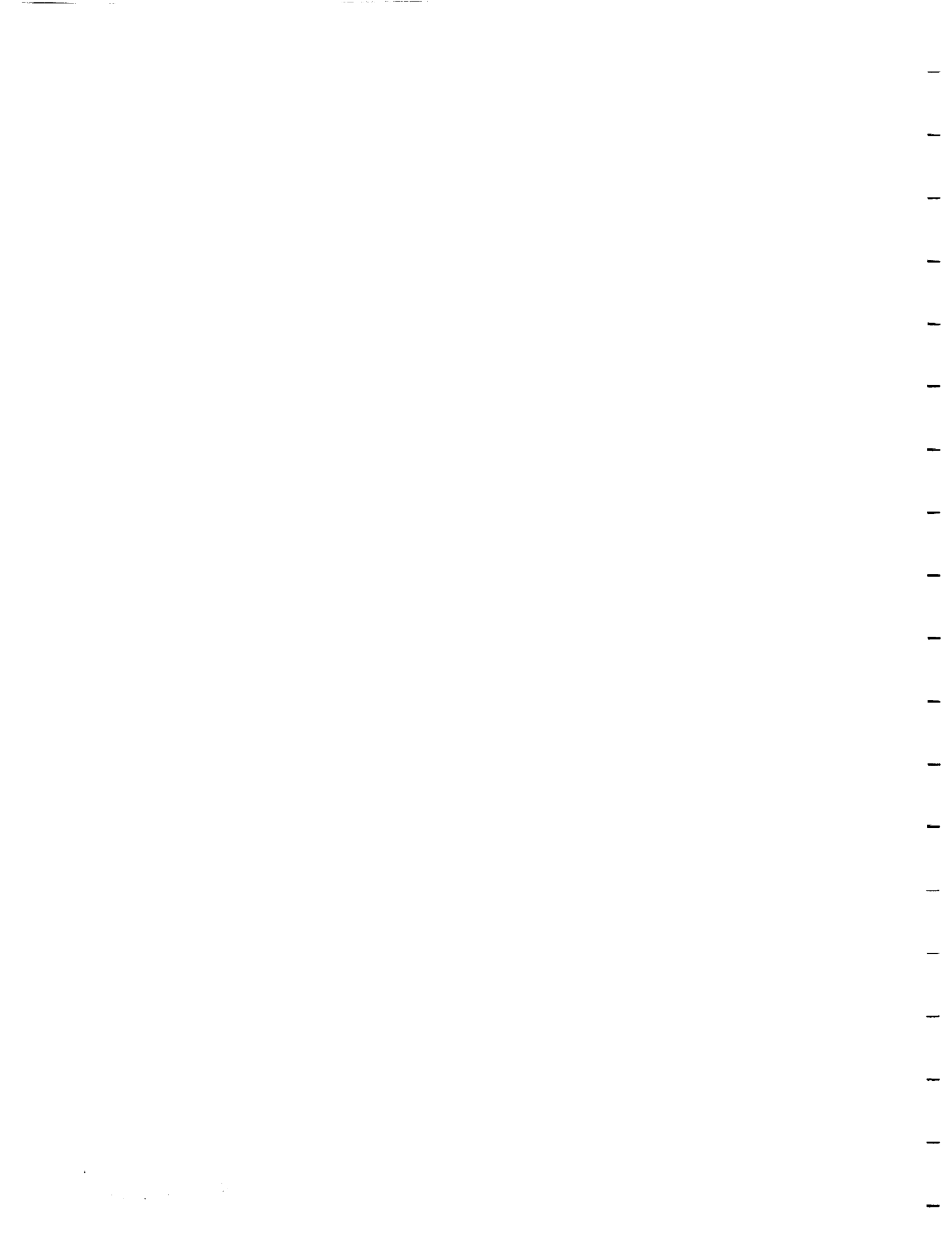
Now consider equation (14) in further detail. The kinetic quantities σ_{Lij}^C may be interpreted as generalized stresses which are energy conjugates to the kinematic strain-like internal state variables u_{Lij}^M . It can be inferred from this that there exists a constitutive relation between these variables of the form

$$\sigma_{Lij}^C = \sigma_{Lij}^C(\epsilon_{Lk}, T_L, u_{Lk}^M) \quad (15)$$

which depends on loading history via the explicit inclusion of the internal state variables.

Therefore, substituting (15) into (14) will give

$$u_L^C(t_1) - \int_{t_0}^{t_1} \dot{u}_L^C(t) dt = u_L^C(\epsilon_{Lk}(t_1), T_L(t_1), u_{Lk}^M(t_1)) \quad (16)$$



Thus, expanding equation (16) in a Taylor series, substituting (2) and (16) into equation (13) and neglecting higher order terms yields [20]:

$$\sigma_{Lij} = E_{Lij} \epsilon_{Lij} + C'_{Lijk} \epsilon_{Lk} + l_{ijk}^M \alpha_{k}^M \quad (17)$$

Restricting the damage to small quantities constitutes a sufficient but not a necessary condition for dropping the higher order terms. Equations (17) may be written in the following incremental form for isothermal conditions

$$d\sigma_{Lij} = C'_{Lijk} d\epsilon_{Lk} \quad (18)$$

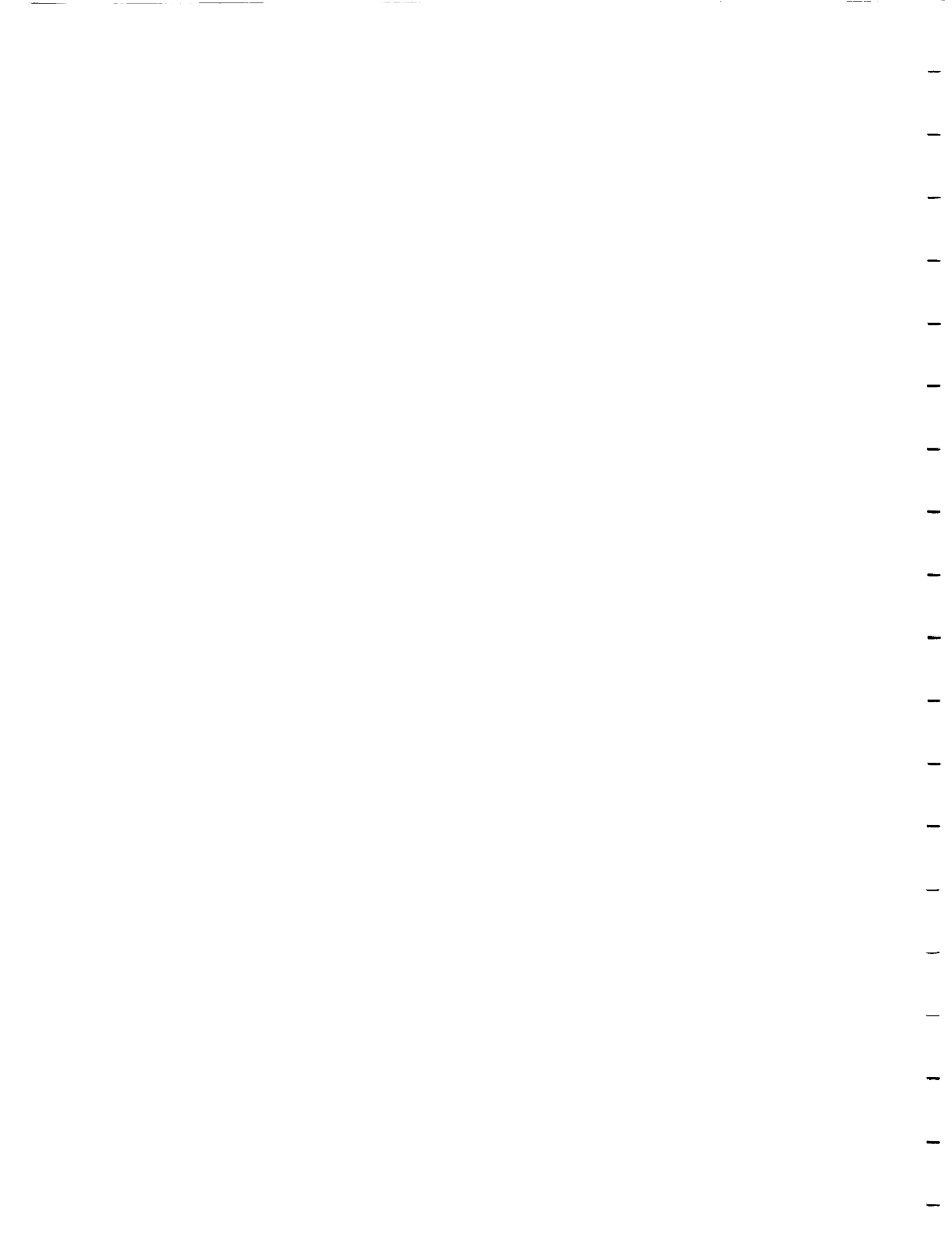
where

$$C'_{Lijk} = \frac{\partial \sigma_{Lij}}{\partial \epsilon_{Lk}} \quad (19)$$

Thus, it can be seen that the constitutive equations can be represented equivalently by both equations (17) and (18). In the first case, the internal state is represented by a strain-like variable, α_{ij} , whereas in the second case the effect of damage is incorporated within the stiffness tensor, C'_{ijk} , which is implicitly damage dependent. A careful inspection of equations (17) and (18) will show that C'_{ijk} can be determined as a function of the damage internal variables α_{ij} by differentiating (17) with respect to the stress tensor. Thus, it is found that C'_{ijk} is a function of $\partial \alpha_{ij} / \partial \epsilon_{Lij}$, which is a fourth order tensor. Obviously, either α_{ij} or $\partial \alpha_{ij} / \partial \epsilon_{Lij}$ could be termed the damage variable. In this work, the author prefers to call α_{ij} the damage internal variable, and $\partial \alpha_{ij} / \partial \epsilon_{Lij}$ the measure of the damage state. This is due to the fact that in brittle systems, it can be seen from equations (1) that when the damage surface area is constant, α_{ij} changes linearly with strain, so that $\partial \alpha_{ij} / \partial \epsilon_{Lij}$ is constant. Thus, the latter is a better measure of the damage state.

Equation (17) and the associated internal energy have previously been shown to be exact for both a linear elastic isotropic cracked body [22] and a linear elastic orthotropic cracked body [23] when the cracks are evenly spaced. For the case where all matrix cracks are normal to the laminate plane

ORIGINAL PAGE IS
OF POOR QUALITY



the above reduces to the following form [24]:

$$\begin{Bmatrix} \sigma_{Lx} \\ \sigma_{Ly} \\ \sigma_{Lz} \\ \sigma_{Lxz} \\ \sigma_{Lyz} \\ \sigma_{Lxy} \end{Bmatrix} = \begin{bmatrix} Q_{11} & Q_{12} & Q_{13} & Q_{14} & Q_{15} & Q_{16} \\ Q_{12} & Q_{22} & Q_{23} & Q_{24} & Q_{25} & Q_{26} \\ Q_{13} & Q_{23} & Q_{33} & Q_{34} & Q_{35} & Q_{36} \\ Q_{14} & Q_{24} & Q_{34} & Q_{44} & Q_{45} & Q_{46} \\ Q_{15} & Q_{25} & Q_{35} & Q_{45} & Q_{55} & Q_{56} \\ Q_{16} & Q_{26} & Q_{36} & Q_{46} & Q_{56} & Q_{66} \end{bmatrix} \begin{Bmatrix} \epsilon_{Lx} - \frac{M}{u_{xx}} \\ \epsilon_{Ly} - \frac{M}{u_{yy}} \\ \epsilon_{Lz} - \frac{M}{u_{zz}} \\ \gamma_{Lyz} - 0 \\ \gamma_{Lxz} - 0 \\ \gamma_{Lxy} - \frac{M}{u_{xy}} \end{Bmatrix} \quad (20)$$

where Q_{ij} are components of the elastic (undamaged) modulus tensor in ply coordinates. When the matrix cracks are not normal to the midplane, a more complex procedure is required [25]. Fortunately, this circumstance appears to arise only when several adjacent plies are stacked at the same orientation [25].

Damage Dependent Lamination Theory

Unlike the ply level model for matrix cracking, statistical homogeneity cannot be assumed for delaminations. Although the delaminations appear to be evenly distributed in the plane of the laminate, the same cannot be said for the through-thickness direction. The damage is therefore accounted for via area averaging in the laminate plane, accompanied by a kinematic assumption through the thickness. Accordingly, the laminate equations are constructed by assuming that the Kirchhoff-Love hypothesis may be modified to include the effects of jump displacements u_i^D , v_i^D , and w_i^D , as well as jump rotations θ_i^D and ψ_i^D for the i th delaminated ply interface, as shown in Fig. 6. Mathematically, then [26]

$$u(x,y,z) = u^0(x,y) - z [\psi^0 + H(z-z_i) \psi_i^D] + H(z-z_i) u_i^D \quad (21)$$

$$v(x,y,z) = v^0(x,y) - z [\psi^0 + H(z-z_i) \psi_i^D] + H(z-z_i) v_i^D \quad (22)$$

and



$$w(x,y,z) = w^0(x,y) + H(z-z_i) w_i^D \quad (23)$$

where the superscripts "0" imply undamaged midsurface quantities, and $H(z-z_i)$ is the heavyside step function. Also, a repeated index i in a product is intended to imply summation, and the superscripts D imply displacement components across the delamination.

The displacement equations are averaged over the local area, A_L , shown in Fig. 4, in order to produce locally averaged displacements to be utilized in the laminate formulation. Thus,

$$u_L(x,y,z) = \frac{1}{A_L} \int_{A_L} [u^0 + z(\epsilon^0 + H(z-z_i)(\epsilon_i^D)) + H(z-z_i) u_i^D] dx dy \quad (24)$$

$$v_L(x,y,z) = \frac{1}{A_L} \int_{A_L} [v^0 + z(\epsilon^0 + H(z-z_i)(\epsilon_i^D)) + H(z-z_i) v_i^D] dx dy \quad (25)$$

and

$$w_L(x,y,z) = \frac{1}{A_L} \int_{A_L} [w^0 + H(z-z_i) w_i^D] dx dy \quad (26)$$

By averaging the displacements, the delamination jump discontinuities are also averaged over A_L .

The laminate strains are given by

$$\epsilon_{L_x} = \frac{\partial u_L}{\partial x} \quad (27)$$

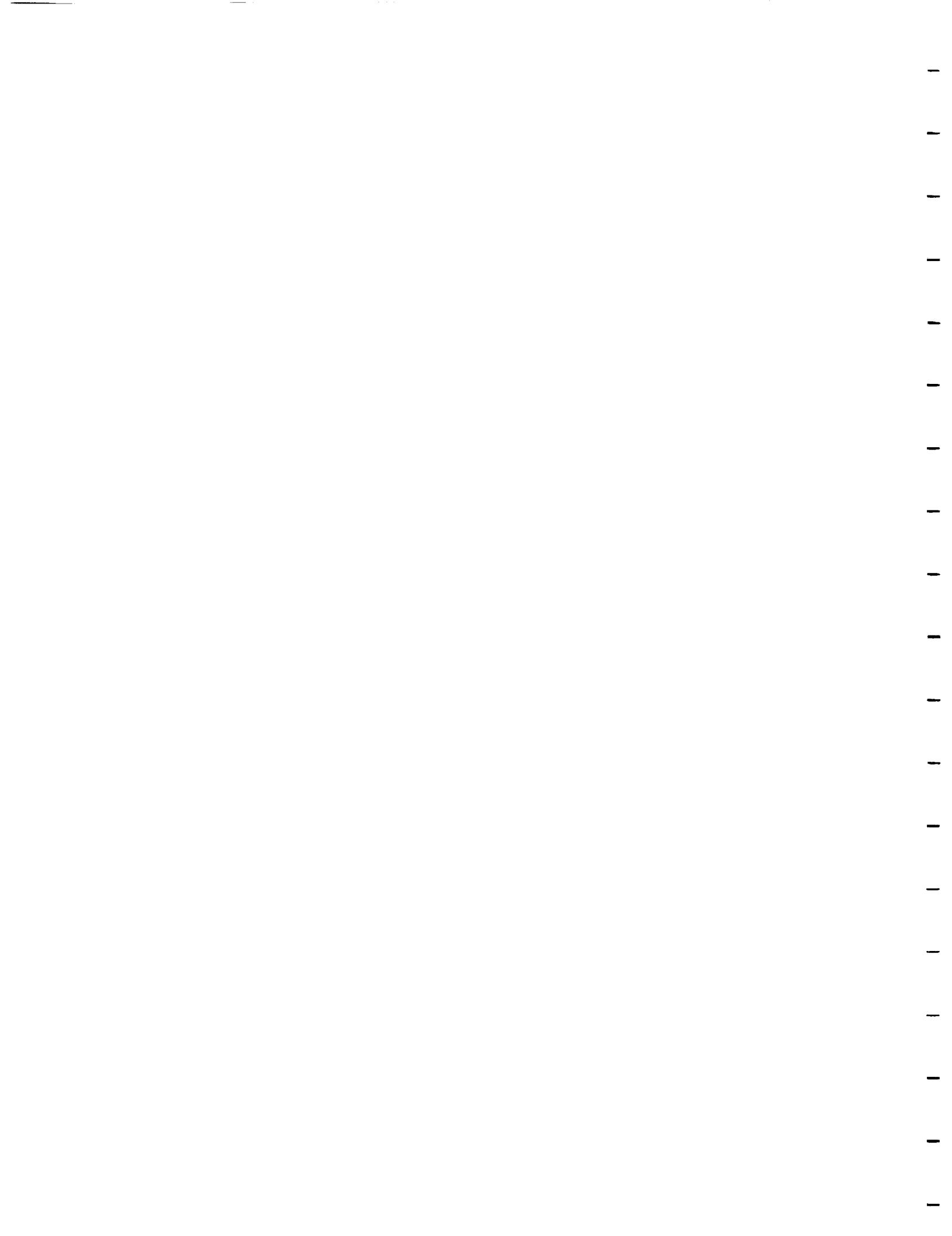
$$\epsilon_{L_y} = \frac{\partial v_L}{\partial y} \quad (28)$$

$$\epsilon_{L_z} = \frac{\partial w_L}{\partial z} \quad (29)$$

$$\gamma_{L_{yz}} = \frac{\partial v_L}{\partial z} + \frac{\partial w_L}{\partial y} \quad (30)$$

$$\gamma_{L_{xz}} = \frac{\partial u_L}{\partial z} + \frac{\partial w_L}{\partial x} \quad (31)$$

ORIGINAL PAGE IS
OF POOR QUALITY



$$\gamma_{L_{xy}} = \frac{\partial u_L}{\partial y} + \frac{\partial v_L}{\partial x} \quad (32)$$

The laminate constitution is obtained by integrating the stress in each lamina over the laminate thickness. The resultant midplane forces and moments per unit width of region Δx in the laminate are thus given by

$$\begin{matrix} N_x \\ N_y \\ N_{xy} \end{matrix} = \int_{-t/2}^{t/2} \begin{Bmatrix} \sigma_{L_x} \\ \sigma_{L_y} \\ \sigma_{L_{xy}} \end{Bmatrix} dz \quad (33)$$

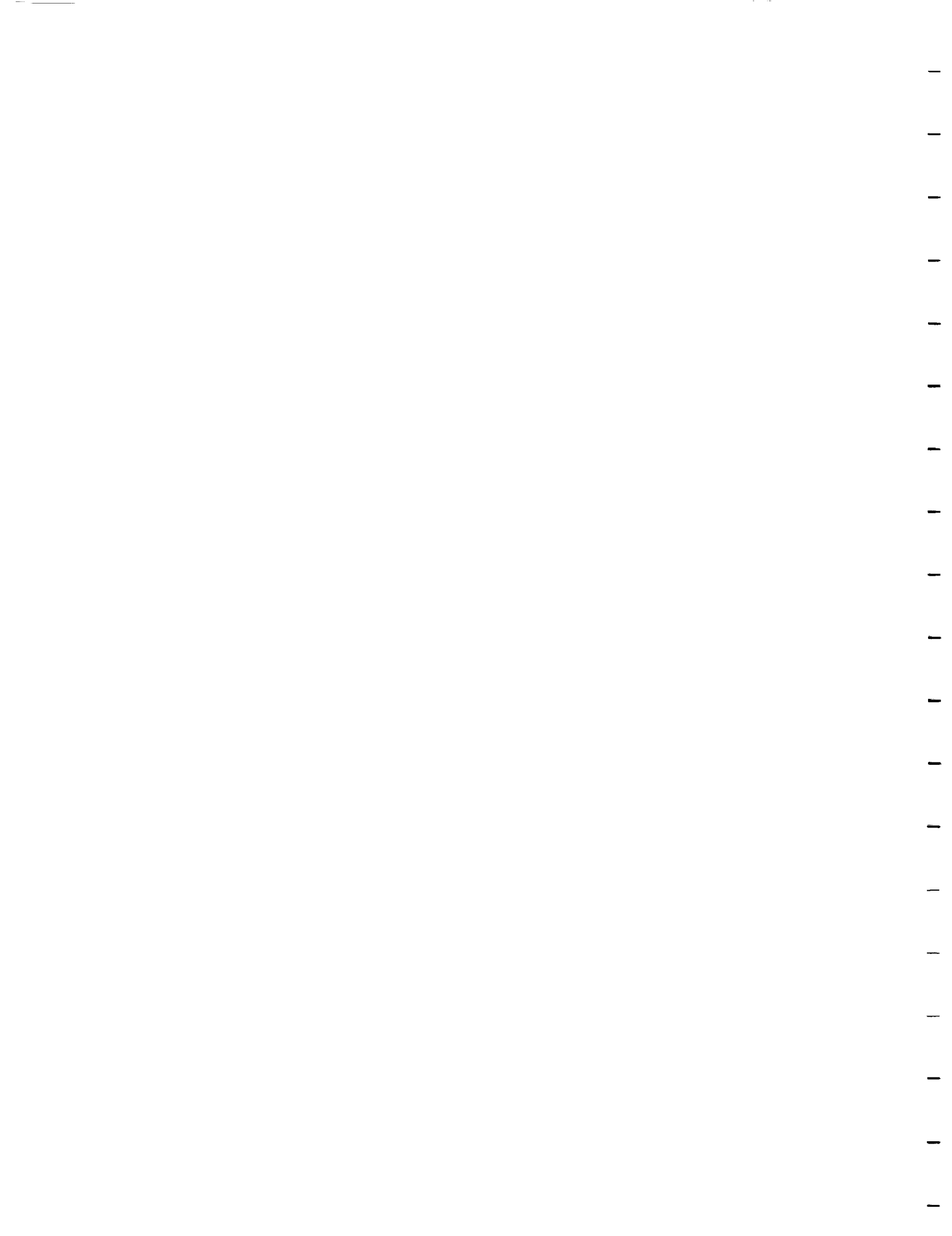
and

$$\begin{matrix} M_x \\ M_y \\ M_{xy} \end{matrix} = \int_{-t/2}^{t/2} \begin{Bmatrix} \sigma_{L_x} \\ \sigma_{L_y} \\ \sigma_{L_{xy}} \end{Bmatrix} z \, dz \quad (34)$$

where t is the laminate thickness.

The resultant laminate equations may be obtained by substituting equations (24) through (26) into equations (27) through (32), and this result into equations (20). This result is then substituted into equations (33) and (34), and the divergence theorem is employed to obtain the following laminate equations [26]:

$$\{N\} = \sum_{k=1}^n [Q]_k (z_k - z_{k-1}) \{\epsilon_L^0\} - \frac{1}{2} \sum_{k=1}^n [Q]_k (z_k^2 - z_{k-1}^2) \{\kappa_L\}$$



$$\begin{aligned}
& + \sum_{i=1}^d |\bar{Q}_1|_i t_i \begin{Bmatrix} 0 \\ 0 \\ 0 \\ u_{1i} \\ 0 \\ u_{2i} \\ 0 \\ u_{3i} \\ 0 \end{Bmatrix} + \sum_{i=1}^{d+1} (z_i - z_{i-1}) |\bar{Q}_2|_i \begin{Bmatrix} 0 \\ 0 \\ 0 \\ 0 \\ u_{4i} \\ 0 \\ u_{5i} \\ 0 \end{Bmatrix} \\
& + \sum_{k=1}^n |Q|_k (z_k - z_{k-1}) \{u^M\}_k \quad (35)
\end{aligned}$$

$$\begin{aligned}
\{M\} &= \frac{1}{2} \sum_{k=1}^n |Q|_k (z_k^2 - z_{k-1}^2) \{u^D\} + \frac{1}{3} \sum_{k=1}^n |Q|_k (z_k^3 - z_{k-1}^3) \{u^L\} \\
& + \sum_{i=1}^d |\bar{Q}_3|_i t_i^2 \begin{Bmatrix} 0 \\ 0 \\ 0 \\ u_{1i} \\ 0 \\ u_{2i} \\ 0 \\ u_{3i} \\ 0 \end{Bmatrix} + \sum_{i=1}^{d+1} |\bar{Q}_4|_i (z_i^2 - z_{i-1}^2) \begin{Bmatrix} 0 \\ 0 \\ 0 \\ 0 \\ u_{4i} \\ 0 \\ u_{5i} \\ 0 \end{Bmatrix} \\
& + \frac{1}{2} \sum_{k=1}^n |Q|_k (z_k^2 - z_{k-1}^2) \{u^M\}_k \quad (36)
\end{aligned}$$

where $\{N\}$ and $\{M\}$ are the resultant forces and moments per unit length, respectively, and $\{u^M\}_k$ and $\{u^D\}_i$ represent the damage due to matrix cracking and interply delamination, respectively. Furthermore, n is the number of plies, and d is the number of delaminated ply interfaces, as shown in Fig. 6.

The internal state variable for delamination, $\{u^D\}_i$, is obtained by employing the divergence theorem on a local volume element of the laminate.



The resulting procedure gives [26]

$$a_{1i}^D = \frac{2}{V_{1i}} \int_{S_{2i}} w_i^D n_z dS \quad (37a)$$

$$a_{2i}^D = \frac{2}{V_{1i}} \int_{S_{2i}} v_i^D n_z dS \quad (37b)$$

$$a_{3i}^D = \frac{2}{V_{1i}} \int_{S_{2i}} u_i^D n_z dS \quad (37c)$$

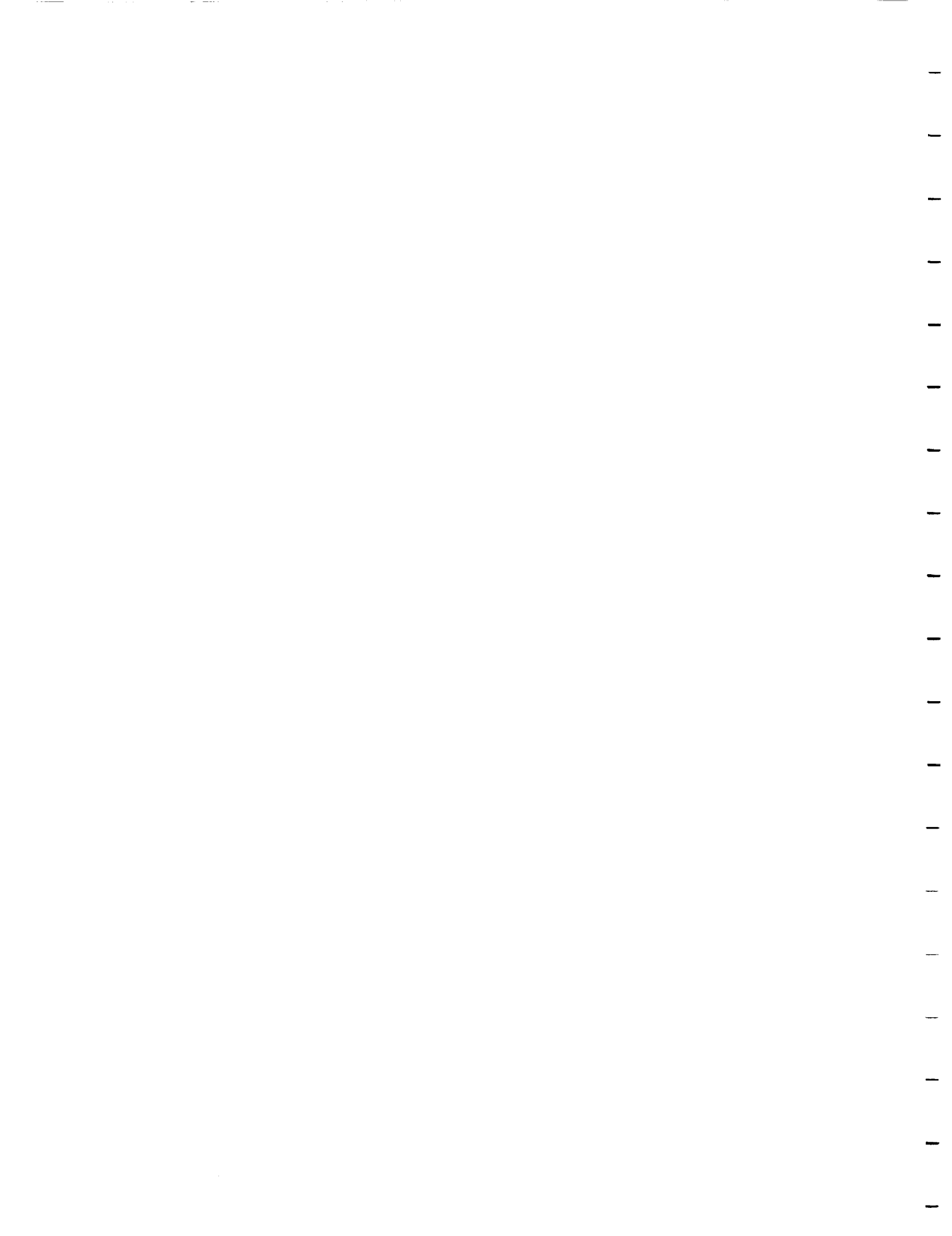
$$a_{4i}^D = \frac{1}{A_i} \int_{S_{2i}^B} \psi_i^D n_z dS \quad (37d)$$

$$a_{5i}^D = \frac{1}{A_i} \int_{S_{2i}^B} \varphi_i^D n_z dS \quad (37e)$$

where the subscript i is associated with the i th delaminated ply interface. Furthermore, V_{1i} is equivalent to $t_i A_L$, where t_i is the thickness of the two plies above and below the delamination, as shown in Fig. 9. By definition, the z component of the unit normal, n_z , is equivalent to unity. The matrices $[Q]$ with subscripts k are the standard elastic property matrices for the undamaged plies. The matrices $[\bar{Q}]$ with subscripts i apply to the i th delaminated ply interface. They represent average properties of the plies above and below the delamination. For example,

$$\bar{Q}_{15} = \frac{N_{xz}}{e_{1xz}} = \frac{\bar{Q}_{11}^T \bar{Q}_{1z}^b}{\bar{Q}_{11}^T - \bar{Q}_{11}^b} \quad (38)$$

$$\bar{Q}_{14} = \frac{N_{yz}}{e_{1yz}} = \frac{\bar{Q}_{12}^T \bar{Q}_{1z}^b}{\bar{Q}_{12}^T - \bar{Q}_{12}^b} \quad (39)$$



$$\bar{Q}_{25} = \frac{N_y}{\epsilon_{x2}} = \frac{\bar{Q}_{21}^T \bar{Q}_{21}^B}{\bar{Q}_{21}^T - \bar{Q}_{21}^B} \quad (40)$$

and

$$\bar{Q}_{24} = \frac{N_x}{\epsilon_{y1}} = \frac{\bar{Q}_{22}^T \bar{Q}_{22}^B}{\bar{Q}_{22}^T - \bar{Q}_{22}^B} \quad (41)$$

where the superscripts A and B designate the properties of the ply immediately above and below the delamination, respectively. These are described in further detail in reference [26].

Determination of Damage Dependent Stiffness

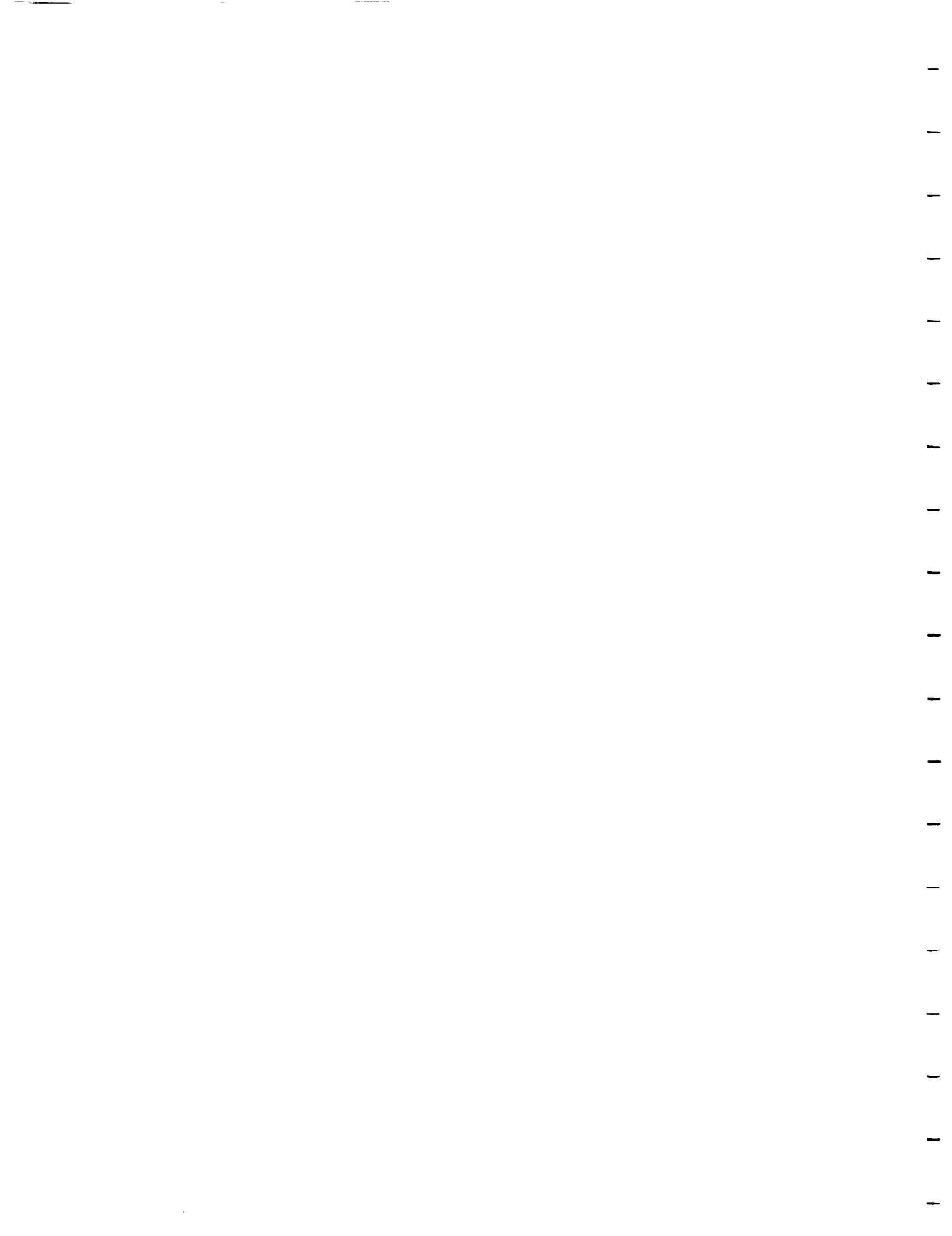
A measure of the accuracy of laminate equations (35) and (36) can be obtained by comparing predictions of damage dependent stiffness to experimental results. In order to do this, it is necessary to construct the (stacking sequence independent) material parameters developed in the previous section. The loading direction engineering modulus, E_x , and Poisson's ratio, ν_{xy} , of the laminate are defined by [27]

$$E_x = \frac{1}{t} \frac{\partial N_x}{\partial \epsilon_x} \quad (42)$$

$$\nu_{xy} = \frac{\frac{1}{t} \frac{\partial N_x}{\partial \epsilon_y}}{\frac{1}{t} \frac{\partial N_y}{\partial \epsilon_y}} \quad (43)$$

where t is the laminate thickness.

For the purpose of comparing the model predictions to experimental results, this development is confined to the case of a symmetric, balanced laminate with delamination sites symmetrically located with respect to the laminate midplane. For this special case, the following expressions for E_x



and ν_{xy} may be obtained [27]

$$E_x = \frac{1}{n} \sum_{k=1}^n (Q_{11})_k \left(1 - \frac{\partial u_x^M}{\partial \epsilon_x}\right)_k + 2\left(\frac{2}{n}\right) (\bar{Q}_{14} \frac{\partial u_2^D}{\partial \epsilon_x} + \bar{Q}_{15} \frac{\partial u_3^D}{\partial \epsilon_x}) \quad (44)$$

$$\nu_{xy} = \frac{\frac{1}{n} \sum_{k=1}^n (Q_{12})_k \left(1 - \frac{\partial u_x^M}{\partial \epsilon_y}\right)_k + 2\left(\frac{2}{n}\right) (\bar{Q}_{14} \frac{\partial u_2^D}{\partial \epsilon_y} + \bar{Q}_{15} \frac{\partial u_3^D}{\partial \epsilon_y})}{\frac{1}{n} \sum_{k=1}^n (Q_{22})_k \left(1 - \frac{\partial u_y^M}{\partial \epsilon_y}\right)_k + 2\left(\frac{2}{n}\right) (\bar{Q}_{24} \frac{\partial u_2^D}{\partial \epsilon_y} + \bar{Q}_{25} \frac{\partial u_3^D}{\partial \epsilon_y})} \quad (45)$$

where it is assumed that all plies have the same thickness so that

$$z_k - z_{k-1} = t_{ply} \quad (46)$$

$$\frac{t_{ply}}{t} = \frac{1}{n} \quad (47)$$

$$\frac{t_1}{t} = \frac{2}{n} \quad (48)$$

Implementation of equations (44) and (45) to predict the damage degraded laminate moduli requires the specification of the partial derivatives of the internal state variables with respect to strain for a given damage state. In the absence of ISV evolution laws, the damage state must be determined experimentally. Expressions for the internal state variables have been previously developed [28] by employing energy principles.

For example, in the case of matrix cracking in cross-ply laminates where only the opening mode of fracture is involved the following expression has been developed

$$\frac{\partial u_x^M}{\partial \epsilon_x} = \frac{1}{2} m \frac{(p+q)}{q} - \frac{E_{x0}}{E_{22}} \left(\frac{E_{x1}}{E_{x0}} \right)_{S_{M1}} - 1 \quad (49)$$



where m is the number of consecutive 90° plies, p is the number of 0° plies, q is the number of 90° plies, E_{x0} is the initial undamaged modulus, and E_{x1} is the damage degraded modulus corresponding to matrix crack damage state S_{M1} . The term in the parentheses has been determined experimentally from tests on a $[0/90/0]_S$ graphite/epoxy laminate and is given by [27]

$$\frac{E_{x1}}{E_{x0}} = 0.99969 - 0.061607 S + 0.04623 S^2 \quad (50)$$

Other components are as determined in reference [27].

While the damage-dependent laminate analysis model may be used to predict any of the effective engineering moduli for a laminate, experimental results are only available for the axial modulus and Poisson's ratio. Therefore, the general utility of the model is demonstrated by comparing model predictions to experimental results for E_x and ν_{xy} for the fully developed damage states illustrated in Figs. 10-14. The delamination interface location has been determined experimentally and the delamination area has been estimated from the x-ray radiographs using an optical planimeter procedure. In both the model analysis and data reduction, it is assumed that the delamination sites are symmetrically located about the laminate midplane and contain the same delamination surface area.

Model predictions have been made for a typical graphite/epoxy system with properties shown in Table 1. The bar chart shown in Fig. 15 compares the model predictions to the experimental values for the engineering modulus, E_x , for combined matrix cracking and delamination. The delamination interface location and percent of delamination area are listed in the figure underneath the laminate stacking sequence. As can be seen, the comparison between model results and the experimental results is quite good. Some limited results for Poisson's ratio are given in Fig. 16 using the same bar chart format. With the exception of the $[0/90_2]_S$ laminate, these results are also quite good. Note that these results have been obtained for a single set of input data which do not depend on stacking sequence. On the basis of these results it is concluded that the theory proposed in equations (35) and (36) is a candidate

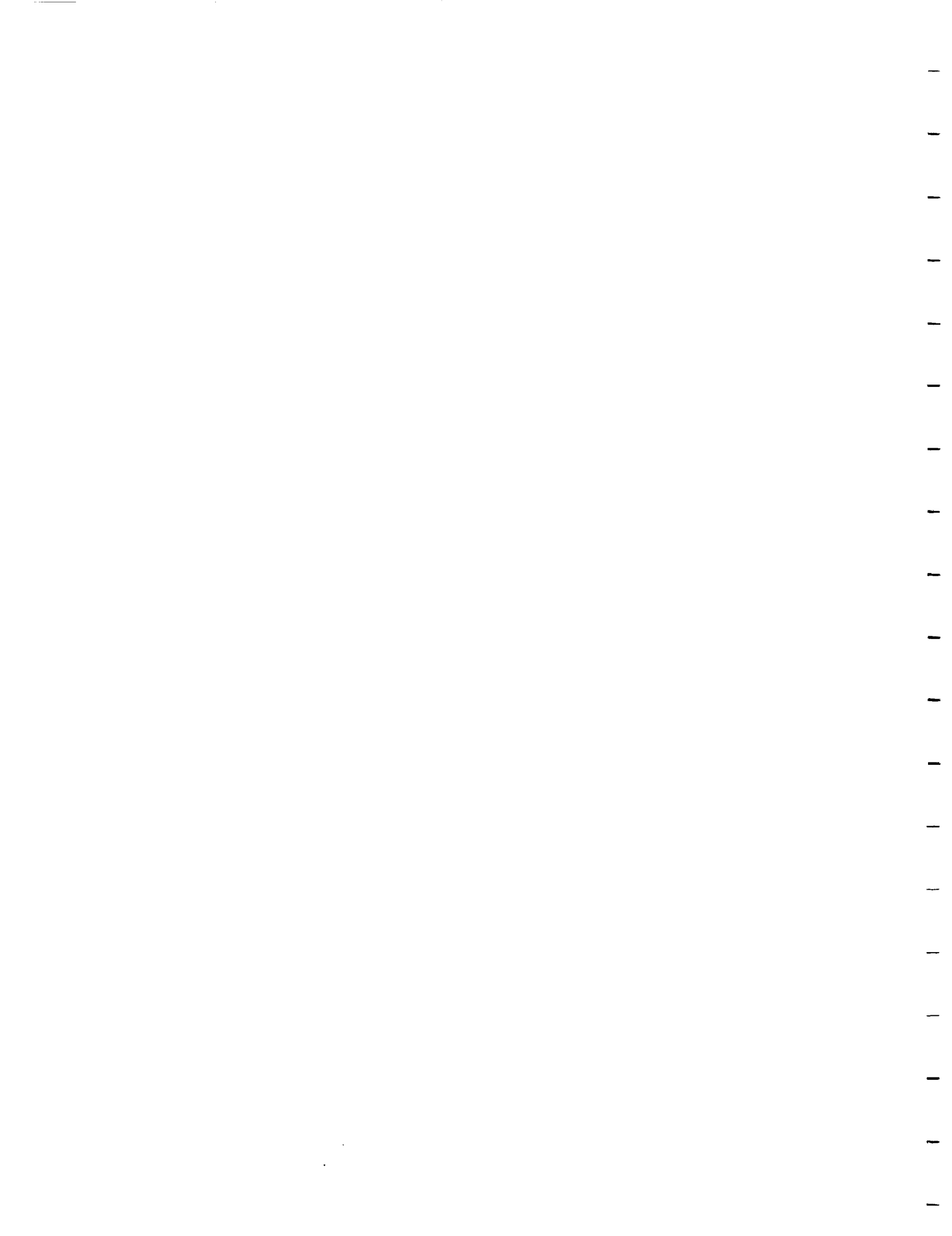


Table 1. AS4/3502 Graphite/Epoxy Lamina Properties

E_{11} 21.0×10^6 psi (144.8 GPa)

E_{22} 1.39×10^6 psi (9.58 GPa)

ν_{12} 0.312

G_{12} 0.694×10^6 psi (4.79 GPa)

ORIGINAL PAGE IS
OF POOR QUALITY

for damaged laminates.

Evaluation of Ply Stresses

In order to evaluate the stress state in each ply, it is first necessary to substitute displacement equations (24) through (26) into the locally averaged strain definitions (27) through (32). Utilizing the divergence theorem on this result will then give the following equations for the strains in each ply.

$$\epsilon_{L_x} = \epsilon_{L_x}^0 - z [\kappa_{L_x} + H(z-z_i) a_{5i}^D] + H(z-z_i) a_{3i}^D \quad (51)$$

$$\epsilon_{L_y} = \epsilon_{L_y}^0 - z [\kappa_{L_y} + H(z-z_i) a_{4i}^D] + H(z-z_i) a_{2i}^D \quad (52)$$

$$\epsilon_{L_z} = \epsilon_{L_z}^0 + H(z-z_i) a_{1i}^D \quad (53)$$

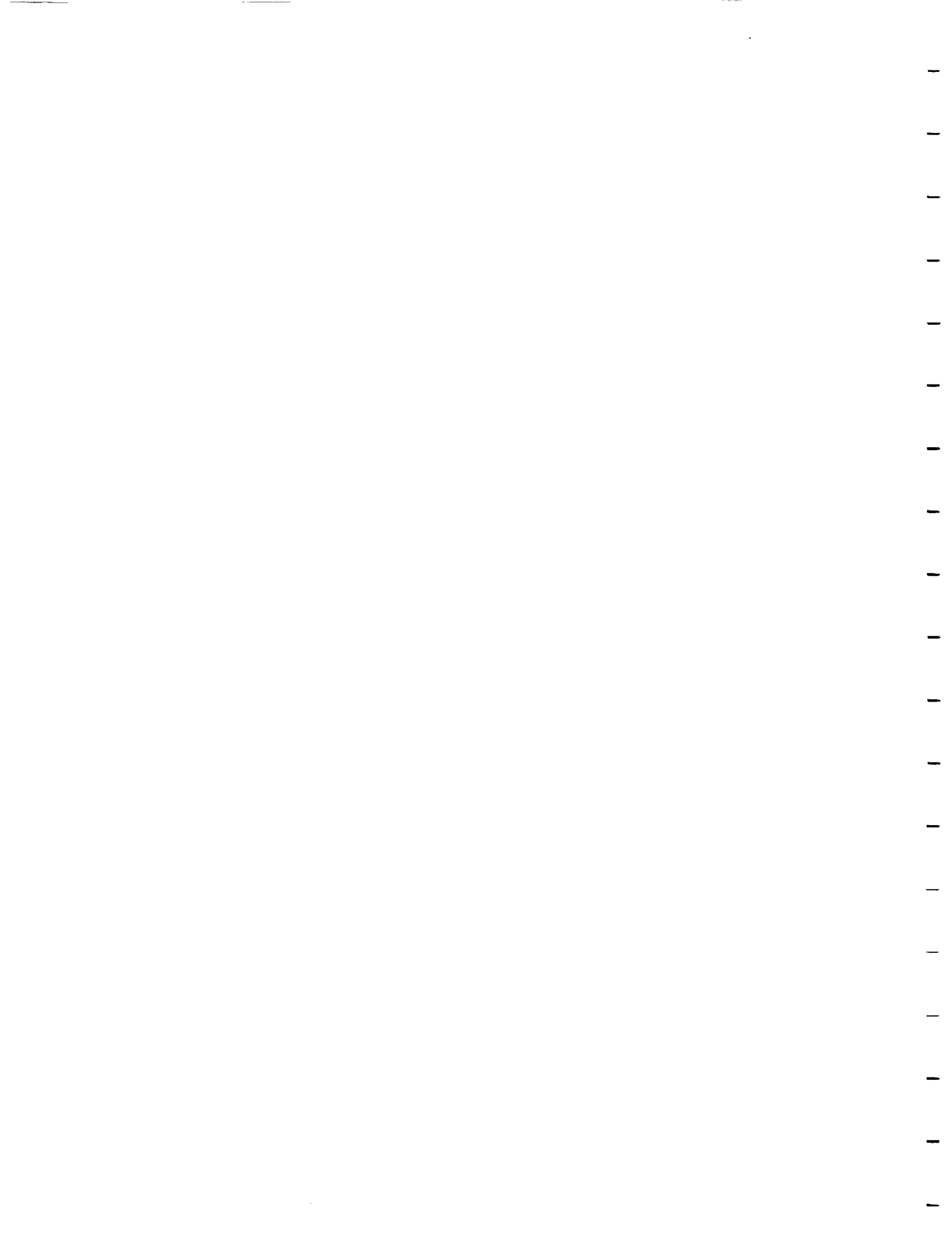
$$\epsilon_{L_{yz}} = \epsilon_{L_{yz}}^0 - [\kappa_{L_{yz}} + H(z-z_i) a_{4i}^D] \quad (54)$$

$$\epsilon_{L_{xz}} = \epsilon_{L_{xz}}^0 - [\kappa_{L_{xz}} + H(z-z_i) a_{5i}^D] \quad (55)$$

$$\epsilon_{L_{xy}} = \epsilon_{L_{xy}}^0 - \epsilon_{L_{xy}} \quad (56)$$

The above equations may be utilized to obtain the ply strains, and these results may be substituted into equation (20) to obtain the stresses in each ply [29]. Since the ply stresses determined by this procedure represent locally averaged values, they must be considered to be far-field stresses, so that stress intensity factors would be needed in order to determine matrix crack-tip stresses. This point will be discussed further in the section on damage evolution laws.

A computer code has been constructed to determine the effect of damage on the "far-field" ply stresses in composite laminates [29]. Results presented are for a given laminate strain $\epsilon_{x0} = .01$ (all other strains assumed to be zero). Damage variables were calculated for matrix cracks in a saturated damage state using equations (38) and (39) assuming $u_0^M = 0.0001"$. The off-axis and 90° plies use the matrix crack damage terms of u_8^M and u_2^M , respectively. No damage is assumed in the 0° plies. Since the laminate is



subjected only to ϵ_{x0} , a_3^D is assumed to be the only delamination damage component. This term is calculated for an equivalent delamination area by the use of equation (40) with $u_0^D = .00001$ ".

The results obtained from the model are shown in Table 2 and Figures 17-22. As evidenced by the results, the damage significantly affects the far-field ply stresses. Damage variables were calculated by using equations (38) through (40) to simulate damage existing in several previously tested laminates. Matrix cracks caused substantial stress reductions in ply stresses in the 90° plies in cross-ply laminates. For example, in the 90° plies of the $[0_2/90_2]_S$ laminate the matrix cracks resulted in a thirty-four percent far-field ply stress reduction. The two quasi-isotropic laminates developed different damage resulting in dissimilar far-field ply stresses. The $[90/\pm 45/0]_S$ laminate exhibited little matrix cracking, thus producing only a small reduction in ply stress in both the 90° and $\pm 45^\circ$ plies. The $[0/\pm 45/90]_S$ laminate exhibited a similar stress reduction in the $\pm 45^\circ$ plies, but showed a substantial stress reduction (fifteen percent verses one percent) in the 90° plies when compared to the $[90/\pm 45/0]_S$ laminate. This alteration in ply stresses should significantly affect the growth of new damage in the composite.

Damage Evolution Laws

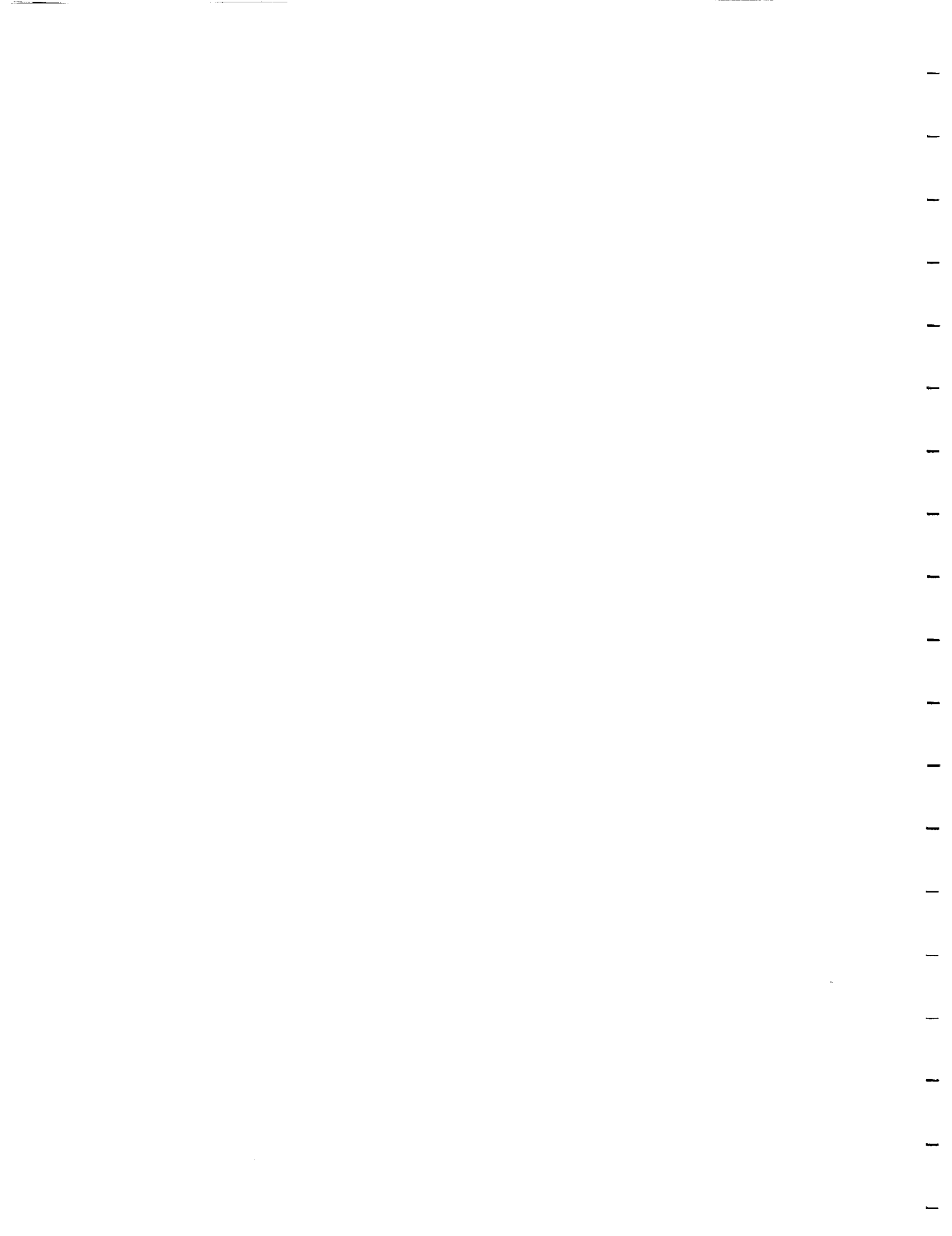
It is hypothesized that the evolution of damage in each ply is driven by the current stress state at the crack tips within that ply [20]. This stress state depends upon the strains, temperature, and internal variables within that ply. In addition, since these are locally averaged values, they must be regarded as far-field quantities, and the stress intensity factors should be included in order to account for the crack tip stresses. Thus, the internal state variable evolution laws should more properly be written in the following form:

$$\dot{a}_{ij}^M = \dot{a}_{ij}^M(\epsilon_{Lk}, T, a_{kk}^M, a_{kk}^D, K_I, K_{II}, K_{III}) \quad (57)$$

and

$$\dot{a}_{ij}^D = \dot{a}_{ij}^D(\epsilon_{Lk}, T, a_{kk}^M, a_{kk}^D, K_I, K_{II}, K_{III}) \quad (58)$$

ORIGINAL PAGE IS
OF POOR QUALITY



where K_I , K_{II} , and K_{III} are the stress intensity factors, which relate the far-field stresses to the crack tip stresses for a given crack geometry. However, it is assumed that the geometry of both matrix cracking and delaminations is sufficiently independent of stacking sequence that the stress intensity factors may be treated as "material properties" and thus possess the same stress intensity factor dependence for all stacking sequences. Thus, they are encompassed implicitly in the material constants required to characterize damage evolution laws (57) and (58).

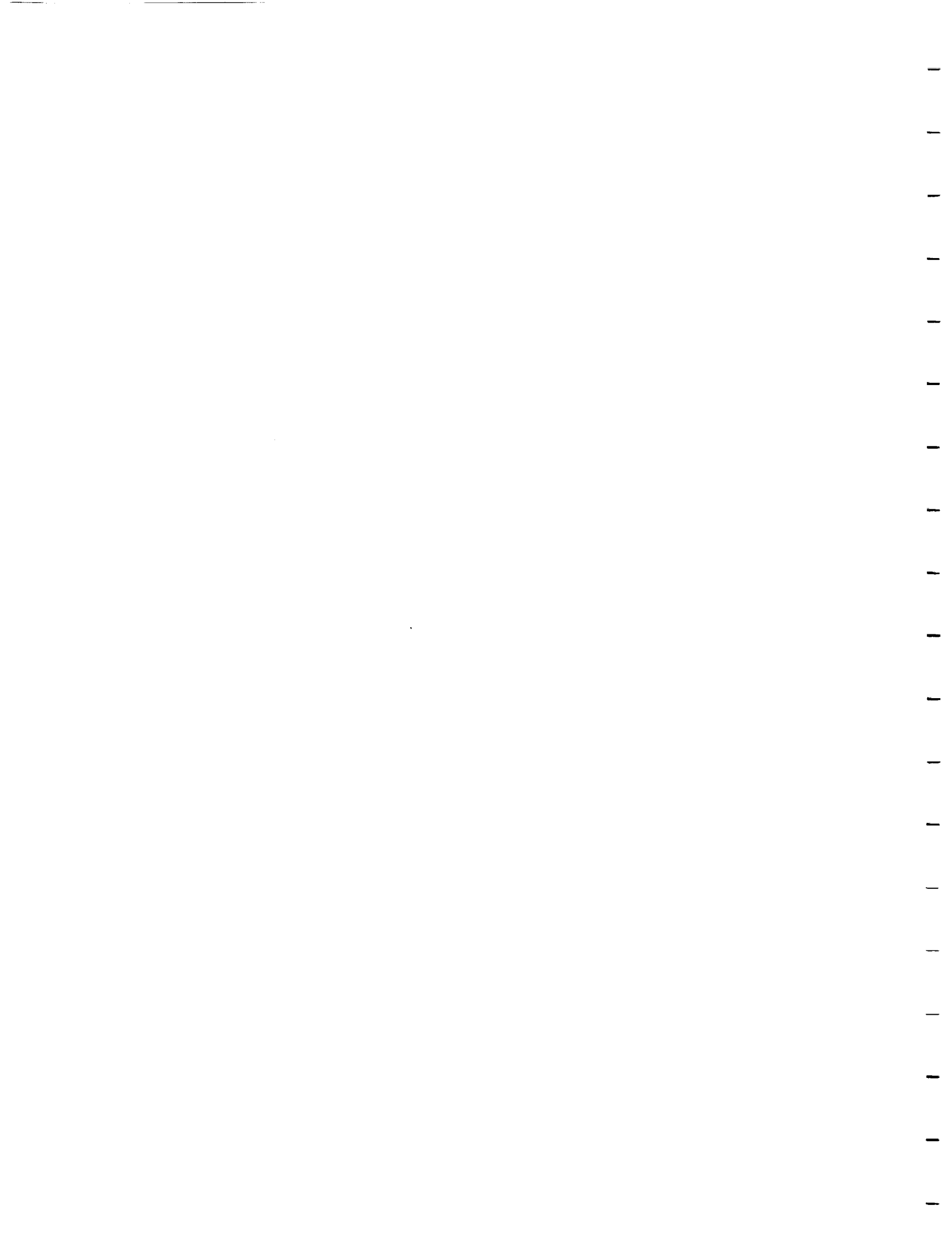
One approach to the formulation of the internal state variable evolutionary relationships is through micromechanical considerations. However, this approach is dependent on the availability of micromechanical solutions that can model the essential physical characteristics of the damage state. For the problem of matrix cracks embedded in an orthotropic medium that is layered between two other orthotropic media, the solutions that are currently available are applicable only to very specific loading conditions and damage geometries. Therefore, the evolutionary equation proposed herein is phenomenological in nature. The form of the damage evolutionary relationship employed in this paper is based on the observation made by Wang, et al. [30] that for some materials the rate of damage surface evolution per load step, $\frac{dS}{dN}$, follows a power law as shown below, in which the strain energy release rate, G , and a material parameter, n , serve as the basis and exponent, respectively. Thus,

$$\frac{dS}{dN} = PG^n \quad (59)$$

where P is a material constant. To develop internal state variable evolutionary equations in the form of equation (59), a_{ij}^M must be related to the surface area of damage. Since a_{ij}^M , as defined by equation (1), represents the kinematics of the crack faces, the damage surface area alone will not be sufficient to describe the crack face displacements. Assuming that each crack in the material volume shares a common geometry and orientation, then the specification of the far field strains will complete this description. The rate of change of the internal state variable can therefore be expressed as follows [31]:

$$\frac{da_{ij}^M}{dN} = \frac{da_{ij}^M}{dS} \frac{dS}{dN} \quad (60)$$

ORIGINAL PAGE IS
OF POOR QUALITY



where the far field strains are reflected in the term da_{ij}^M/dS which relates the changes in the internal state variable during the development of damage surfaces. Thus, using equations (59) and (60), the stable evolution of the internal state variable is given by

$$da_{ij}^M = \frac{da_{ij}^M}{dS} k_1 G^{1/n} dN \quad (61)$$

The term da_{ij}^M/dS reflects the changes in the internal state variable with respect to changes to the damage surfaces. da_{ij}^M/dS can be obtained analytically from relationships describing the kinematics of the crack surfaces for given damage states and loading conditions, should such solutions exist. For transverse matrix cracks in crossply laminates, the average crack face displacement in the pure opening mode can be approximated by a solution obtained by Lee, et al. [23] for a medium containing an infinite number of alternating 0° and 90° plies. Thus, da_{ij}^M/dS can be determined for crossply laminates subjected to uniaxial loading conditions. It has been found that for typical continuous fiber reinforced graphite/epoxy systems da_{ij}^M/dS can be assumed to be constant for a given applied load until the damage state has reached an advanced stage of development. This assumption has facilitated the determination of the material parameters k_1 and n . The damage state at any point in the loading history can now be determined by the integration of equation (61) using the laminate averaged ply responses. This integration is performed numerically because of the nonlinearity of the damage evolutionary equation. The fourth order Runge-Kutta method has been found to be suitable for this application.

The development of the matrix crack damage state in crossply laminates subjected to uniaxial fatigue loading is examined using the proposed damage evolution equation. To maintain the thermodynamic admissibility of the fatigue loading process, it is assumed that the values of the internal state variables remain constant during the unloading portion of the load cycle. It is further assumed that the required thermodynamic force is very small compared to the available thermodynamic force, thus a_{22}^M will change at the onset of load application. The material properties for AS4/3501-6 graphite/epoxy are used in the calculations to enable the comparison of model prediction to experimental measurements made by Chou, et al. [32]. The

material parameters for this polymeric composite system have been found to be

$$k_1 = 4.42 \quad \text{and} \quad n = 6.39 \quad (62)$$

The damage histories for two crossply layups have been predicted using the model. The model predictions for the damage state in the $[0_2/90_3]_s$ laminates fatigue loaded at maximum stress amplitudes of 38 ksi and 43 ksi are shown in Figs. 23 and 24, respectively. The lower stress amplitude is equivalent to eighty percent of the monotonic crack initiation stress, while the higher stress amplitude is equal to ninety percent of the initiation stress. The experimentally measured damage states were originally measured in terms of the crack density. However, the corresponding σ_{22}^M for each damage level can be approximated by the relationship proposed by Lee, et al. [23].

Good agreement is found between the model predictions and the experimental results. The damage evolution for the thicker $[0_2/90_3]_s$ laminate is shown in Fig. 25. This laminate was loaded at a maximum stress amplitude of 26 ksi. This amplitude corresponds to eighty percent of the quasi-static matrix crack initiation stress. The results for this load case indicated good agreement with the experimental data. The effect of the load redistribution on the damage evolution is apparent in this load case. A marked decrease in the rate of damage evolution after fifty thousand load cycles was indicated by the model. On the other hand, the experimental data showed this decrease to occur after only ten thousand load cycles. Since the evolution of delaminations was not included in the analysis, the predicted decrease in the rate of damage evolution is attributed only to the matrix crack induced transfer of load from the 90° plies to the adjacent 0° plies and the resulting decrease in the available thermodynamic force. The measured values of the damage state, however, may have been influenced by the formation of delaminations along the free edges and in the interior. Such occurrences can drastically affect the stress distribution among the plies and the available thermodynamic force for damage evolution.

To examine the amount of stress redistribution that occurs during the damage accumulation, the model was used to determine the axial stress in the 90° plies of the $[0_2/90_3]_s$ laminate fatigue loaded at three different stress amplitudes. Fig. 26 shows that for the stress amplitude of 38 ksi, the axial

stress in the 90° plies after forty thousand cycles was less than fifty percent of the original stress level in the undamaged laminate. Therefore, the rate of damage evolution is expected to be relatively low during the latter stages of the loading history. This is observed in Fig. 27, which shows the corresponding values of the internal state variable, α_{22}^M , for the three load cases. The 26 ksi stress amplitude load case, on the other hand, produced only gradual changes in the axial stress and damage state as compared to the other two stress amplitudes. The percentage decrease from the original undamage stress level increased with the fatigue stress amplitude. These results demonstrate that the stress redistribution characteristics among the plies in the laminate are dependent on the loading conditions. These redistribution characteristics will affect the manner in which damage develops in the surrounding plies as well as eventual failure of the laminate.

An Algorithm for Structural Analysis

In order to model the response of a structural component with spatially variable stresses, it is necessary to incorporate the damage dependent lamination theory into a structural analysis algorithm. This will be accomplished via the finite element method. To do this, first recall the equilibrium equations for a plate [33]:

$$\frac{\partial N}{\partial x} + \frac{\partial N_{xy}}{\partial y} = p_x \quad (63)$$

$$\frac{\partial N_{xy}}{\partial x} + \frac{\partial N_y}{\partial y} = p_y \quad (64)$$

$$\frac{\partial^2 M_x}{\partial x^2} + \frac{\partial^2 M_{xy}}{\partial x \partial y} + \frac{\partial^2 M_y}{\partial y^2} = -p_z \quad (65)$$

It is now advantageous to express equations (35) and (36) in the following matrix form:



$$\{R\} = \{A\} \{u_L^0\} + \{B\} \{u_L\} + \{f^M\} + \{f^D\} \quad (66)$$

$$\{M\} = \{B\} \{u_L^0\} + \{D\} \{u_L\} + \{g^M\} + \{g^D\} \quad (67)$$

where [34]

$$\{A\} = \sum_{k=1}^n (z_k - z_{k-1}) \{Q_1\}_k \quad (68)$$

$$\{B\} = \frac{1}{2} \sum_{k=1}^n (z_k^2 - z_{k-1}^2) \{Q_1\}_k \quad (69)$$

$$\{D\} = \frac{1}{3} \sum_{k=1}^n (z_k^3 - z_{k-1}^3) \{Q_1\}_k \quad (70)$$

$$\{f^M\} = - \sum_{k=1}^n (z_k - z_{k-1}) \{Q_2\}_k \{a^M\}_k \quad (71)$$

$$\{g^M\} = - \frac{1}{2} \sum_{k=1}^n (z_k^2 - z_{k-1}^2) \{Q_2\}_k \{a^M\}_k \quad (72)$$

$$\{f^D\} = \sum_{i=1}^d t_i \{\bar{Q}_1\}_i \{a_1^D\}_i + \sum_{i=1}^{d+1} (z_i - z_{i-1}) \{\bar{Q}_2\}_i \{a_2^D\}_i \quad (73)$$

$$\{g^D\} = \sum_{i=1}^d t_i^2 \{\bar{Q}_3\}_i \{a_1^D\}_i + \sum_{i=1}^{d+1} (z_i^2 - z_{i-1}^2) \{\bar{Q}_4\}_i \{a_2^D\}_i \quad (74)$$

Substituting equation (66) into equations (63) and (64) results in the in-plane equilibrium equations [34]. Similarly, substituting equation (67) into equation (65) results in the following governing differential equation for the out-of-plane deformations:

$$\begin{aligned}
& D_{11} \frac{\partial^4 w_L^0}{\partial x^4} + 4D_{16} \frac{\partial^4 w_L^0}{\partial x^3 \partial y} + 2(D_{12} + 2D_{66}) \frac{\partial^4 w_L^0}{\partial x^2 \partial y^2} \\
& + 4D_{26} \frac{\partial^4 w_L^0}{\partial x \partial y^3} + D_{22} \frac{\partial^4 w_L^0}{\partial y^4} - \frac{\partial^2}{\partial x^2} (g_1^M + g_1^D) \\
& - \frac{\partial^2}{\partial y^2} (g_2^M + g_2^D) + 2 \frac{\partial^2}{\partial x \partial y} (g_3^M + g_3^D) = p_z
\end{aligned} \quad (77)$$

Integrating the governing differential equations, (75), (76), and (77) against a variations in the displacement components and employing Green's Theorem twice results in the weak formulation for the laminated plate equilibrium equations. This form is described in detail in reference 34.

The finite element formulation utilizes five degrees of freedom at each node, k . These consist of two in-plane displacements, u_k^0 and v_k^0 , one out-of-plane displacement, w_k^0 , and two rotational terms, θ_k^x and θ_k^y . The following displacement fields are assumed to represent the components of deformation within an element:

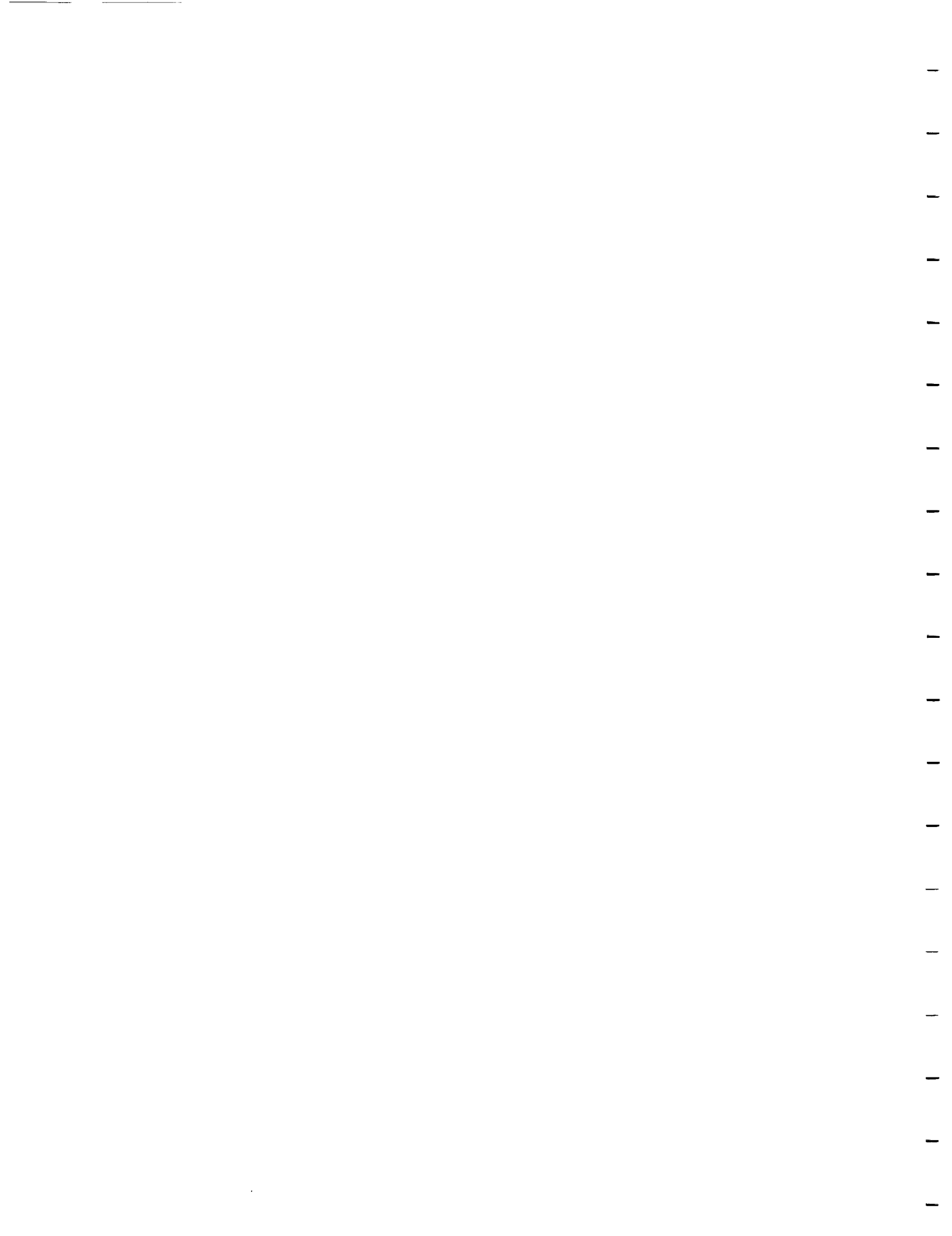
$$u_L^0 = \sum_{j=1}^m \psi_j^e u_j^e \quad (78)$$

$$v_L^0 = \sum_{j=1}^m \psi_j^e v_j^e \quad (79)$$

$$w_L^0 = \sum_{i=1}^p \phi_i^e w_i^e \quad (80)$$

where $(\psi_j = w_j, \theta_j^x, \theta_j^y)$, ψ_j^e and ϕ_i^e represent the shape functions for the element, m is the number of nodes the element contains, and p is three times the number of nodes.

Substitution of equations (78) through (80) into the weak formulation of the plate equilibrium equations results in the following system of algebraic equations for a typical finite element:



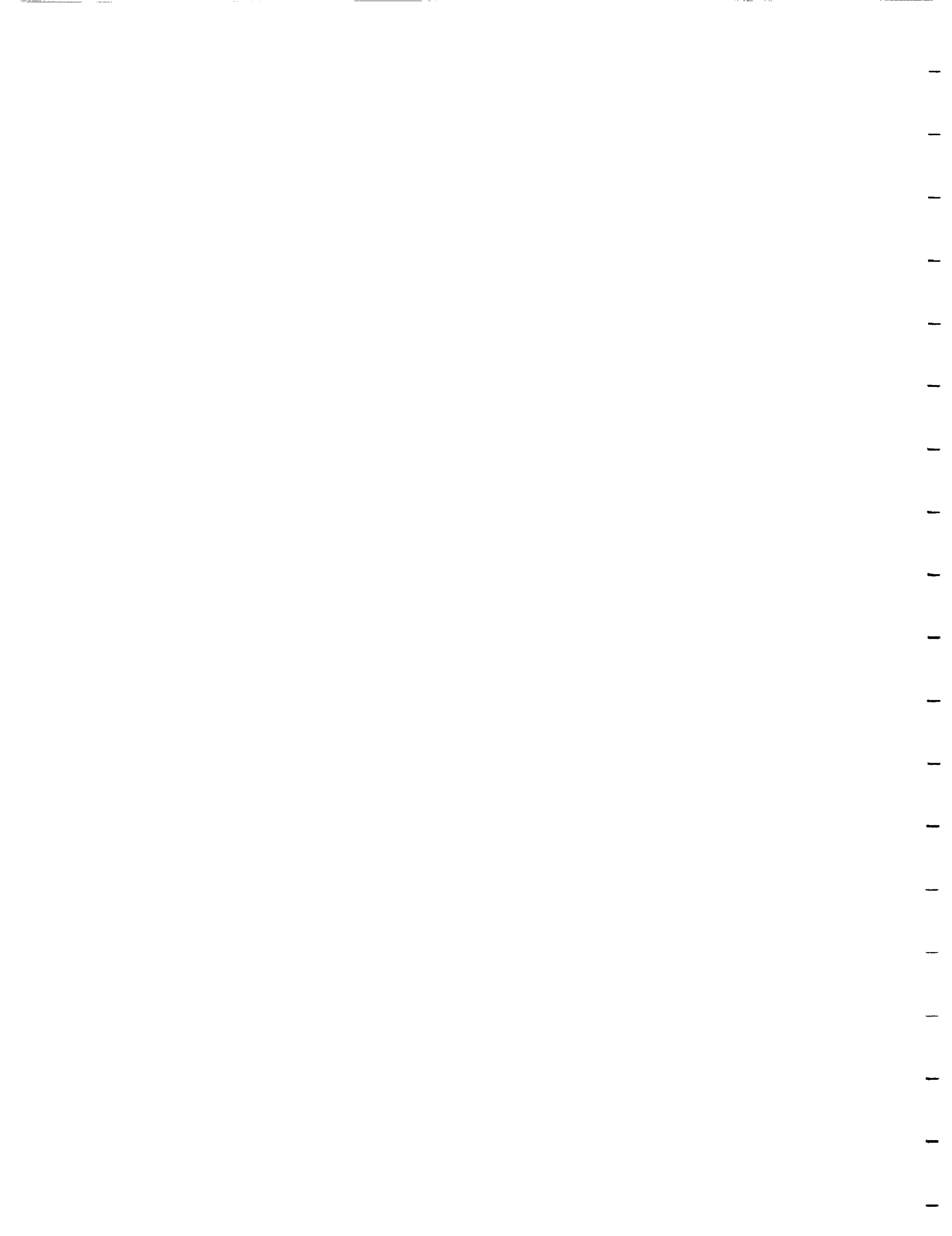
$$\begin{bmatrix} k_{11} & k_{12} & 0 \\ k_{21} & k_{22} & 0 \\ 0 & 0 & k_{33} \end{bmatrix} \begin{Bmatrix} u \\ v \\ z \end{Bmatrix} = \begin{Bmatrix} F_A^1 \\ F_A^2 \\ F_A^3 \end{Bmatrix} + \begin{Bmatrix} F_M^1 \\ F_M^2 \\ F_M^3 \end{Bmatrix} + \begin{Bmatrix} F_D^1 \\ F_D^2 \\ F_D^3 \end{Bmatrix} \quad (81)$$

where the stiffness and force matrices are as described in reference 34.

The system of equations given in (81) can be used in conjunction with any type of element for which the shape functions are known. For the model developed in the present work, a three node triangular element with five degrees of freedom per node is selected [34]. These in turn are assembled by the standard method into a global set of finite element equations.

A finite element code has been developed based on the above formulation. The implementation of the damage evolutionary relationship shown in equation (61) requires that the solution algorithm be repeated for every load cycle. During each cycle, the ply stresses are calculated and used to determine the increment in the matrix crack internal state variable for each ply. The updated damage state is then used in the calculation of the laminate and ply response at the next load cycle.

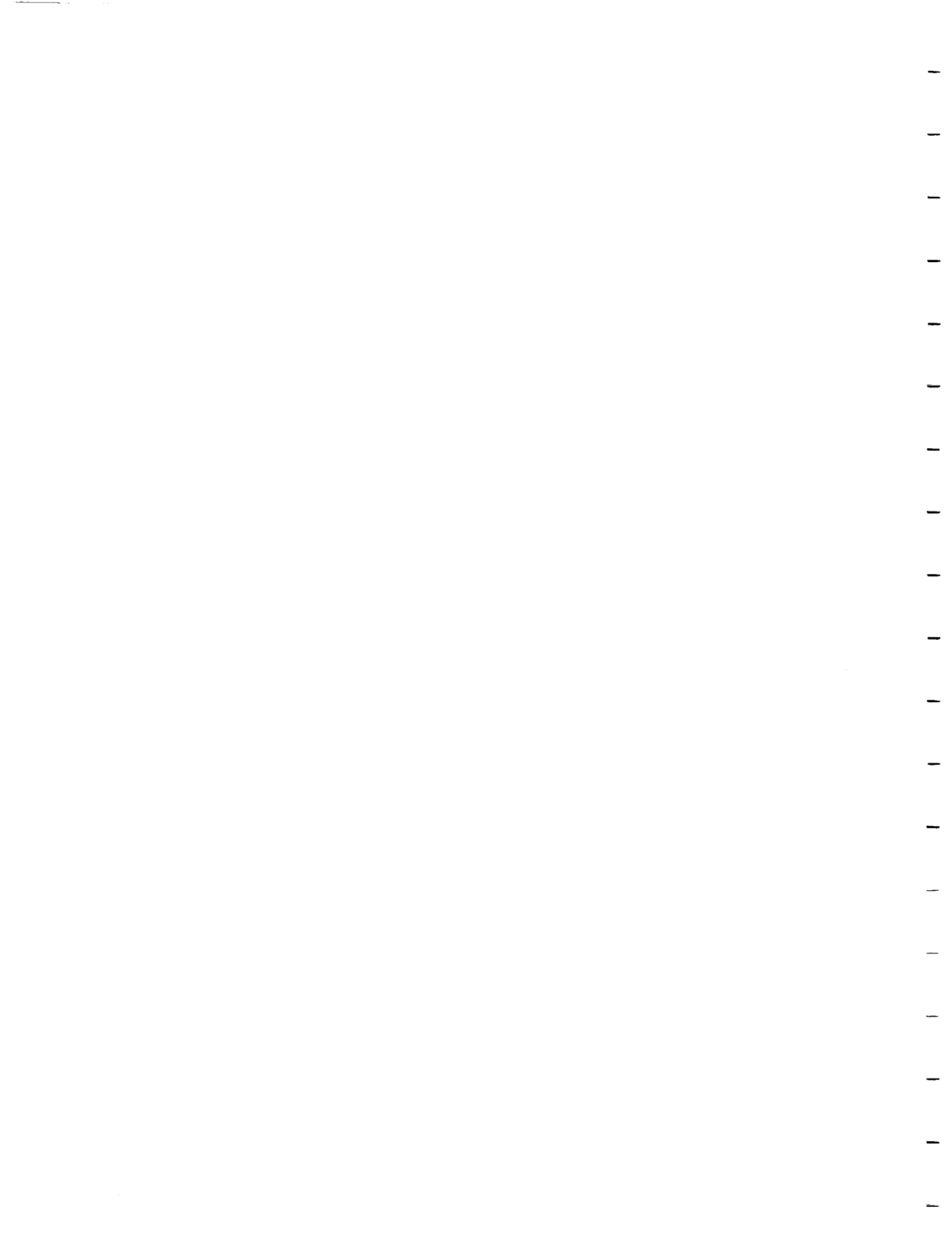
The response of a laminated tapered beam subjected to uniaxial fatigue loading conditions has been examined. This beam has a $[0/90_2]_S$ stacking sequence and possesses the material properties of continuously reinforced AS4/3502 graphite/epoxy. Its length is 17.78 cm and the width is 4.50 cm at the clamped end and tapered to 2.87 cm at the end where the load is applied. The beam is loaded at a distributed load amplitude of 17.5×10^3 N/m and $R = 0.1$. Since the beam is symmetric about its length, it is sufficient to model half of the beam with a mesh containing 28 elements, 24 nodes, and 120 degrees of freedom. The development of matrix cracks during the loading history in the 0° and 90° plies, as represented by the internal state variables, is shown in Figs. 28 and 29, respectively. For clarity, the damage levels in each ply are normalized by the largest value of the internal state variable within that ply at the end of 22495 load cycles. The predicted results indicate that the



matrix cracks first occur in the 90° plies at the narrow end and progress toward the wider end as loading continues. Axial splits in the 0° plies do not develop until after the appearance of the transverse matrix cracks in the 90° plies. Thus, the transverse matrix cracks accumulate and loads carried by the 90° plies are transferred to the 0° plies. Depending on the amplitude of the fatigue load, more than half of the load initially carried by the undamaged 90° plies can be transferred to the 0° plies. The additional loads coupled with the stress concentrations caused by the transverse matrix cracks create suitable conditions for the growth of axial splits. The results also show that the progression of transverse matrix cracks along the length of the tapered beam decelerates near the midway point. The stresses in the region beyond the midway point are most likely to be insufficient in sustaining additional damage. Instead, the intensity of matrix damage increases at the narrow end during the latter portion of the loading history. This process will continue until the matrix cracks have either reached the saturation level or when the laminate fails. The model predictions are qualitatively supported by the experimental result shown in Fig. 30.

Life Prediction:

Usually, ultimate failure of laminated composites is caused by large scale fracture which is induced by fiber fracture at delamination sites. Therefore, there is not only a synergistic effect between matrix cracking and delamination, but also between delamination and the ultimate failure event. Since fiber fracture occurs very near the end of the component life, rather than model it with an additional internal variable, it is preferable to simply treat it as the ultimate failure event and model it with a failure function. Typically, one of two approaches could be taken. A phenomenological approach would entail the use of an existing failure function such as the Isai-Wu [35] and Whitney-Nuismer failure criteria [36] to account for the existing damage state. Since these failure criteria depend on stresses and strains, respectively, in a given ply, they will automatically account for load history dependence, since the model predicts history dependence due to damage evolution. Alternatively, a fracture criterion [37] could also be modified to account for the damage induced stress redistribution. In this case, the energy release rate would have to be



modified to account for the redistribution of stresses. The author is pursuing this subject further at this time.

CONCLUSION

The author has shown that by constructing local averages of the kinematic effects of microcracking it is possible to construct continuous internal variables which appear explicitly in a modified lamination theory for layered composites with damage. Comparisons of predicted stiffness loss as a function of damage state to experimental results lend credence to the model.

Because the lamination theory is damage dependent, it produces predicted stress redistribution as damage develops for a given fatigue load history. This predicted stress redistribution in turn affects the evolution of damage, thus producing a life prediction model which can be used for any stacking sequence regardless of the load history applied to the component. However, while initial model comparisons to experiment are favorable, further research is suggested before the model is utilized in a design setting.



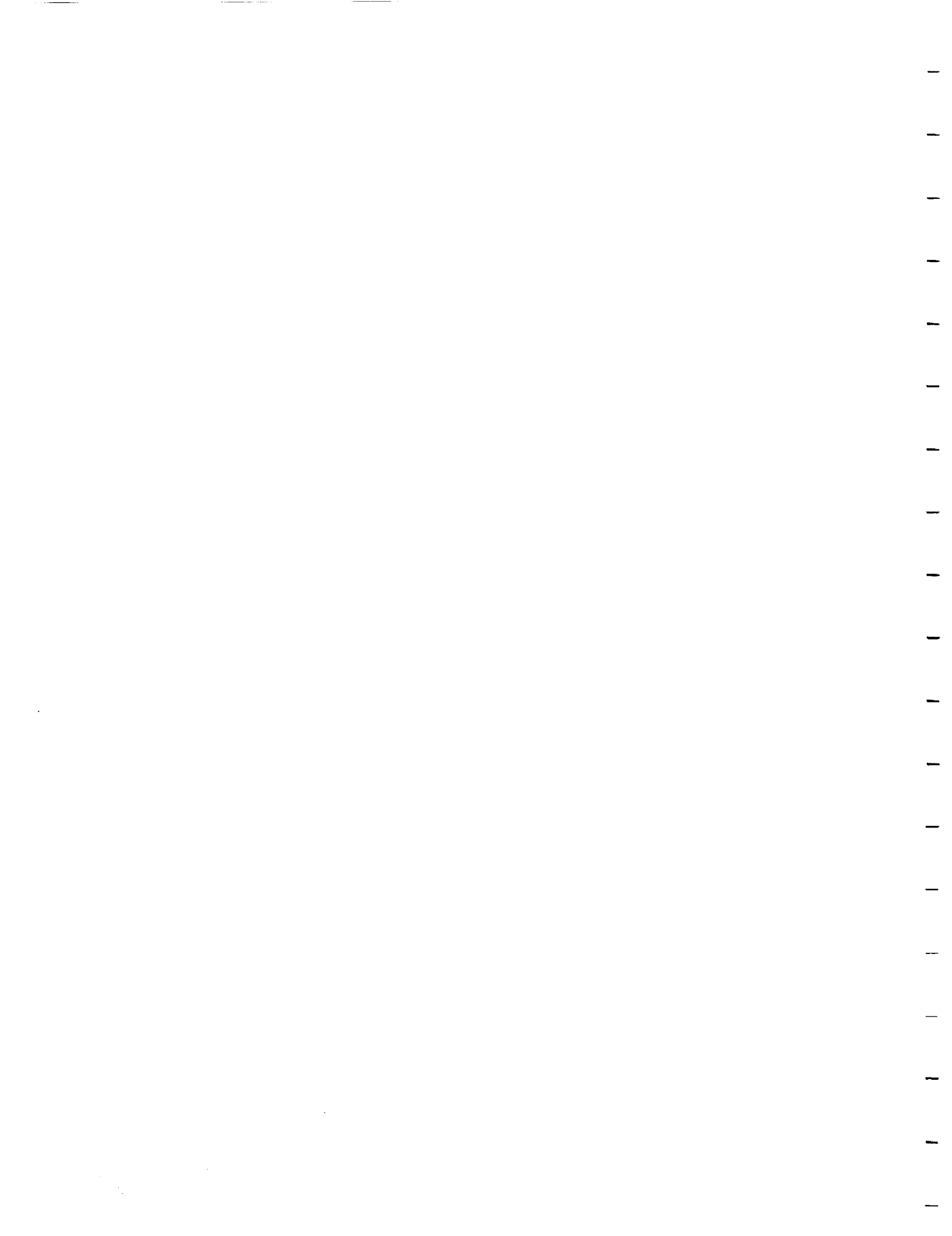
REFERENCES

1. Miner, M.A., "Cumulative Damage in Fatigue," Journal of Applied Mechanics, Vol. 12, p. 159, 1945.
2. Hahn, H.T., "Fatigue Behavior and Life Prediction of Composite Laminates", Composite Materials: Testing and Design (Fifth Conf.), ASTM STP 674, pp. 383-417, 1979.
3. Caruso, J.J. and Chamis, C.C., "Assessment of Simplified Composite Micromechanics Using Three-Dimensional Finite-Element Analysis," J. Composites Technology & Research, Vol. 8, No. 3, pp. 77-83, 1986.
4. Chamis, C.C. and Smith, G.T., "CODSTRAN: Composite Durability and Damage Tolerance: Simplified Predictive Methods," NASA Report TM-100179, NASA, Washington, 1978.
5. Mura, T., "Micromechanics of Defects in Solids," Mechanics of Elastic and Inelastic Solids 3, Martinus Nijhoff Publishers, Netherlands, 1982.
6. Noor, A.K., "Micropolar Beam Models for Lattice Grids with Rigid Joints," Computer Methods in Applied Mechanics and Engineering, Vol. 21, pp. 249-263, 1980.
7. Reifsnider, K.L., "Some Fundamental Aspects of the Fatigue and Fracture Response of Composite Materials," Proceedings 4th Annual Meeting Society Engineering Science, Lehigh University, Bethlehem, Pa., pp. 14-16, 1977.
8. Jamison, R.D., Schulte, K., Reifsnider, K.L., and Stinchcomb, W.W., "Characterization and Analysis of Damage Mechanisms in Tension-Tension Fatigue of Graphite/Epoxy Laminates," Effects of Defects in Composite Materials, ASTM STP 836, American Society for Testing and Materials, pp. 21-55, 1984.
9. Stinchcomb, W.W., and Reifsnider, K.L., "Fatigue Damage Mechanisms in Composite Materials: A Review", Fatigue Mechanisms, Proc. of ASTM-NBS-NSF Symp., Kansas City MO., J.J. Fong, ed., ASTM STP 679, pp. 762-787, 1979.
10. Stinchcomb, W.W., Reifsnider, K.L., Yeung, P., and Masters, J., "Effect of Ply Constraint on Fatigue Damage Development in Composite Material Laminates," Fatigue of Fibrous Composite Materials, ASTM STP 723, pp. 65-84, 1981.
11. Reifsnider, K.L., and Jamison, R., "Fracture of Fatigue-Loaded Composite Laminates," Int. J. Fatigue, pp. 187-197, 1982.
12. Talreja, R., Fatigue of Composite Materials, Technical University of Denmark, Lyngby, Denmark, 1985.
13. Kachanov, L.M., "On the Creep Fracture Time," Izv. AN SSR, Otd. Tekhn. Nauk, No. 8, pp. 26-31, 1958.
14. Talreja, R., "A Continuum Mechanics Characterization of Damage in Composite Materials," Proc. R. Soc. London, Vol. 399A, pp. 195-216, 1985.



15. Talreja, R., "Residual Stiffness Properties of Cracked Composite Laminates," Advances in Fracture Research, Proc. Sixth Int. Conf. Fracture, New Delhi, India, Vol. 4, pp. 3013-3019, 1985.
16. Talreja, R., "Transverse Cracking and Stiffness Reduction in Composite Laminates," Journal of Composite Materials, Vol. 21, pp. 355-371, 1985.
17. Talreja, R., "Stiffness Properties of Composite Laminates with Matrix Cracking and Interior Delamination," Danish Center for Applied Mathematics and Mechanics, The Technical University of Denmark, No. 321, March, 1986.
18. Weitsman, Y., "Environmentally Induced Damage in Composites," Proceedings of the 5th Symposium on Continuum Modeling of Discrete Structures, A.J.M. Spencer, Ed., Nottingham, U.K., 1985.
19. Vakulenko, A.A., and Kachanov, M.L., "Continuum Theory of Cracked Media," Izv. AN SSSR, Mekhanika Tverdogo Tela, Vol. 6, p. 159, 1971.
20. Allen, D.H., Harris, C.E., and Groves, S.E., "A Thermomechanical Constitutive Theory for Elastic Composites with Distributed Damage - Part I: Theoretical Development," Int. Journal Solids & Structures, Vol. 23, No. 9, pp. 1301-1318, 1987.
21. Coleman, B.D., and Gurtin M.E., "Thermodynamics with Internal State Variables," Journal of Chemical Physics, Vol. 47, pp. 597-613, 1967.
22. Kachanov, M.L., "Continuum Theory of Media with Cracks," Izv. AN SSSR, Mekhanika Tverdogo Tela, Vol. 7, pp. 54-59, 1972.
23. Lee, J.W., Allen, D.H., and Harris, C.E., "Internal State Variable Approach for Predicting Stiffness Reductions in Fibrous Laminated Composites with Matrix Cracks," Journal of Composite Materials, Vol. 23, pp. 1273-1291, 1989.
24. Allen, D.H., Harris, C.E., and Groves, S.E., "A Thermomechanical Constitutive Theory for Elastic Composites with Distributed Damage - Part II: Application to Matrix Cracking in Laminated Composites," Int. Journal Solids & Structures, Vol. 23, No. 9, pp. 1319-1338, 1987.
25. Allen, D.H., Harris, C.E., Groves, S.E., and Norvell, R.G., "Characterization of Stiffness Loss in Crossply Laminates with Curved Matrix Cracks," Journal of Composite Materials, Vol. 22, No. 1, pp. 71-80, 1988.
26. Allen, D.H., Groves, S.G., and Harris, C.E., "A Cumulative Damage Model for Continuous Fiber Composite Laminates with Matrix Cracking and Interply Delaminations," Composite Materials: Testing and Design (8th Conference), ASTM STP, American Society for Testing and Materials, 1987.
27. Harris, C.E., Allen, D.H., and Nottorf, E.W., "Damage Induced Changes in the Poisson's Ratio of Cross-Ply Laminates: An Application of a Continuum Damage Mechanics Model for Laminated Composites," Proceedings ASME Winter Annual Meeting, American Society of Mechanical Engineers, 1987.

28. Allen, D.H., Harris, C.E., and Groves, S.E., "Damage Modelling in Laminated Composites," to appear in Proceedings IUTAM/ICM Symposium on Yielding, Damage and Failure of Anisotropic Solids, Grenoble, France, 1987.
29. Allen, D.H., Nottorff, E.W., and Harris, C.E., "Effect of Microstructural Damage on Ply Stresses in Laminated Composites," Recent Advances in the Macro- and Micro-Mechanics of Composite Materials Structures, AD-Vol. 13, ASME, pp. 135-146, 1988.
30. Wang, A.S.D., Chou, P.C., and Lei, S.C., "A Stochastic Model for the Growth of Matrix Cracks in Composite Laminates," Journal of Composite Materials, Vol. 18, pp. 239-254, 1984.
31. Lo, D.C., Allen, D.H. and Harris, C.E. "A Continuum Model for Damage Evolution in Laminated Composites," Proceedings IUTAM Symposium, Troy, N.Y., 1990 (to appear).
32. Chou, P.C., Wang, A.S.D., and Miller, H., "Cumulative Damage Model for Advanced Composite Materials, AFWAL-TR-82-4083, 1982.
33. Timoshenko, S.P. and Woinowsky-Krieger, S., Theory of Plates and Shells, second edition, McGraw-Hill, New York, 1959.
34. Buie, K.D., "A Finite Element Model for Laminated Composite Plates with Matrix Cracks and Delaminations," Texas A&M University Thesis, December, 1988.
35. Tsai, S.W. and Wu, E.M., "A General Theory of Strength for Anisotropic Materials," Journal Composite Materials, pp. 58-80, 1971.
36. Whitney, J.M. and Nuismer, R.J., "Stress Fracture Criteria for Laminated Composites Containing Stress Concentrations," Journal Composite Materials, Vol. 8, No. 2, p. 253, 1974.
37. Harris, C.E. and Morris, D.N., "Fracture of Thick Graphite/Epoxy Laminates with Part-Through Surface Flaws," Composite Materials: Fatigue and Fracture, Hahn, H.T., Ed., ASTM STP 907, American Society for Testing and Materials, Philadelphia, pp. 100-114, 1986.





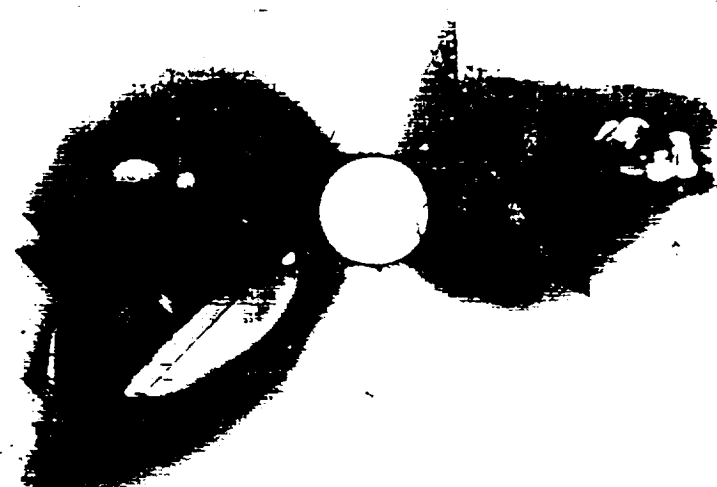
A



B



C



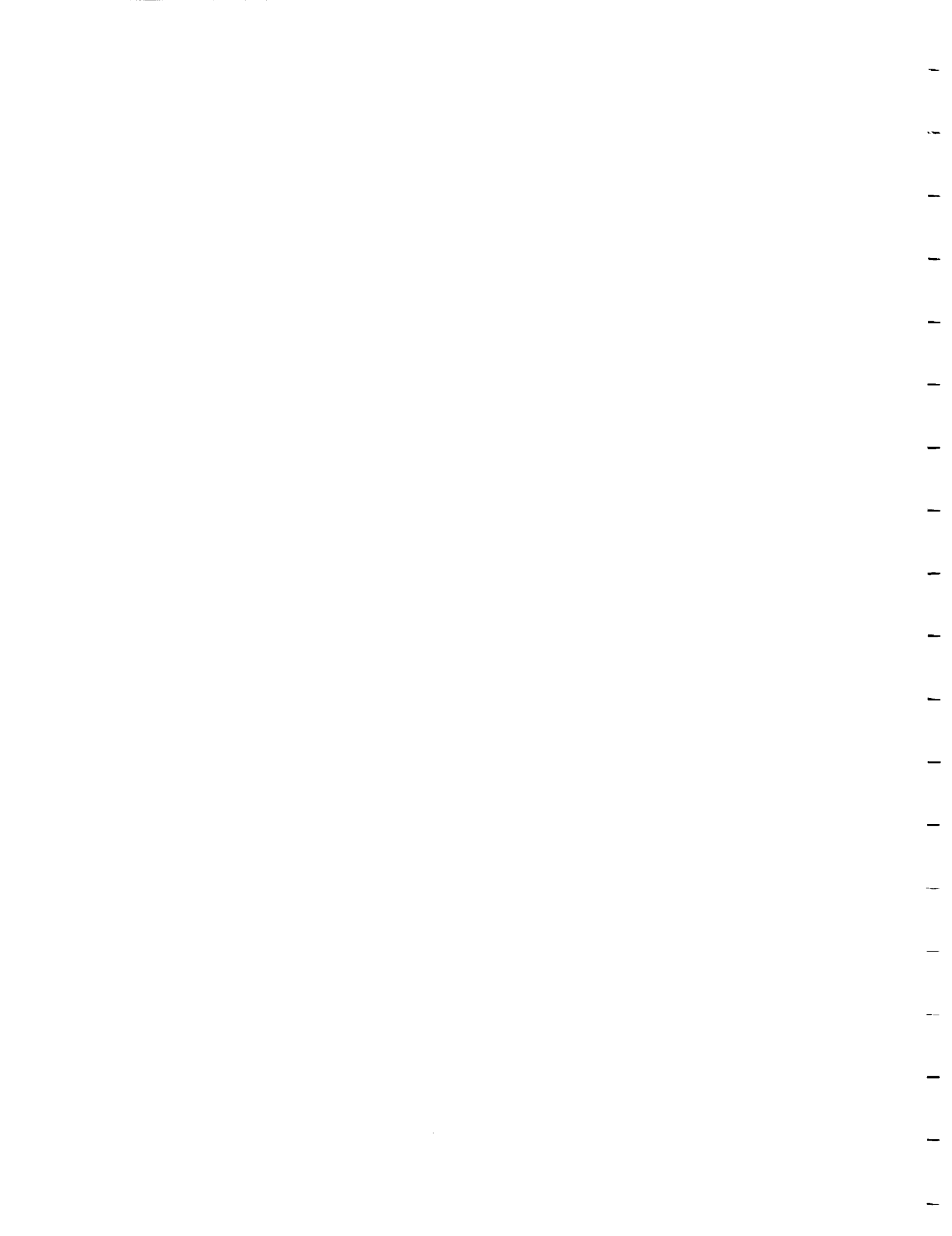
D



E

PROGRESSION OF DAMAGE AT A CIRCULAR HOLE IN AN $[45/90/-45/0]_{2s}$ LAMINATE

ORIGINAL PAGE IS
OF POOR QUALITY



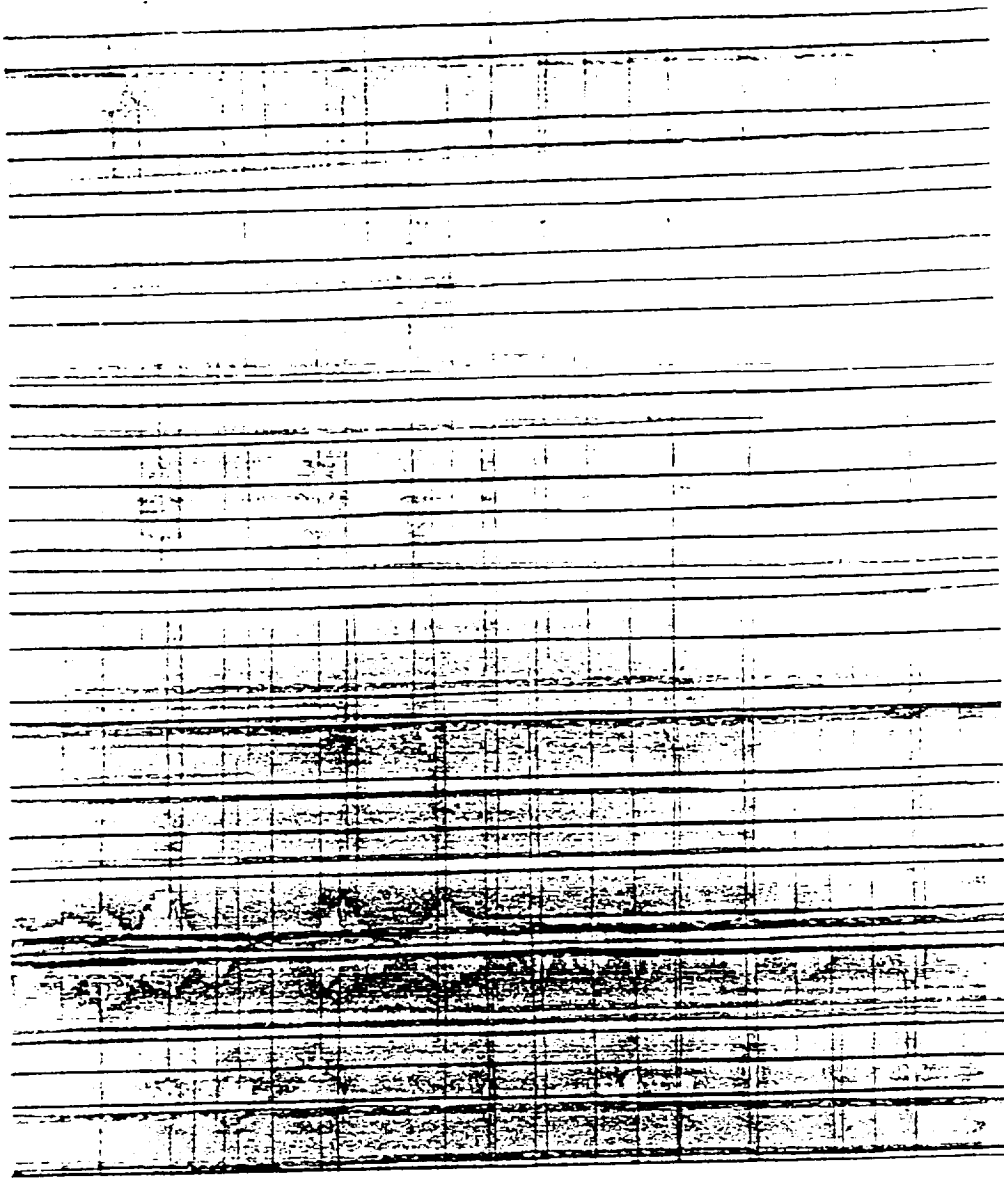
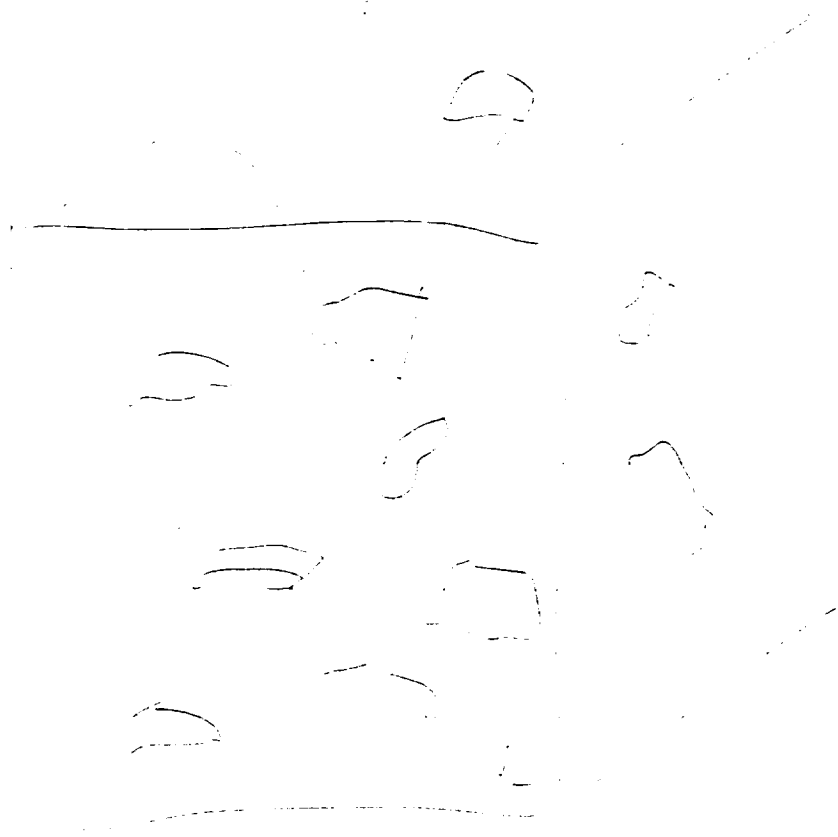
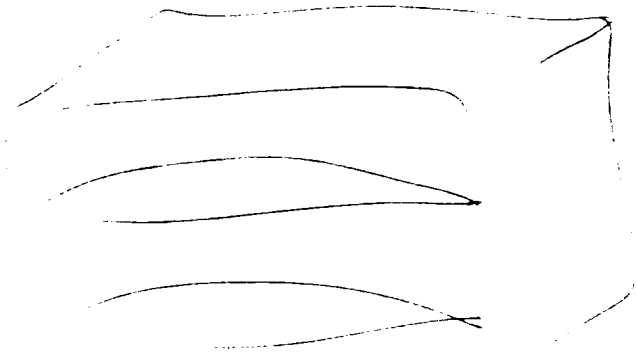


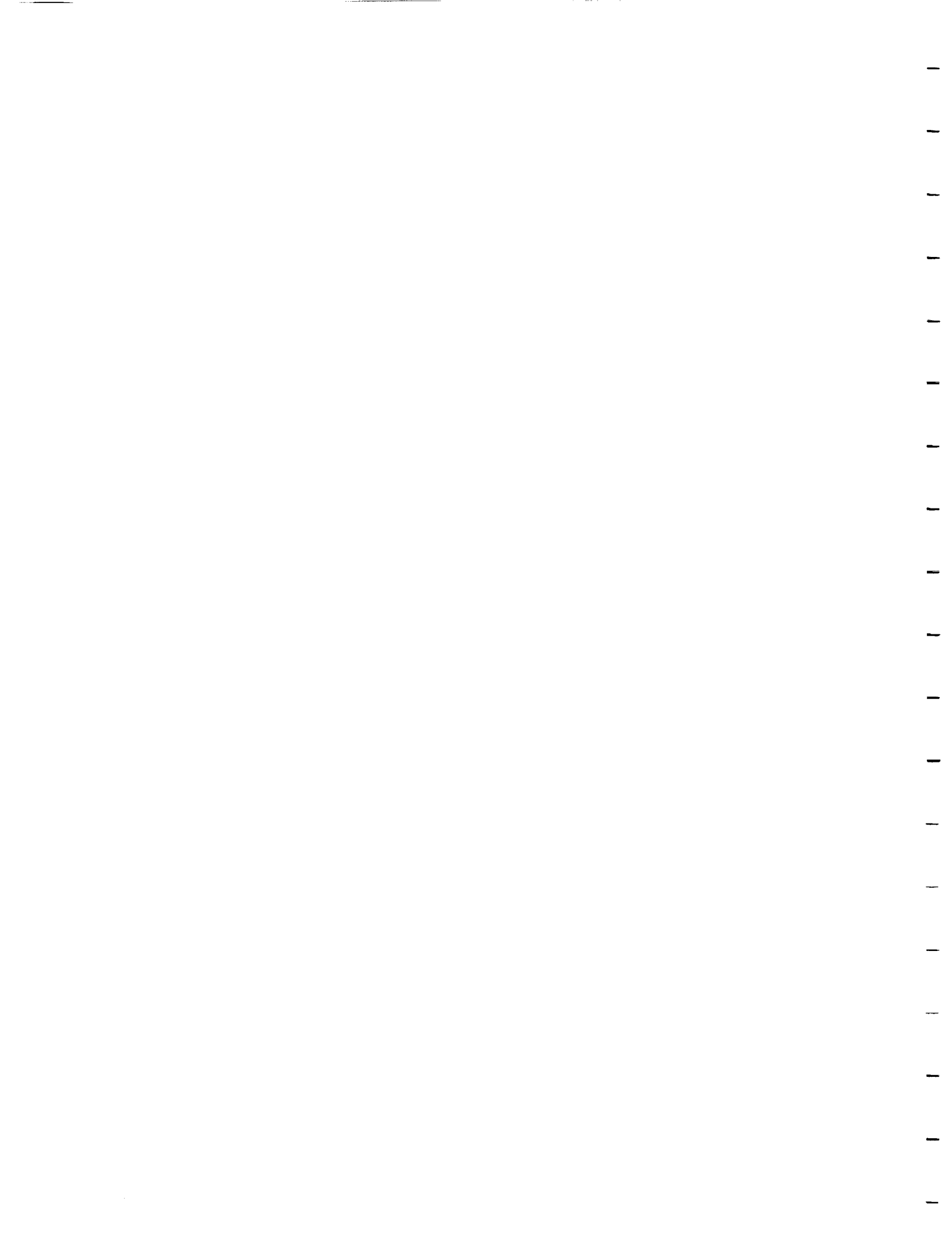
Figure 38. State of grouping of delaminations, shown in Fig. 31 in
#1 (0/90₃)_s laminate, C=200,000
(f=2.0 Hz, R=0.1, L_{max}=10.230 KN)

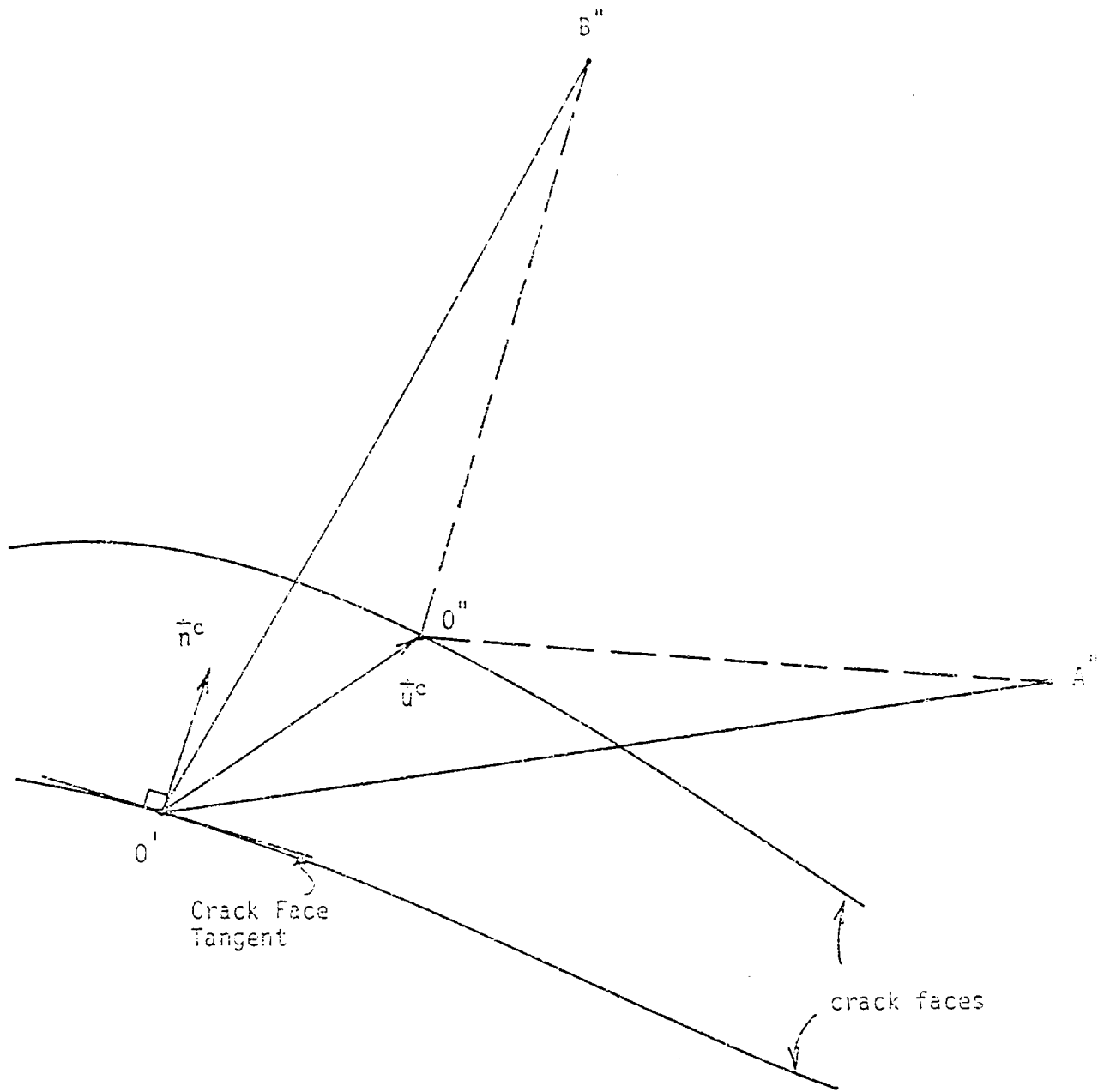
ORIGINAL PAGE IS
OF POOR QUALITY



Handwritten text, possibly a signature or a note, located at the bottom of the page. The text is written in a cursive, handwritten style and is difficult to decipher.

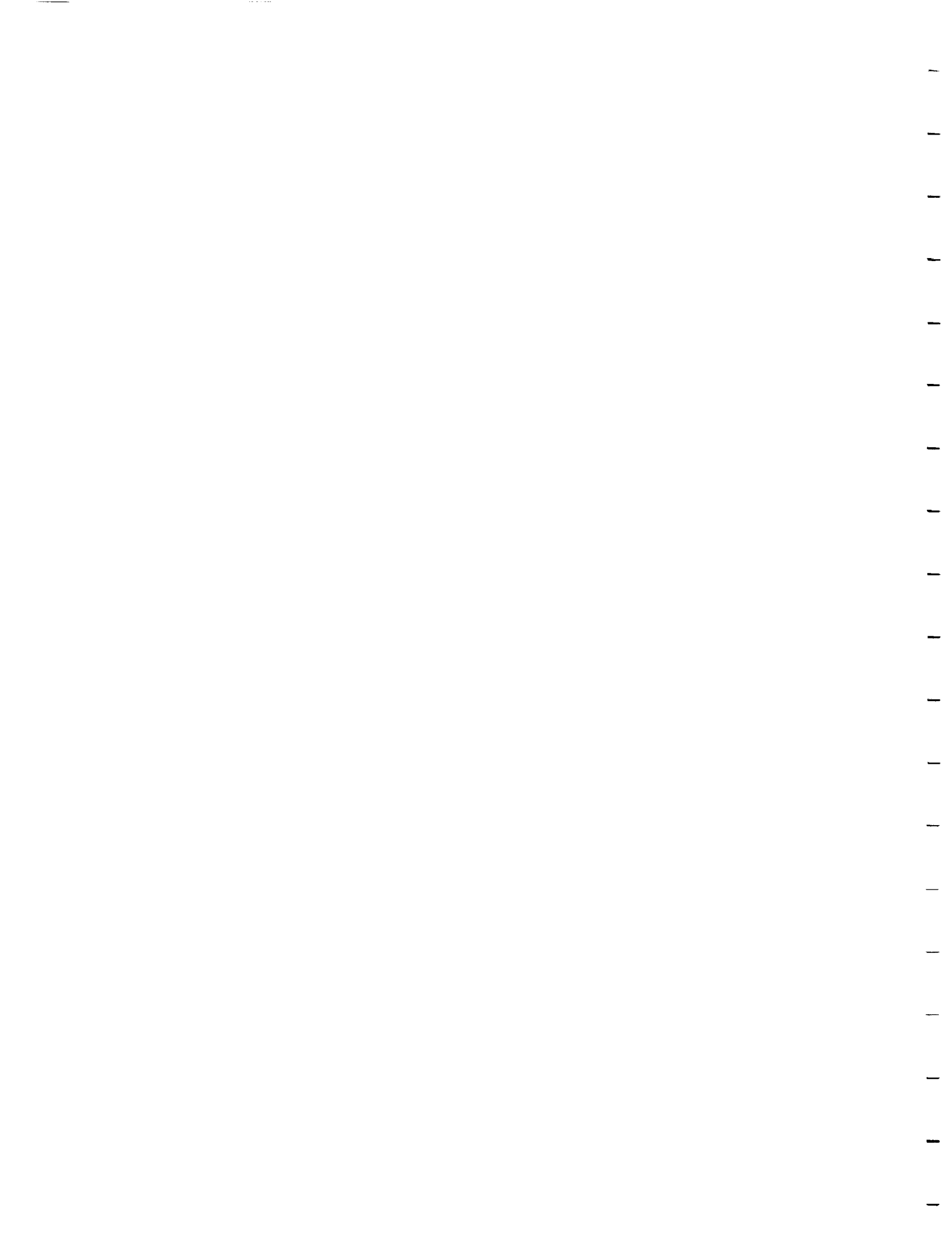
ORIGINAL PAGE IS
OF POOR QUALITY





Description of the Internal State at Point O' .





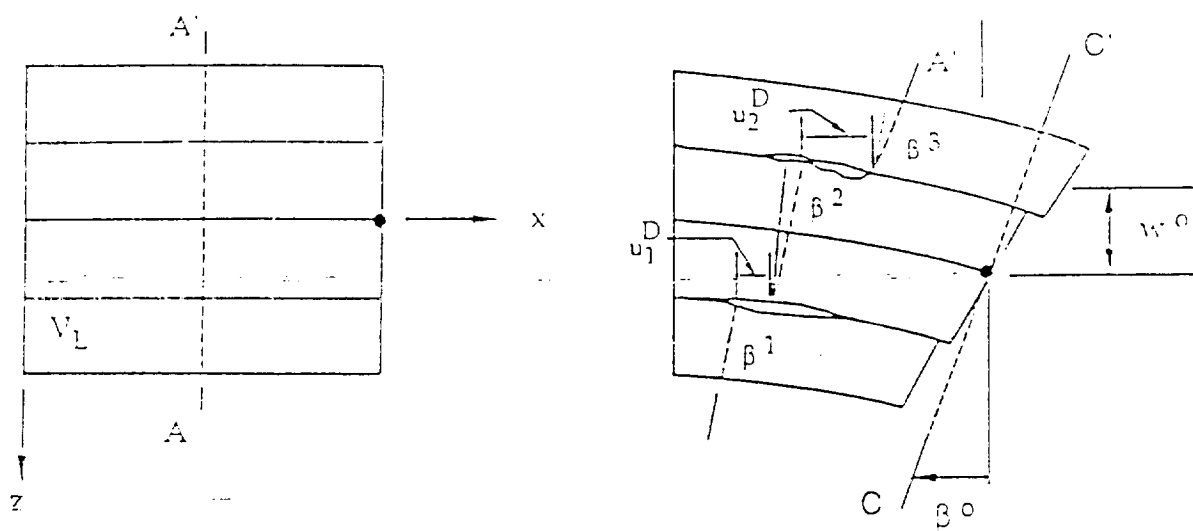
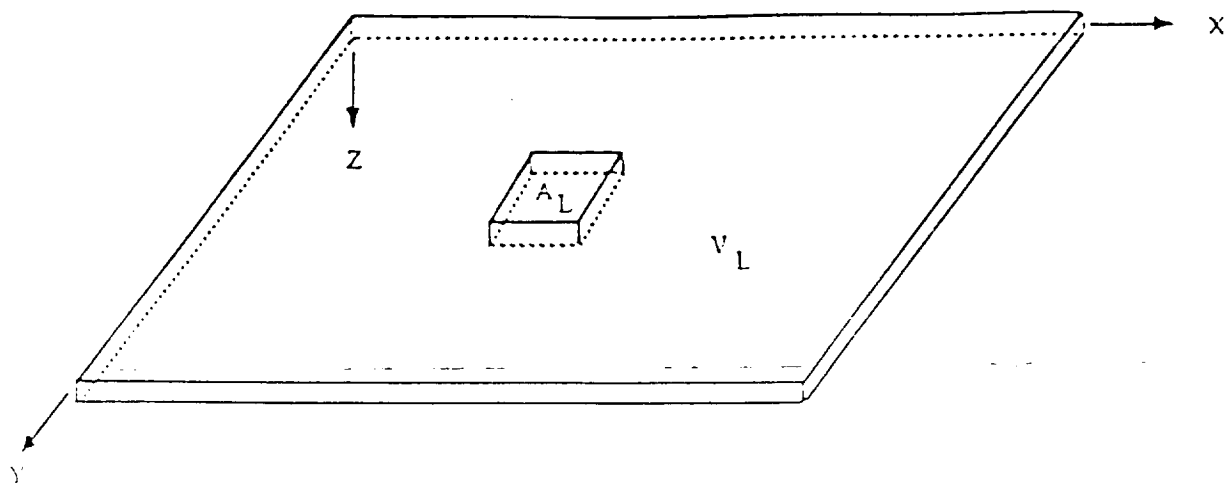
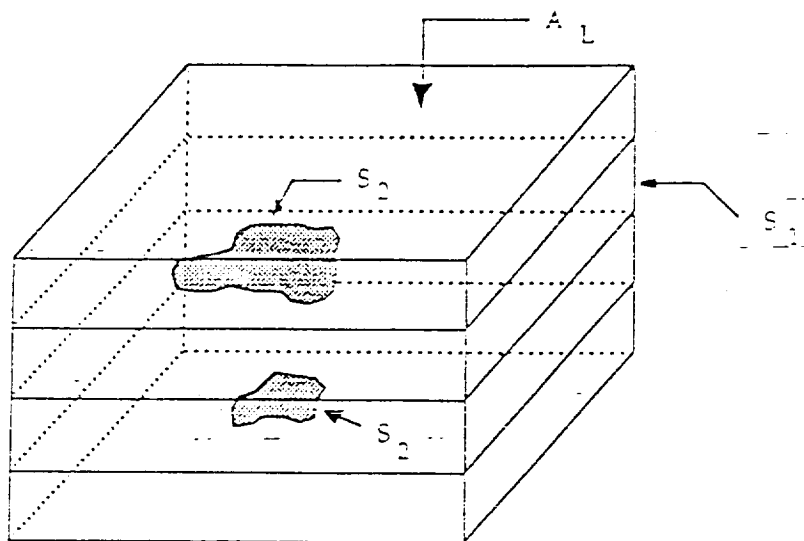


Figure 1. Deformation Geometry for Region A_L .

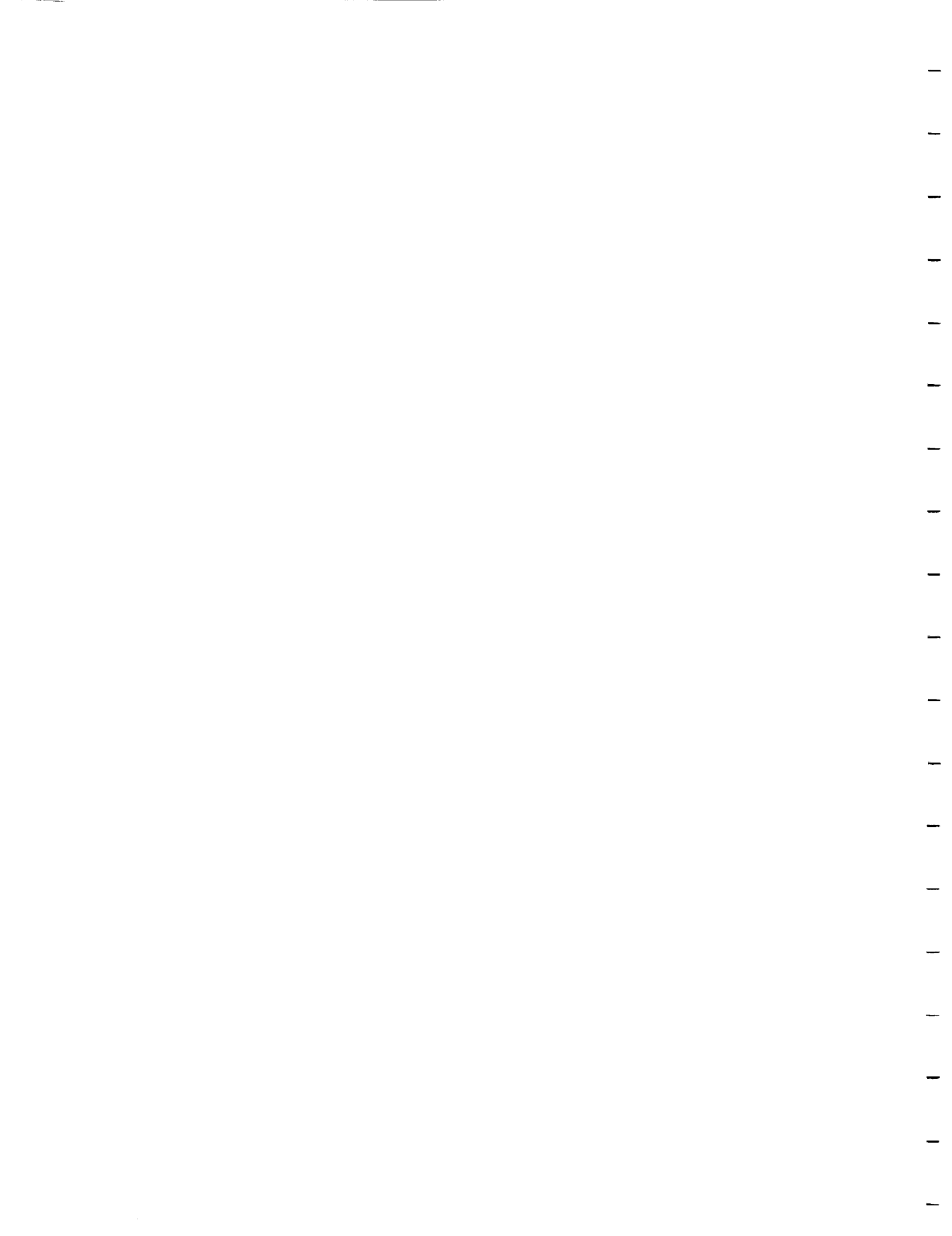


A) General Laminate



B) Exploded View with Damage

Figure 2. Characteristic Local Region of Damage.



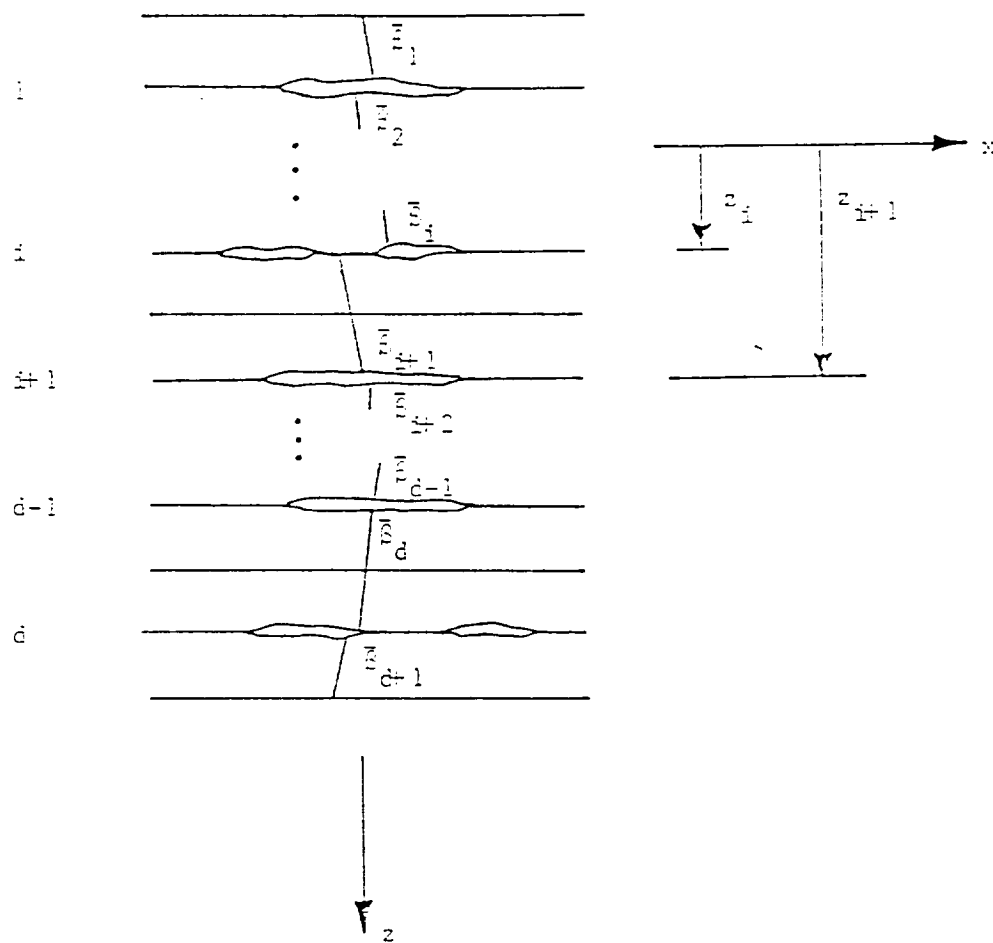
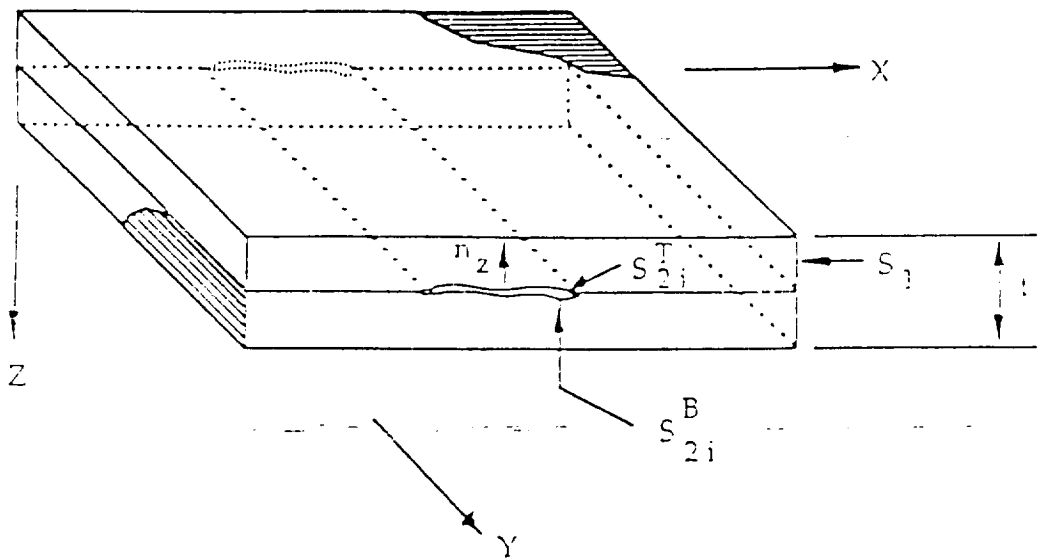


Fig. 7. Schematic of Delaminated Region
in a Composite Layup



$$\begin{aligned} \vec{u} &= u^D \hat{e}_x + v^D \hat{e}_y + w^D \hat{e}_z \\ \vec{n} &= 0 \hat{e}_x + 0 \hat{e}_y + n \hat{e}_z \\ S &= S_1 + S_2 \end{aligned}$$

Figure 3. Interply Delamination in a Laminated Continuous Fiber Composite.

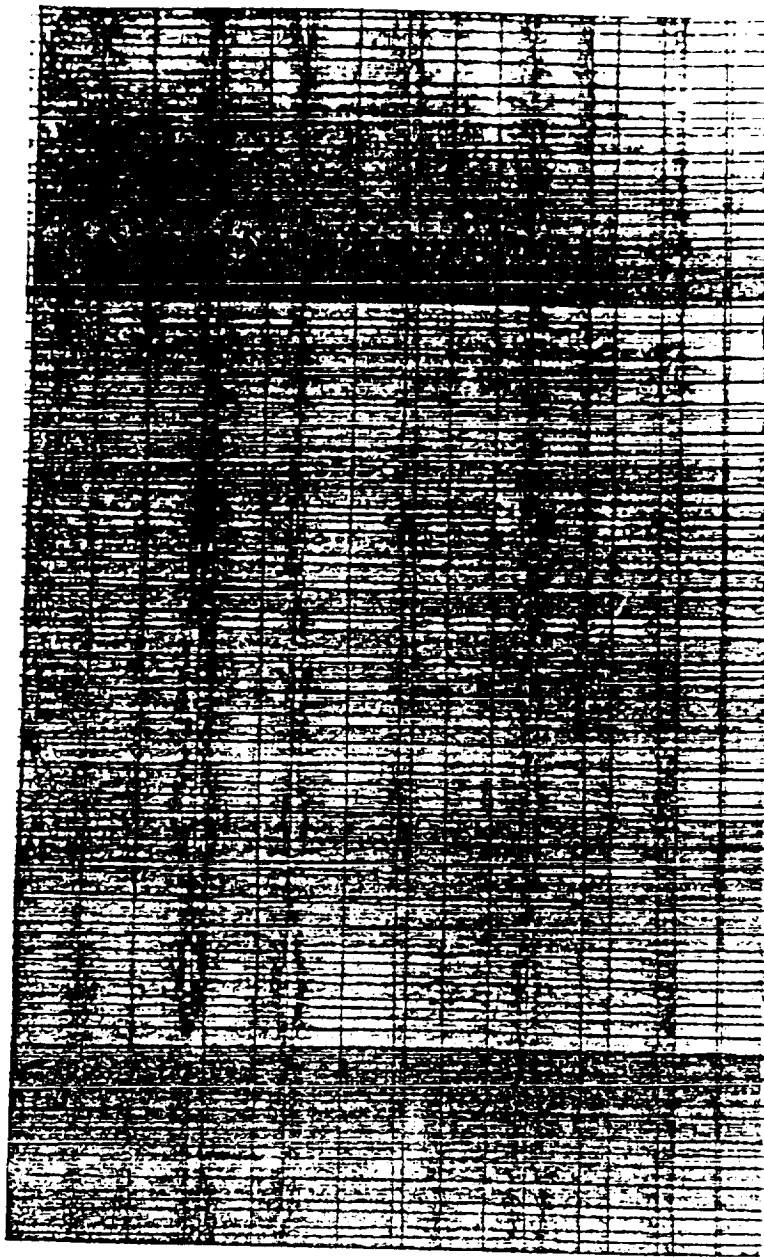
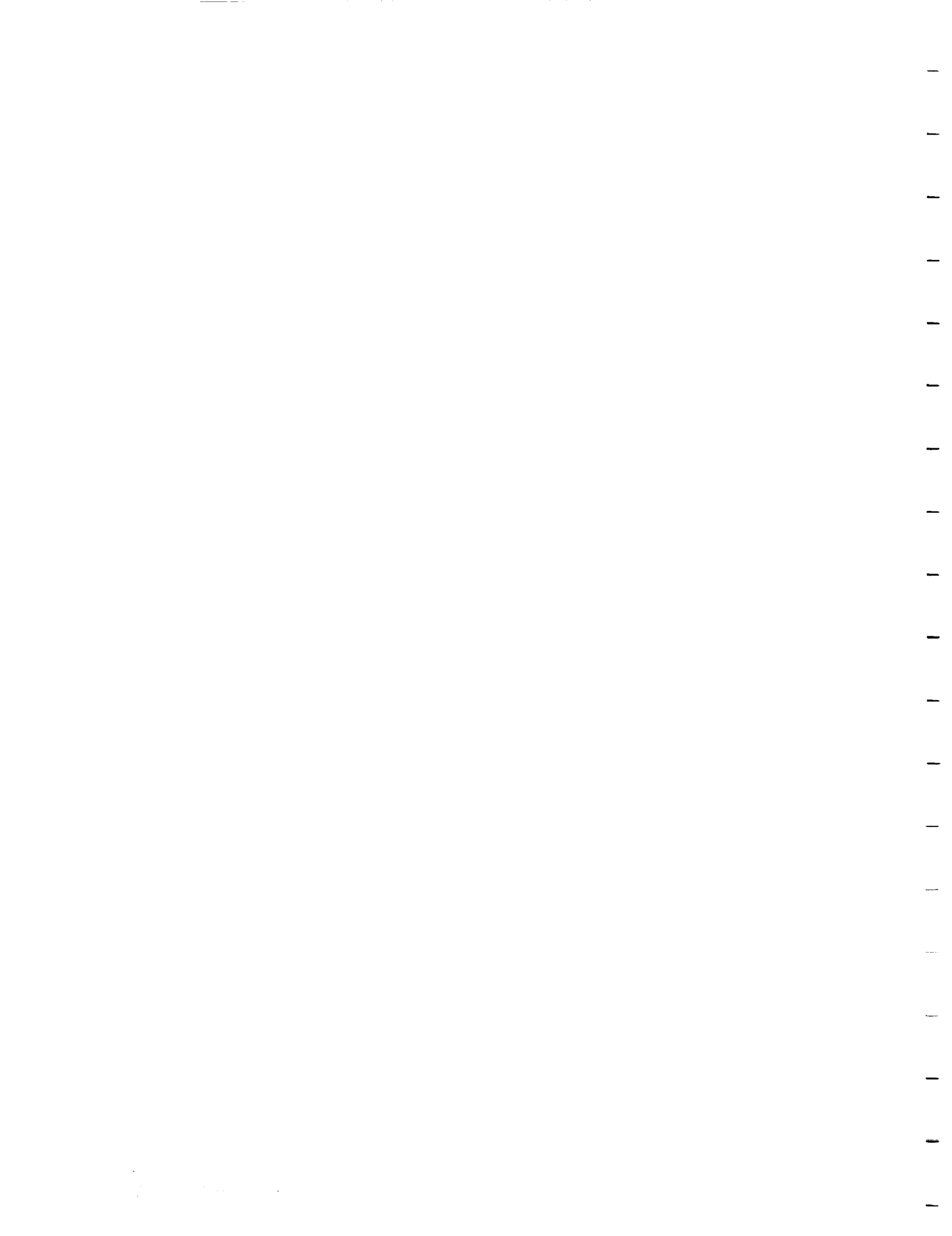


Fig. 2 Enlarged X-ray Radiograph of Damage in a $[0_2/90_2]_s$ Laminate at 400,000 Cycles with $S_{max} = 75\%$ of S_{ULT}

ORIGINAL PAGE IS
OF POOR QUALITY



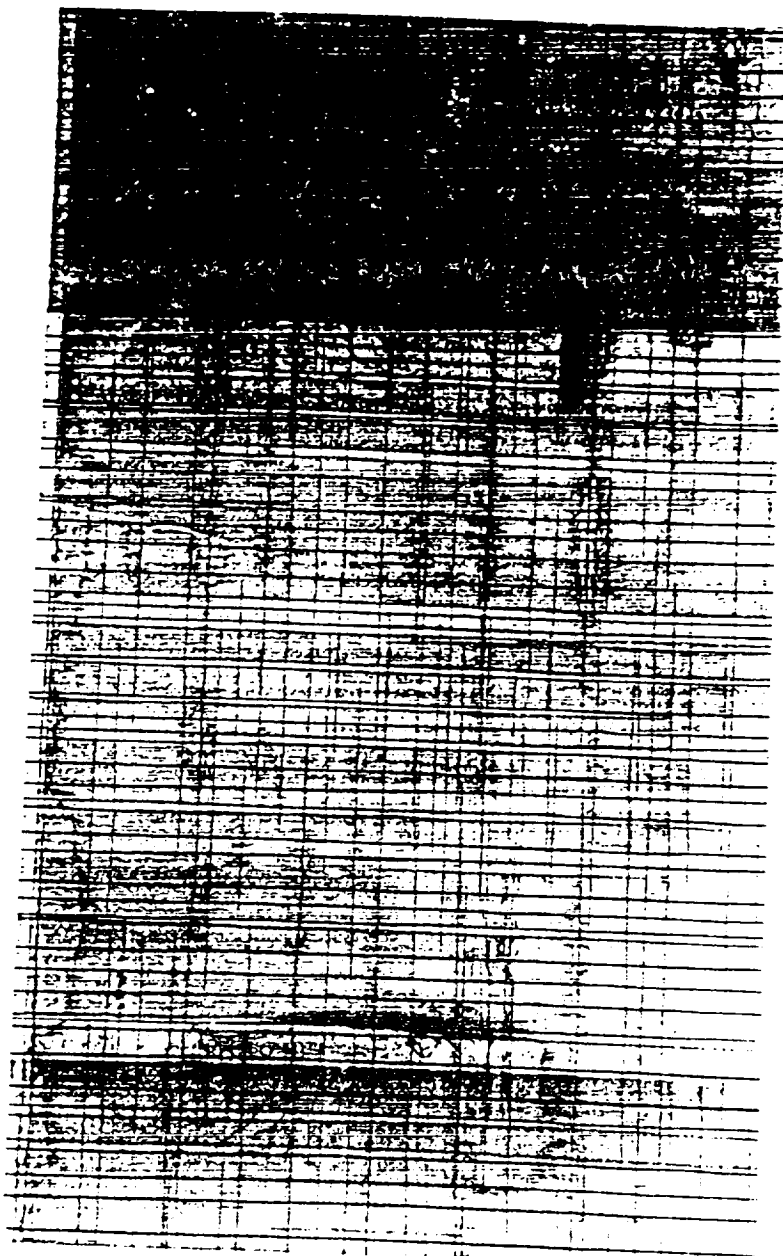
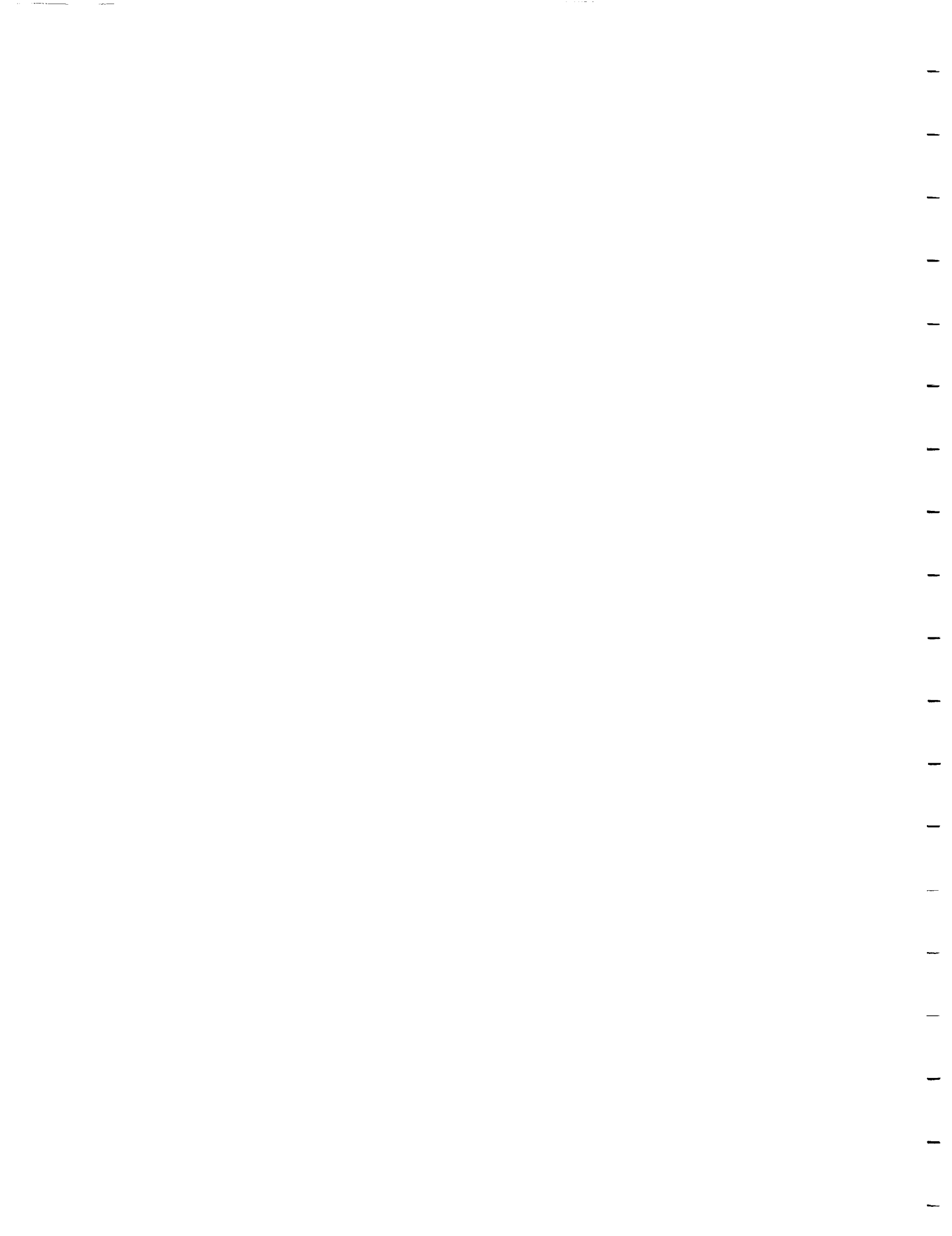


Fig. 4 Enlarged X-ray Radiograph of Damage in a $[0/90_2]_s$ Laminate at 1,003,000 Cycles with $S_{max} = 71\%$ of S_{ULT}

ORIGINAL PAGE IS
OF POOR QUALITY



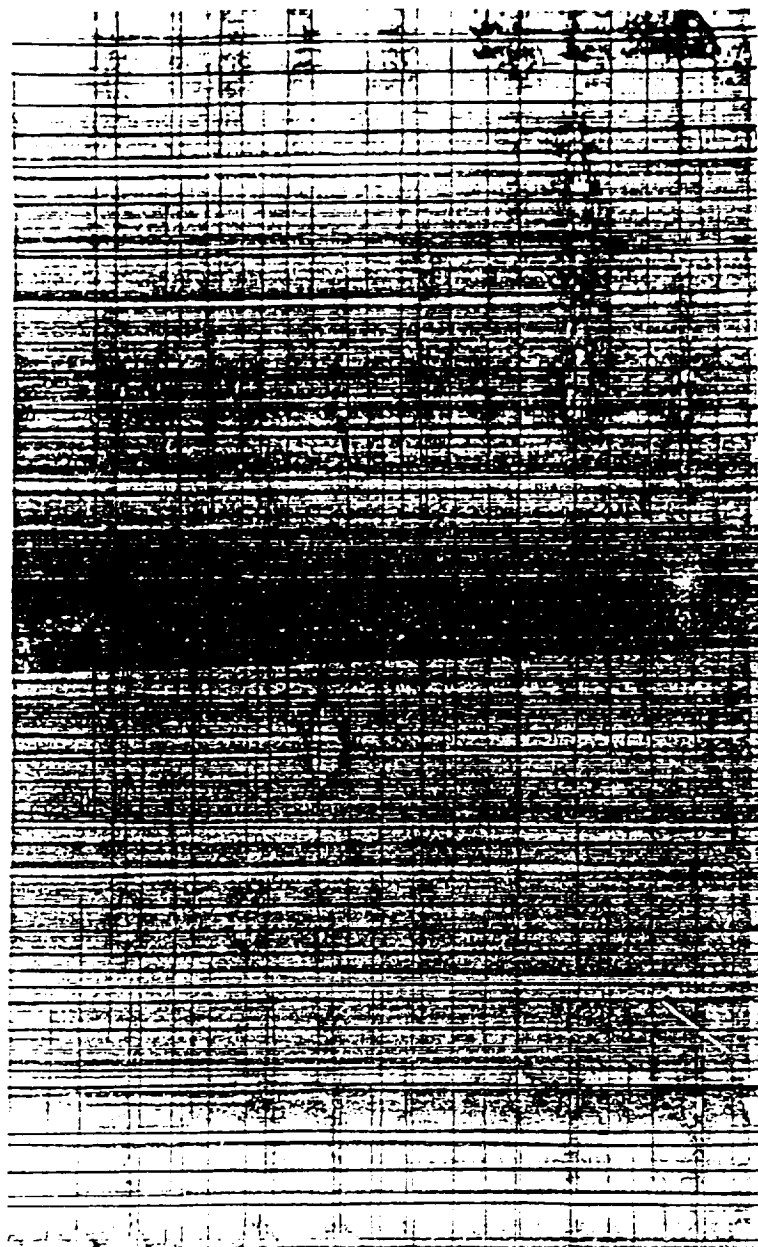


Fig. 5 Enlarged X-ray Radiograph of Damage in a $[0/90_3]_s$ Laminate at 200,000 Cycles with $S_{max} = 73\%$ of S_{ULT}

ORIGINAL PAGE IS
OF POOR QUALITY

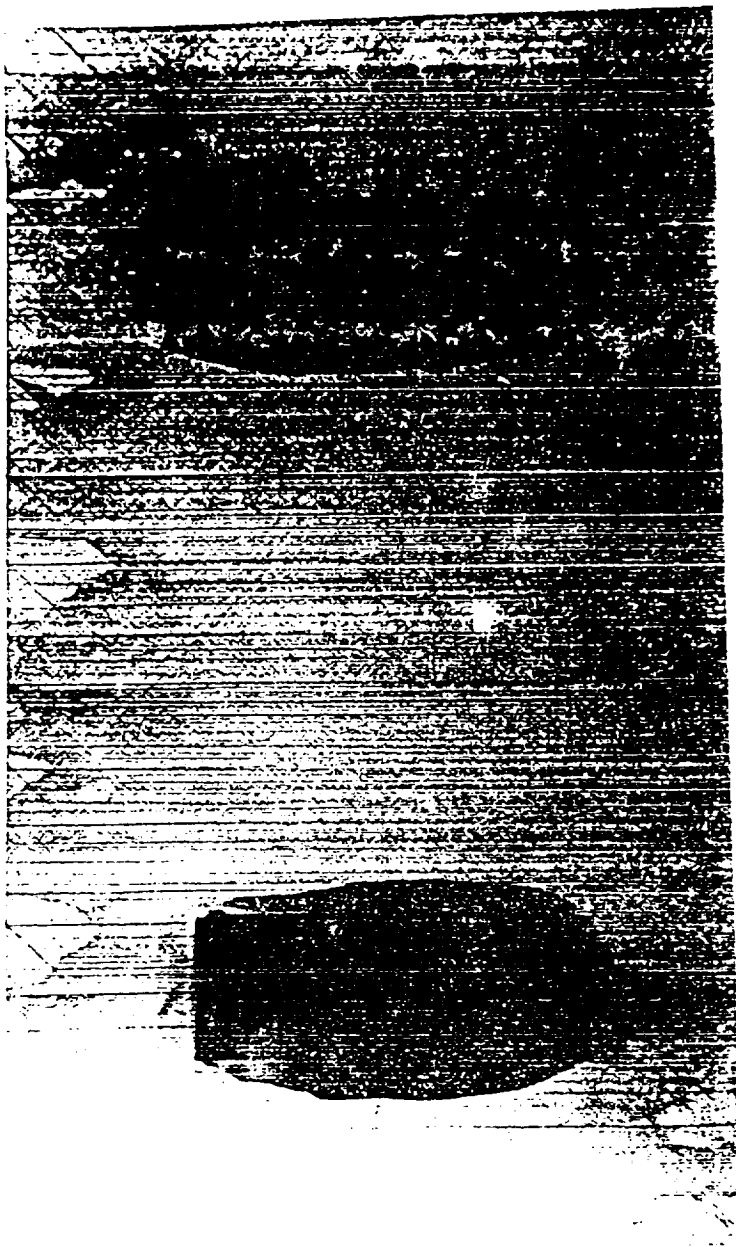
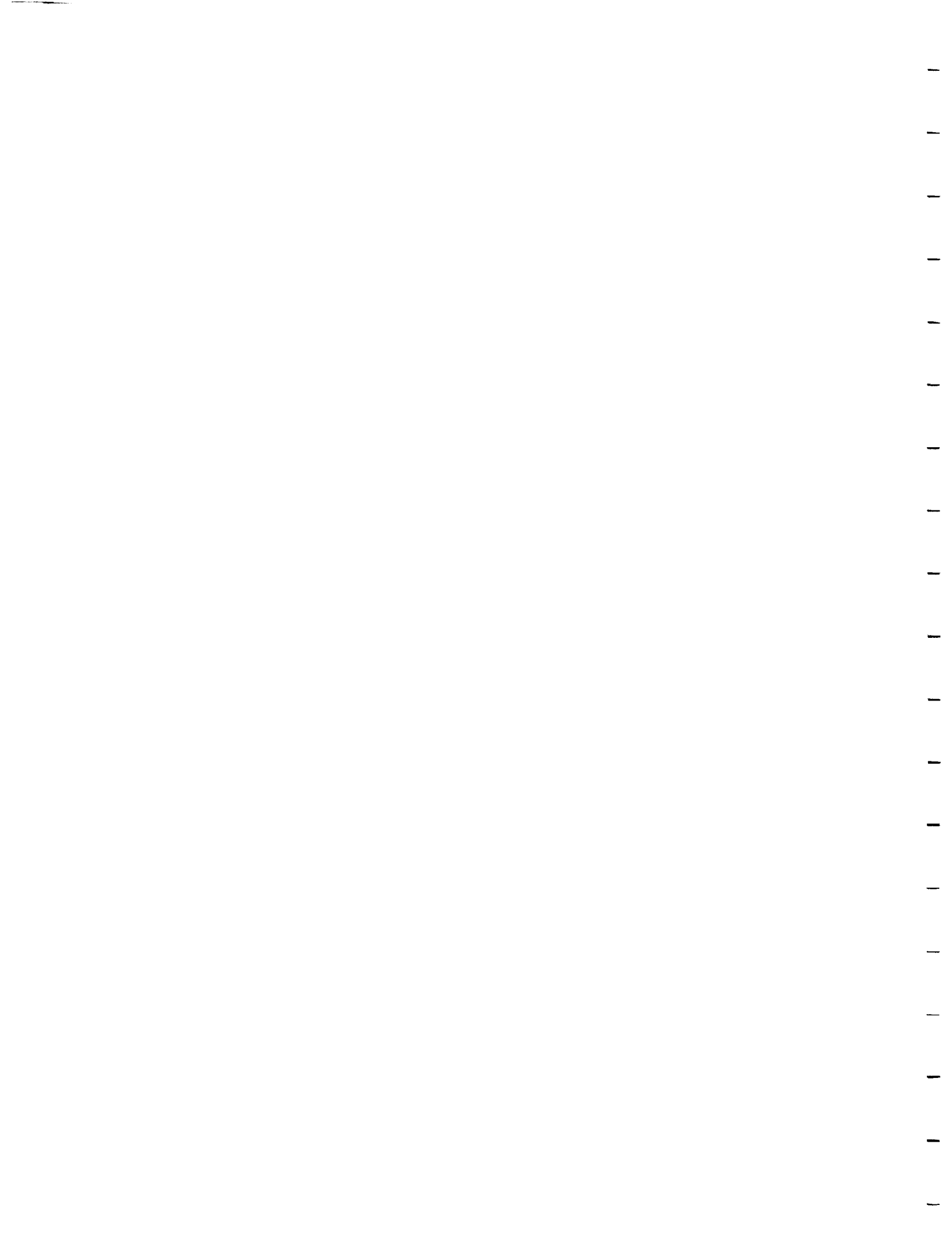


Fig. 6 Enlarged X-ray Radiograph of Damage in a $[90/\pm 45/0]_s$ Laminate at 50,000 Cycles with $S_{\max} = 73\%$ of S_{ULT}

ORIGINAL PAGE IS
OF POOR QUALITY



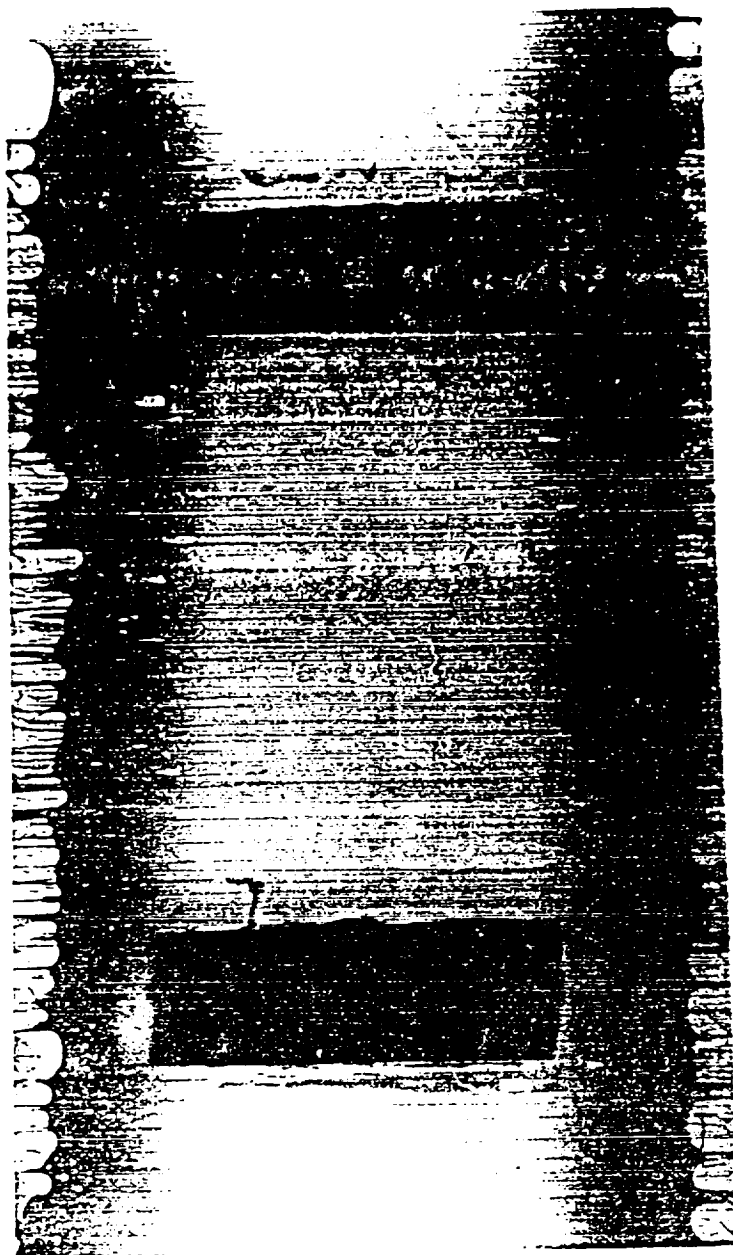
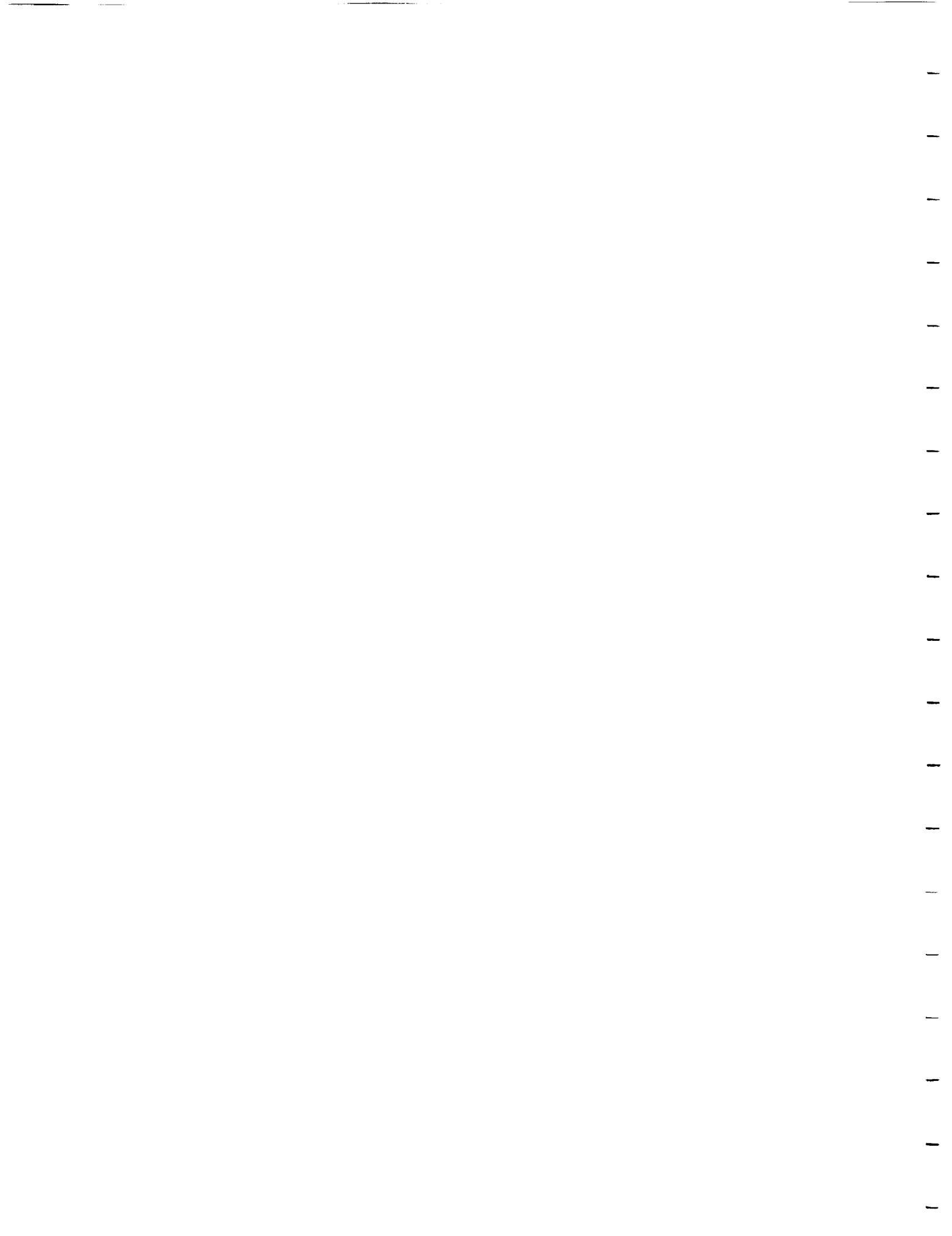


Fig. 7 Enlarged X-ray Radiograph of Damage in a $[0/\pm 45/90]_s$ Laminate at 17,000 Cycles with $S_{\max} = 76\%$ of S_{ULT}

ORIGINAL PAGE IS
OF POOR QUALITY



Damage Dependent Laminate E_x

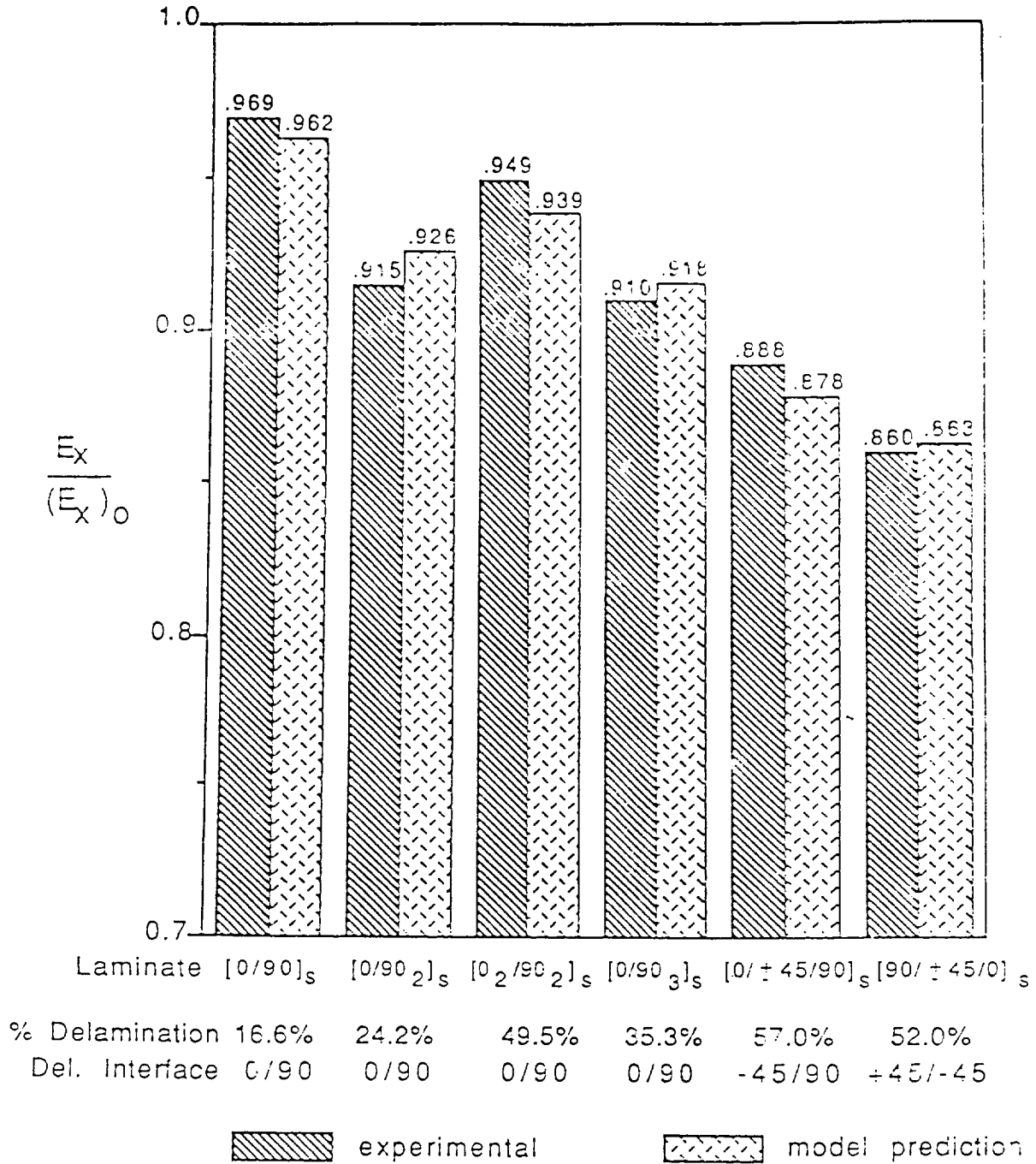


Fig. 5 Comparison of Experimental Results and Model Predictions of the Laminate Engineering Modulus, E_x , Degraded by Both Matrix Cracking and Delamination Damage.

Damage Dependent Laminate ν_{xy}

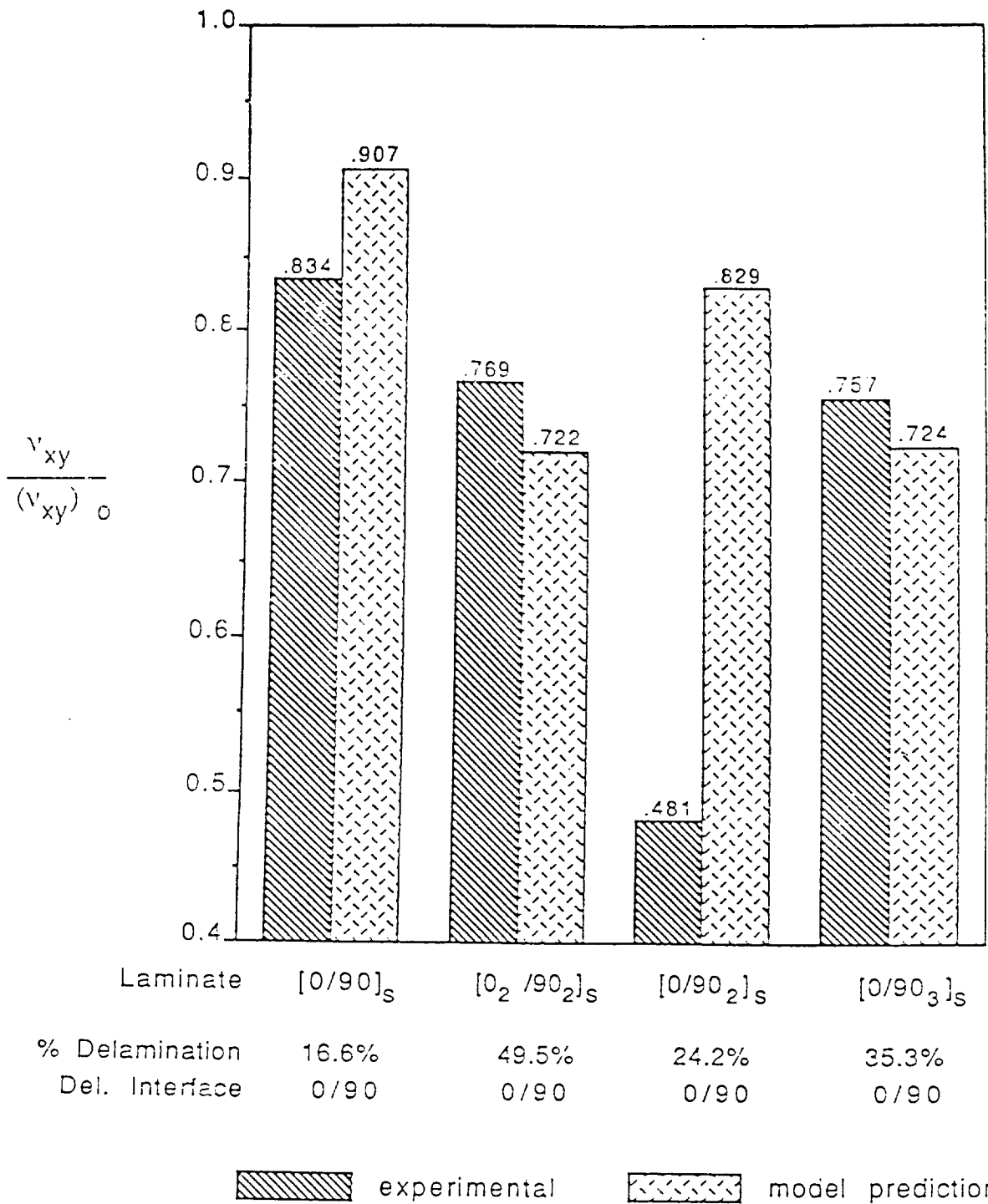


Fig. 6 Comparison of Experimental Results and Model Predictions of the Laminate Engineering Poisson's Ratio, ν_{xy} , Degraded by Both Matrix Cracking and Delamination Damage.

2
Table X. PLY STRESSES RESULTING FROM MATRIX
CRACKING AND DELAMINATION

LAMINATE	PLY	INITIAL PLY STRESS σ (ksi)	STRESS W/MATRIX CRACKS	STRESS W/MATRIX CRACKS & DELAM.	DELAMINATION LOCATION AND MAGNITUDE	MATRIX DAMAGE VARIABLES	
			σ (ksi)	σ (ksi)		μ ϵ_2	μ ϵ_3
[0/90]s	0	211.4	211.4	211.4	0/90	0	0
	90	14.0	9.6	8.5	16.6% .00078	.00318	0
[0/90 ₂]s	0	211.4	211.4	211.4	0/90	0	0
	90	14.0	9.5	7.9	24.2% .001109	.00316	0
	90	14.0	9.5	7.9		.00326	0
[0 ₂ /90 ₂]s	0	211.4	211.4	211.4		0	0
	0	211.4	211.4	211.4	0/90	0	0
	90	14.0	9.2	6.0	49.5% .002267	.00344	0
	90	14.0	9.2	6.0		.00344	0
[0/90 ₃]s	0	211.4	211.4	211.4		0	0
	90	14.0	10.6	8.3	0/90	.00247	0
	90	14.0	10.6	8.3	35.3% .001617	.00247	0
	90	14.0	10.6	8.3		.00247	0
[0/ \pm 45/90]s	0	211.4	211.4	211.4		0	0
	45	64.4	64.0	64.0	-45/90	0	.00067
	-45	64.4	64.0	64.0	57% .002611	0	-.00067
	90	14.0	11.8	8.2		.00157	0
[90/ \pm 45/0]s	90	14.0	13.9	13.9		.00060	0
	+45	64.4	64.0	64.0	+45/-45	0	.00067
	-45	64.4	64.0	48.7	52% .002382	0	-.00067
	0	211.4	211.4	161.0		0	0

ORIGINAL PAGE IS
OF POOR QUALITY

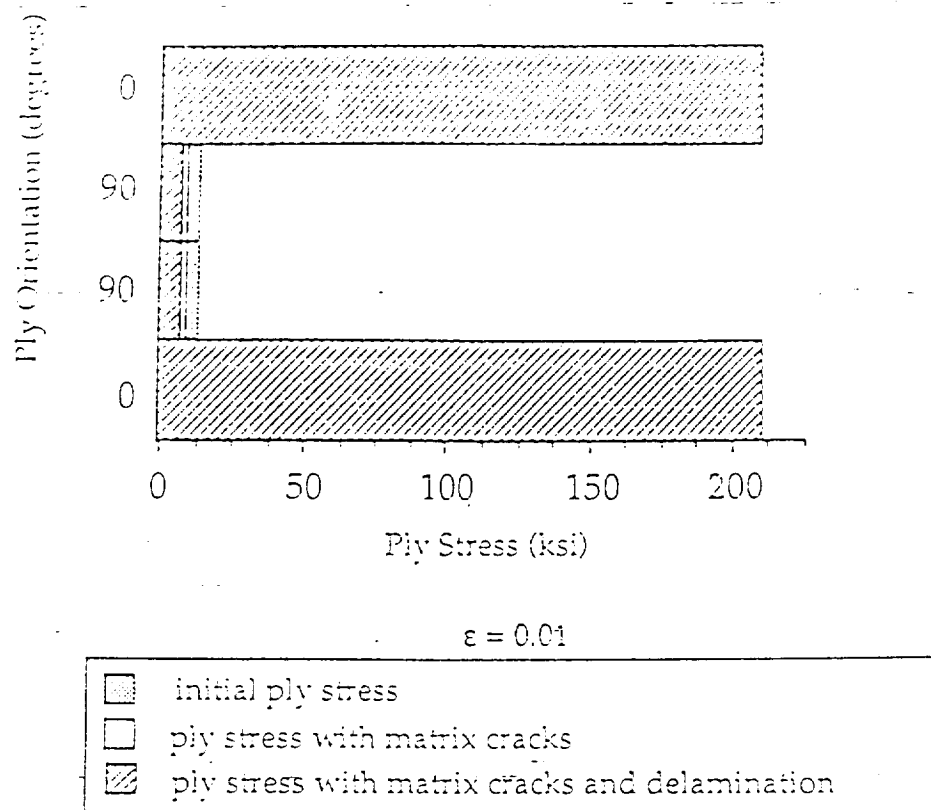
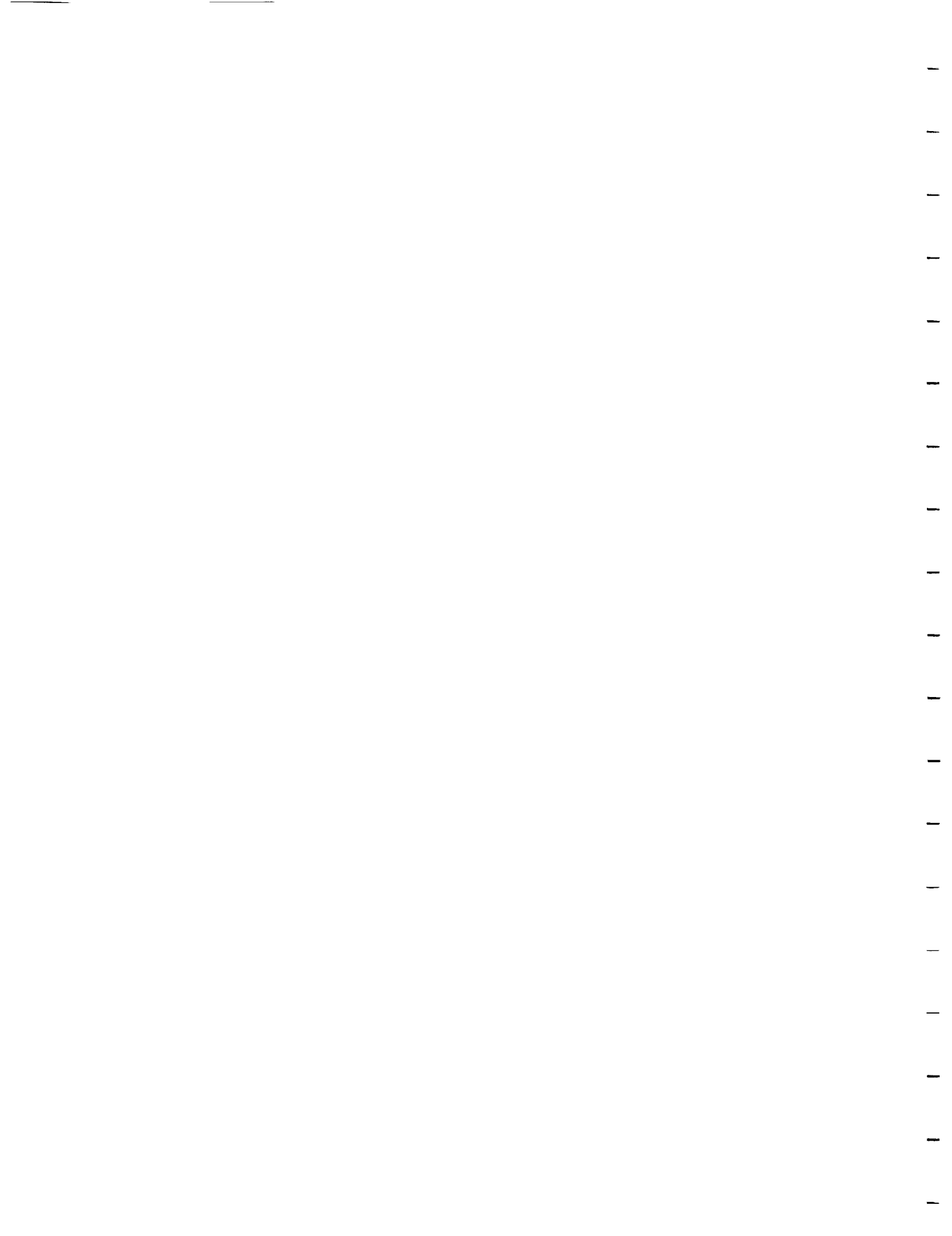
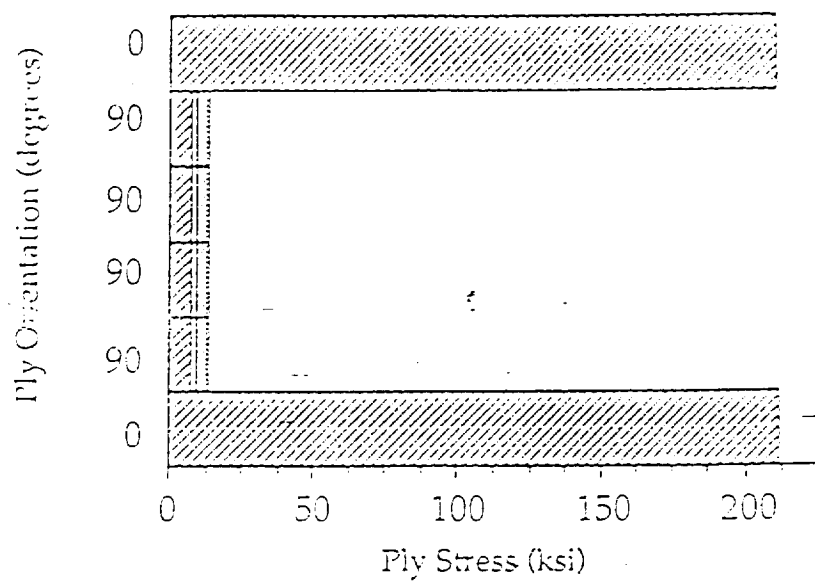


Figure 6. Far Field Ply Stresses in a [0/90]_s Laminate





$\epsilon = 0.01$

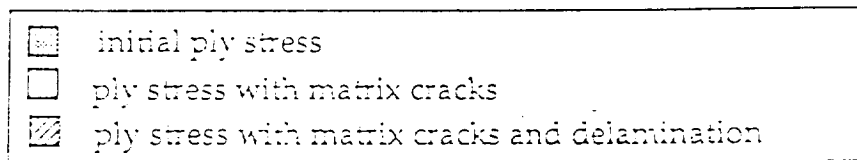
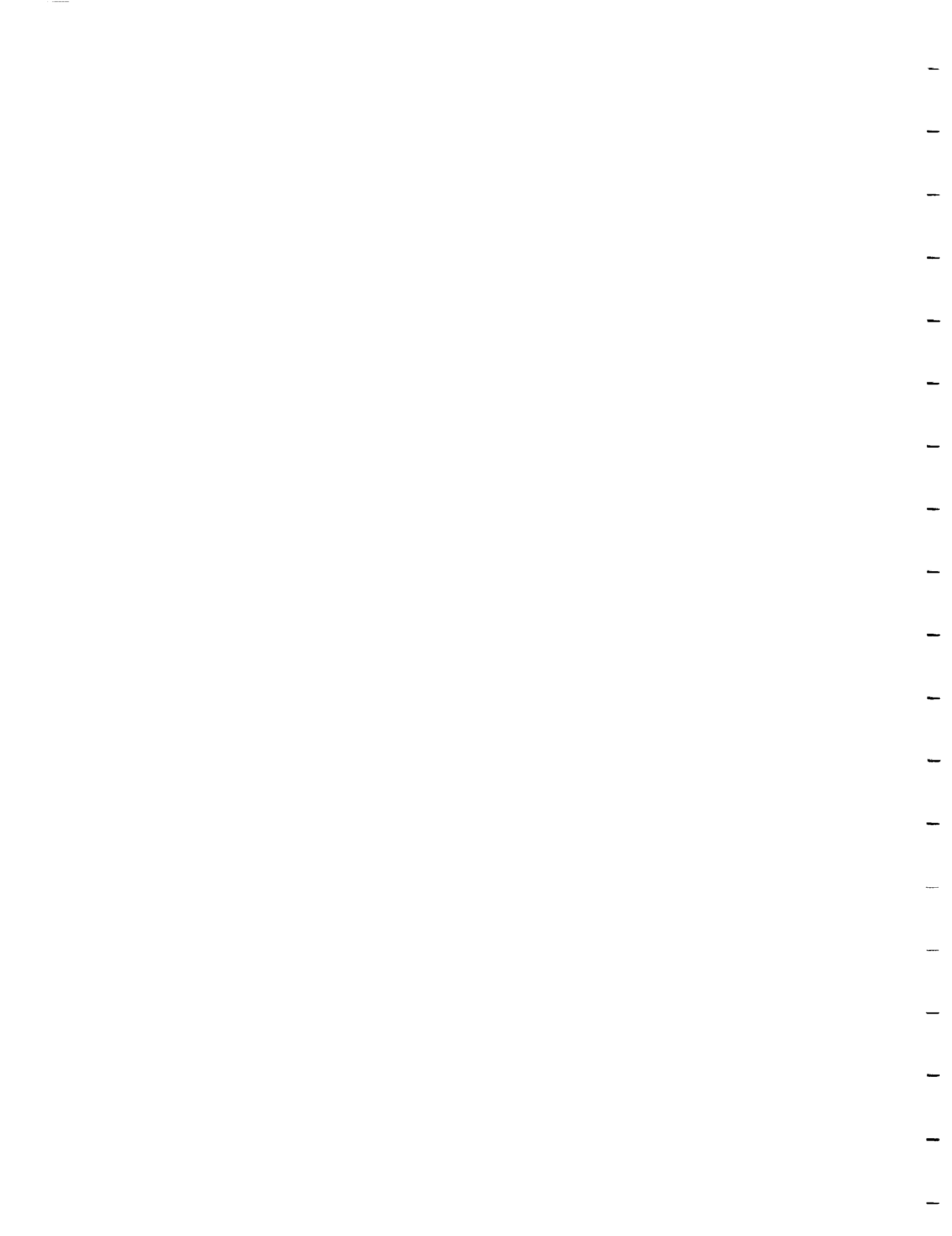
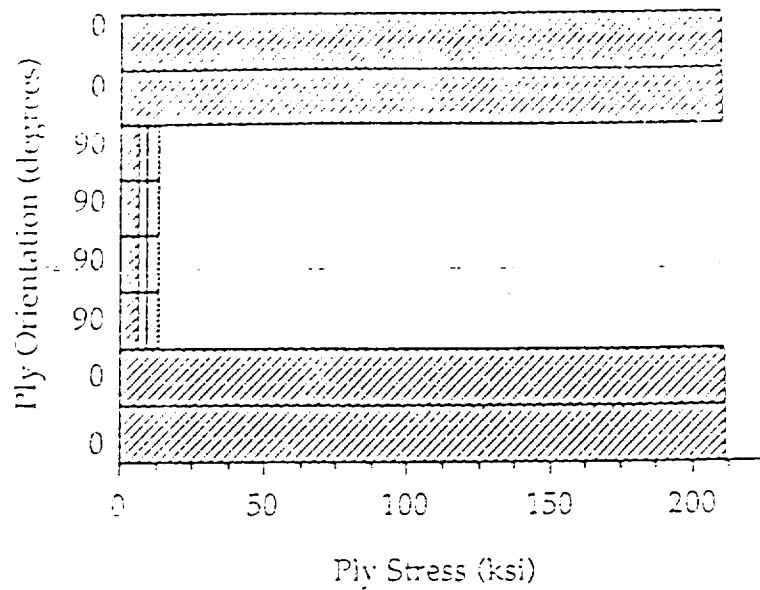


Figure 7. Far Field Stresses in a $[0/90_2]_s$ Laminate





$\epsilon = 0.01$

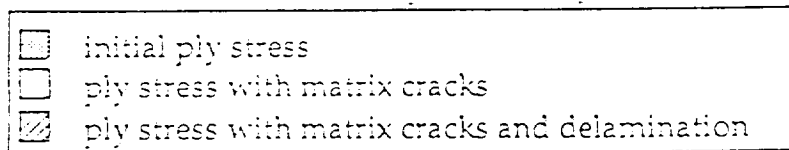
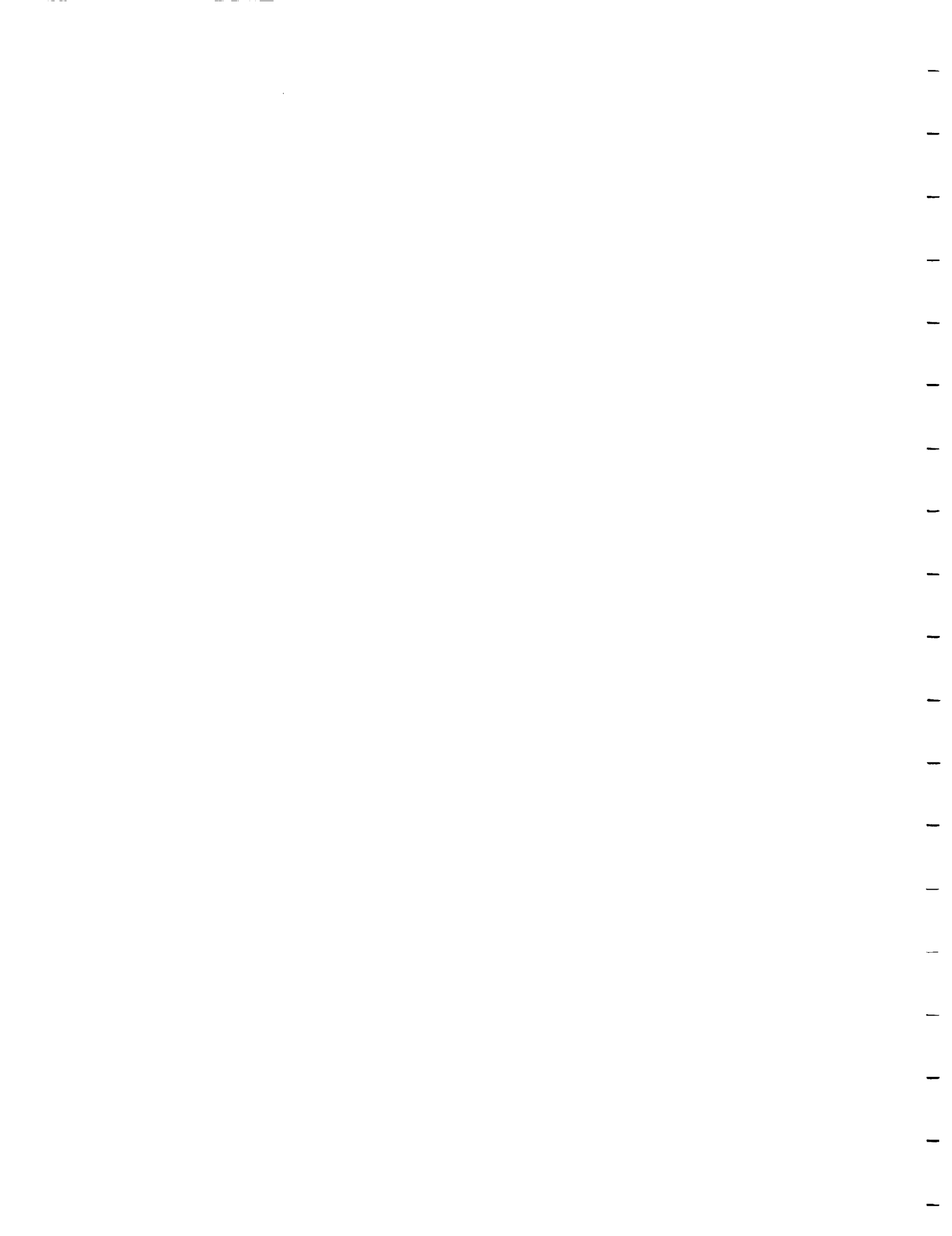
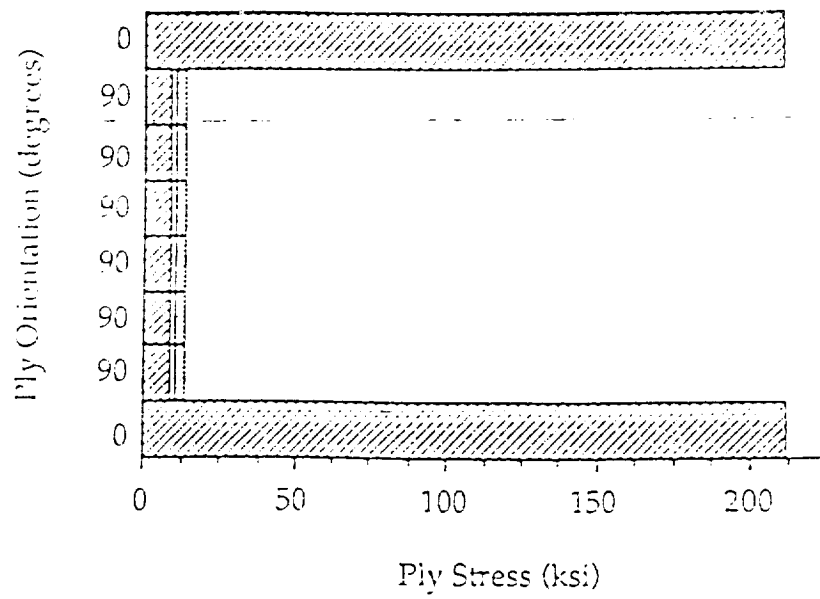


Figure 8. Far Field Stresses in a $[0_2/90_2]_s$ Laminate





$\epsilon = 0.01$

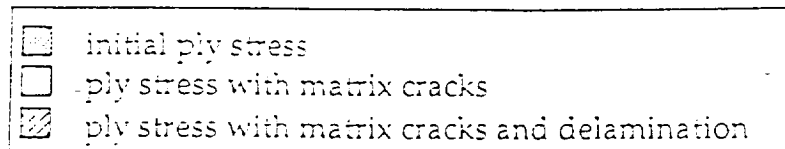
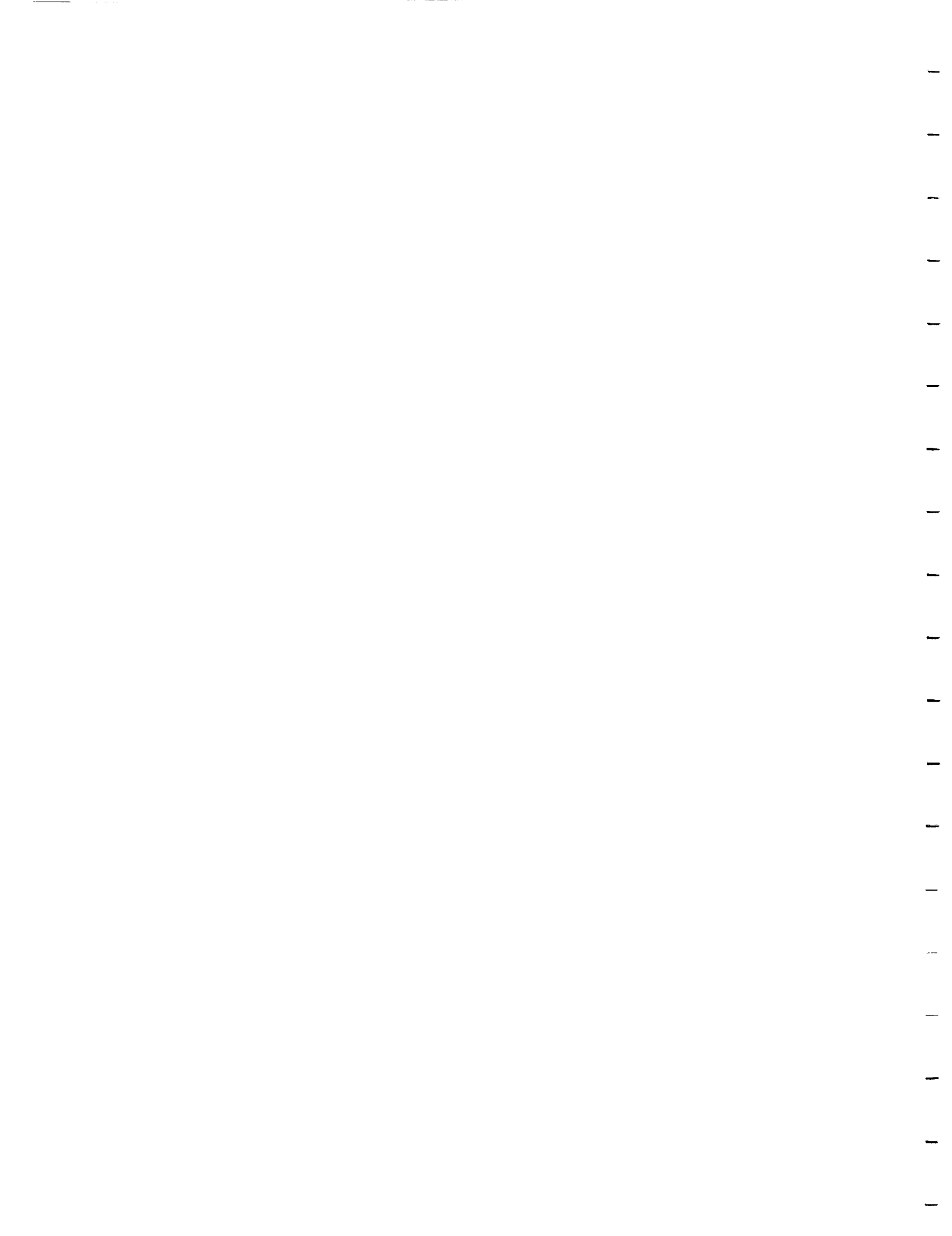
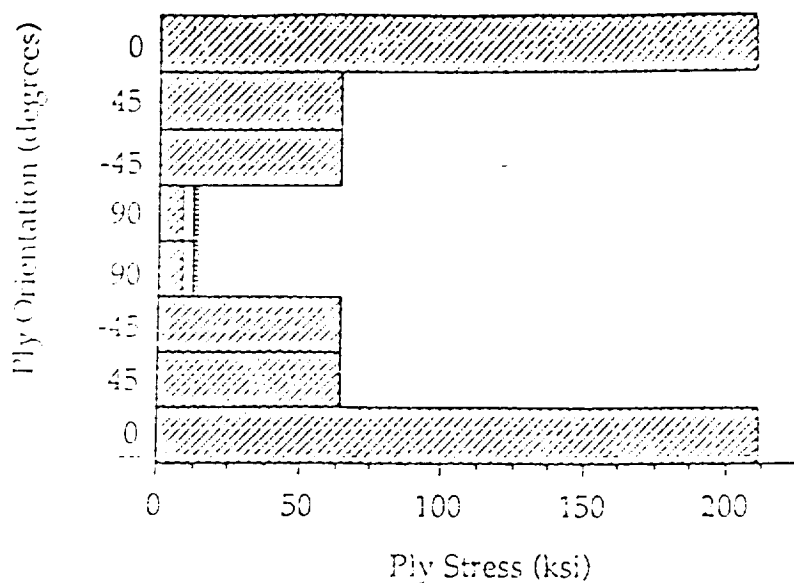


Figure 9. Far Field Ply Stresses in a $[0/90_3]_s$ Laminate





$\epsilon = 0.01$

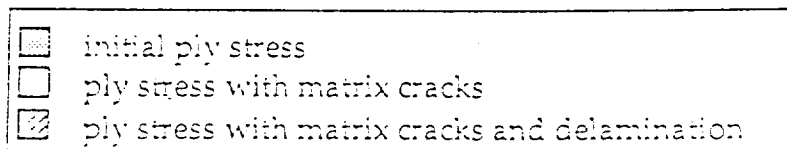
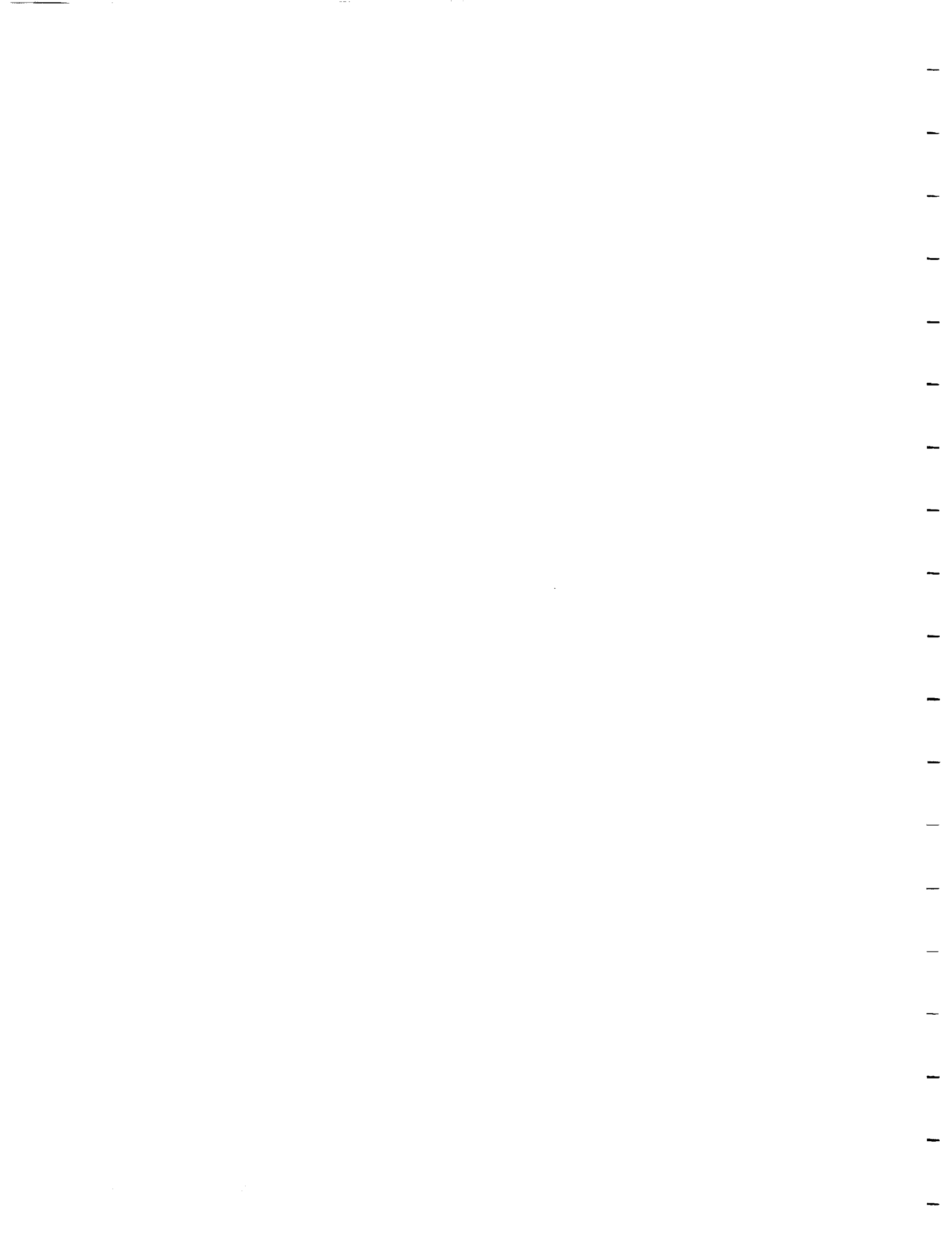
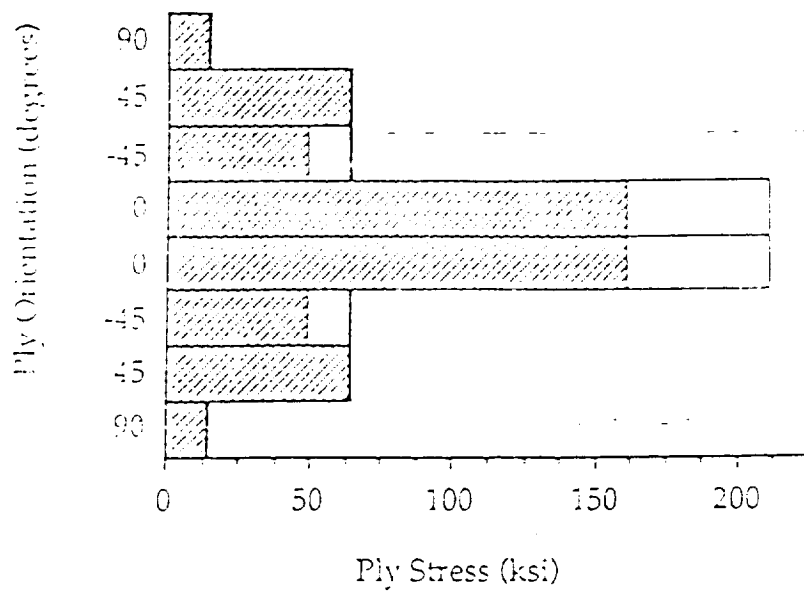


Figure 10. Far Field Ply Stresses in a $[0/\pm 45/90]_s$ Laminate





$\epsilon = 0.01$

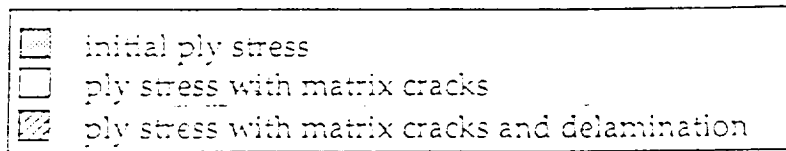
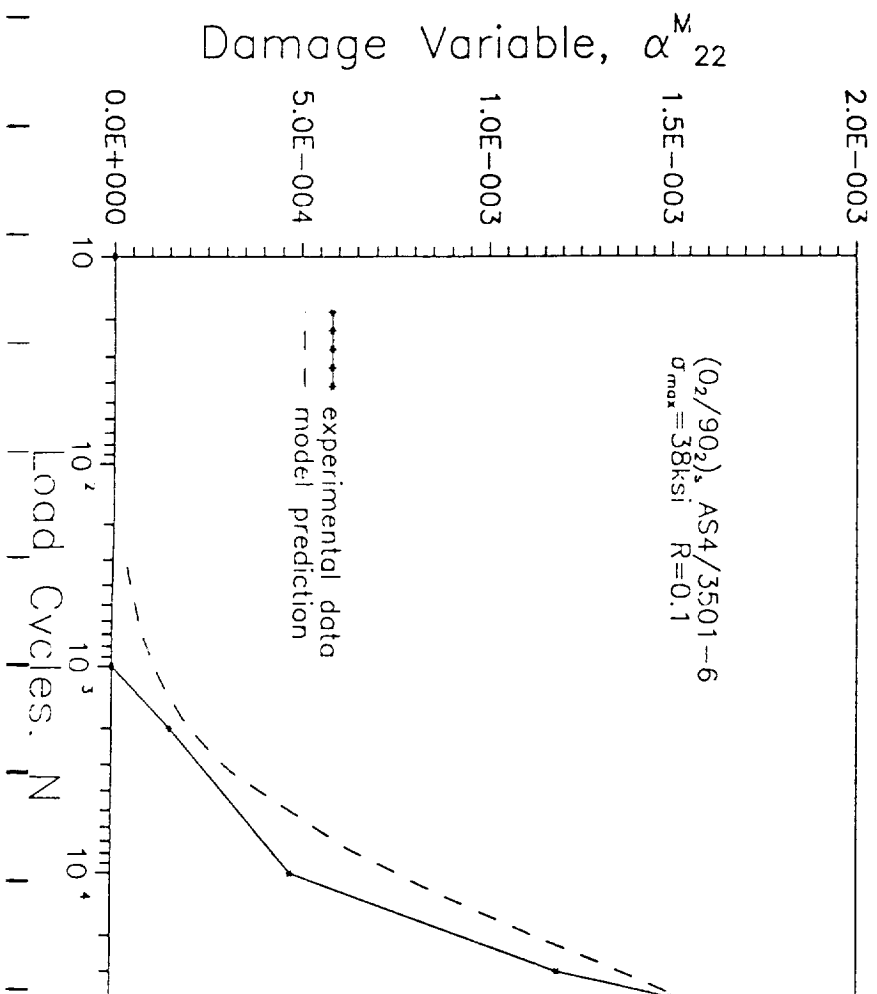


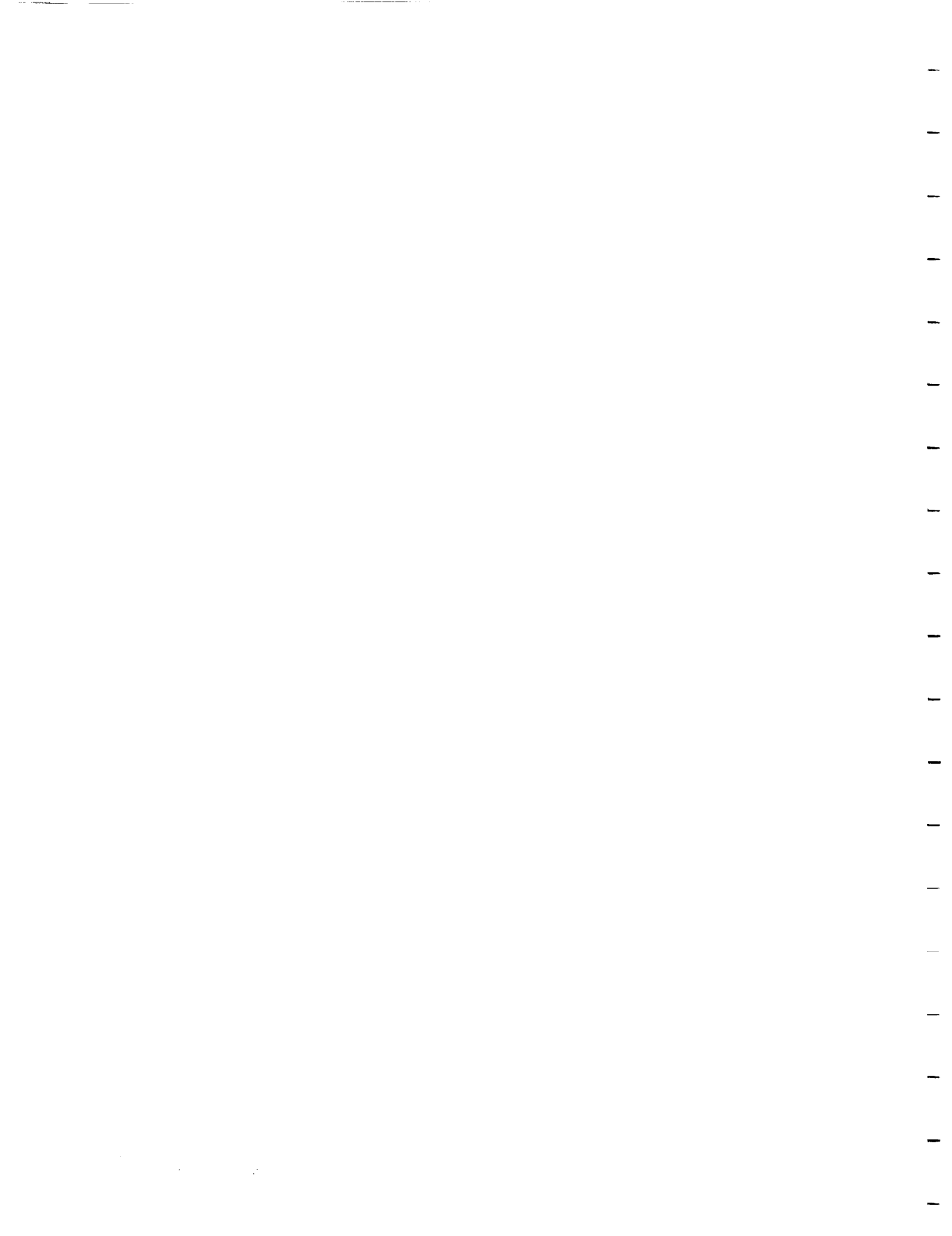
Figure 11. Far Field Ply Stresses in a $[90/\pm 45/0]_s$ Laminate

ORIGINAL PAGE IS
OF POOR QUALITY



Max. Damage = 1.5E-003
at $N = 10^4$
Cycles to Failure = 10,000
Time to Failure = 10,000
Time to Failure = 10,000

ORIGINAL PAGE IS
OF POOR QUALITY



Damage Variable, α^M_{22}

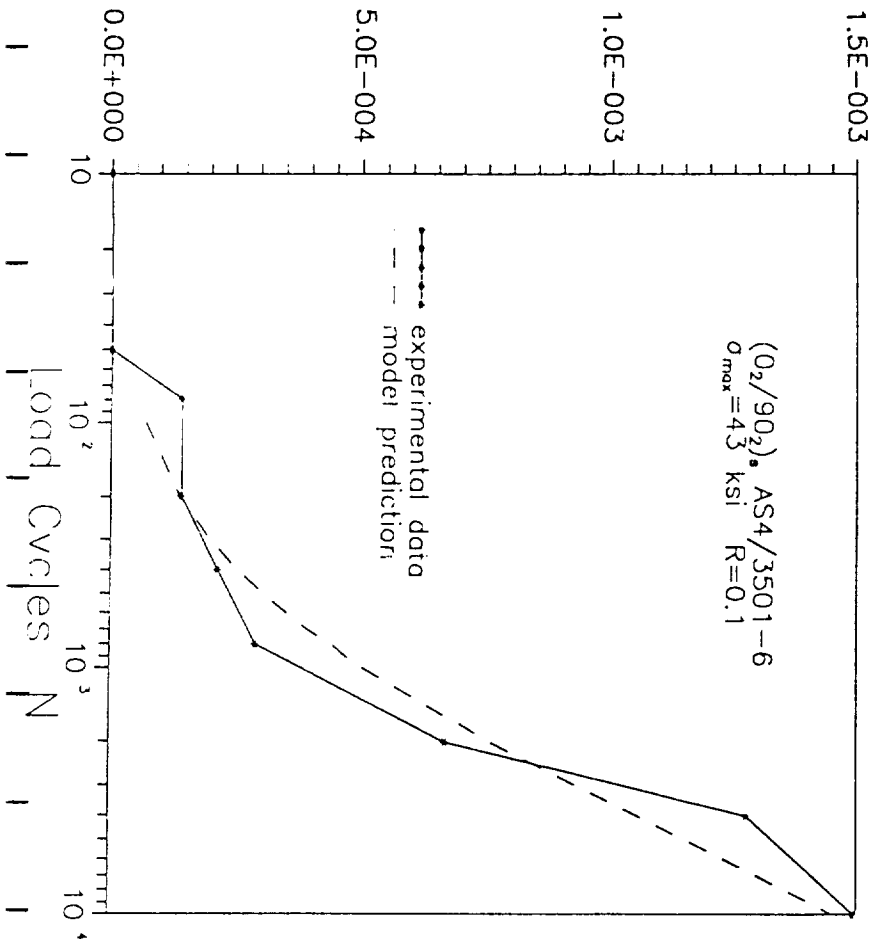
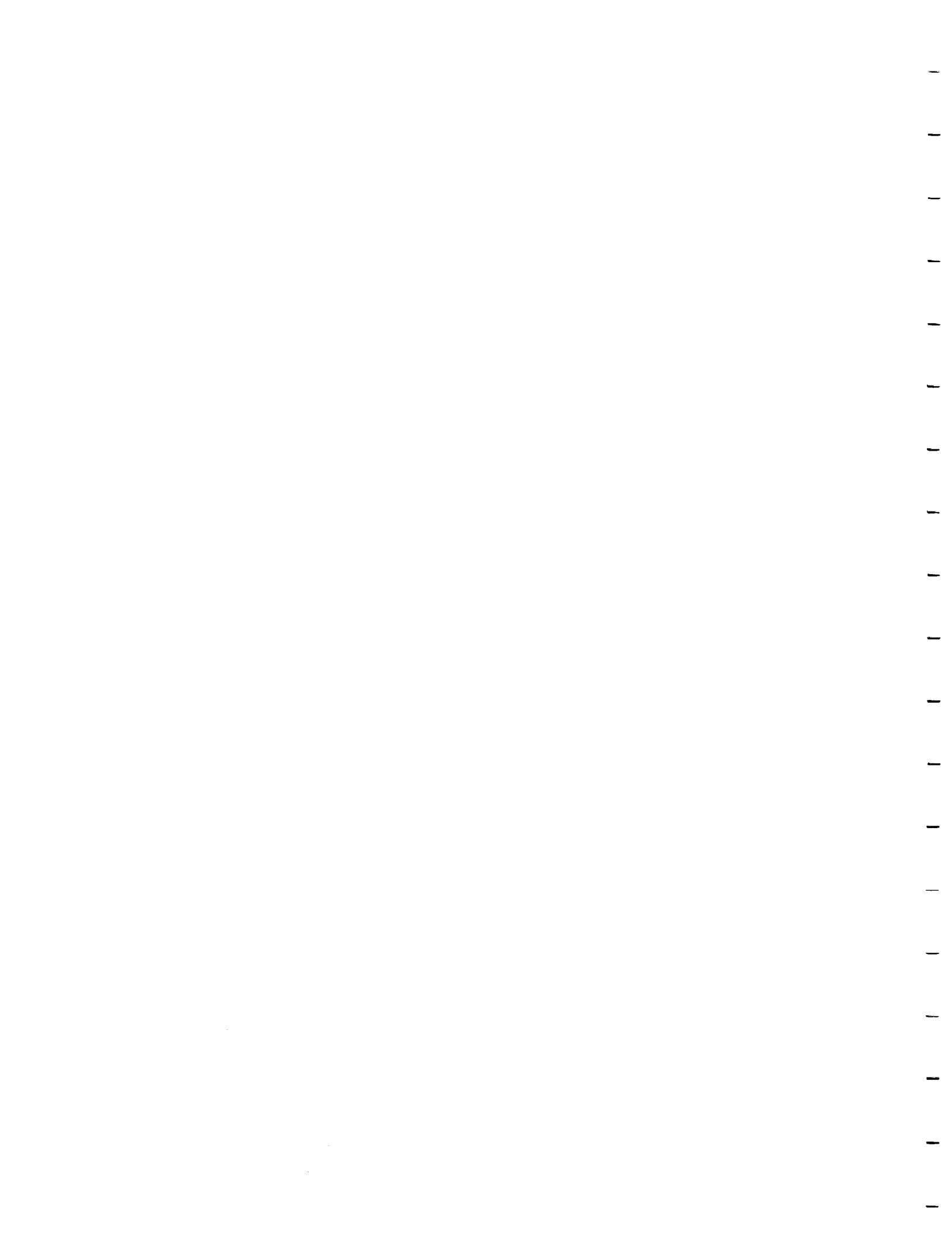
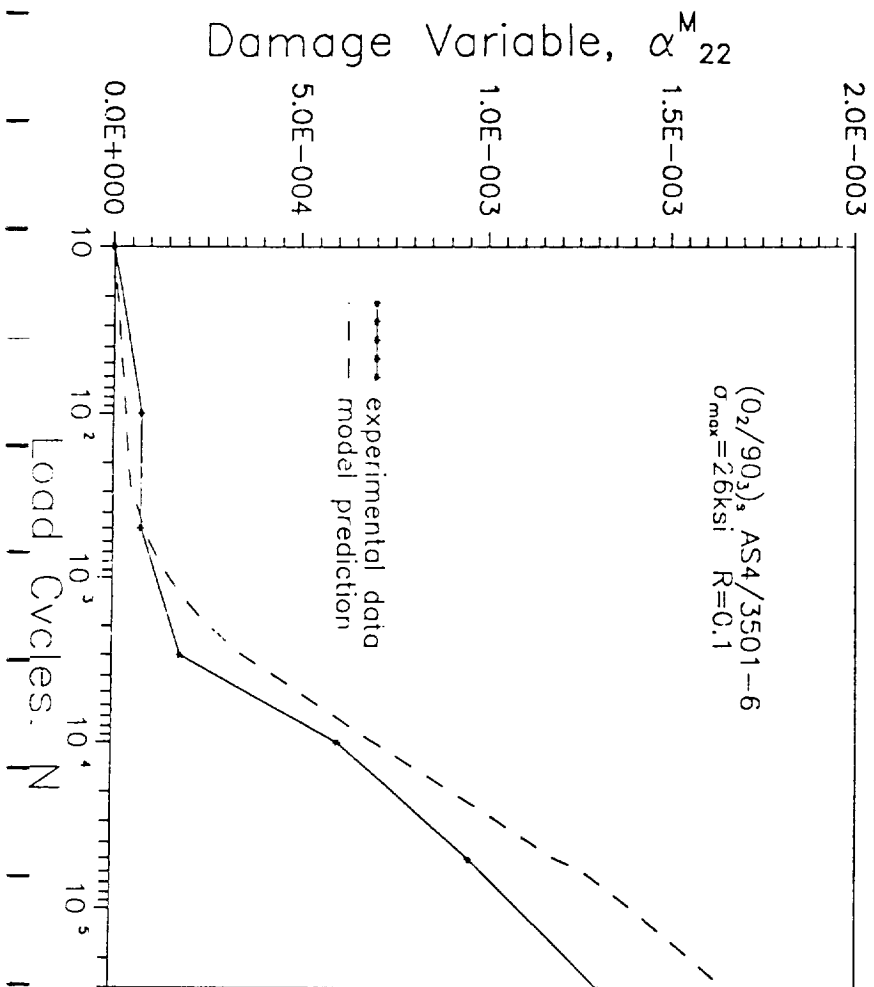


Fig. 24
 Comparison of
 experimental data
 and model prediction
 for damage evolution
 in AS4/3501-6
 under cyclic loading

ORIGINAL PAGE IS
OF POOR QUALITY



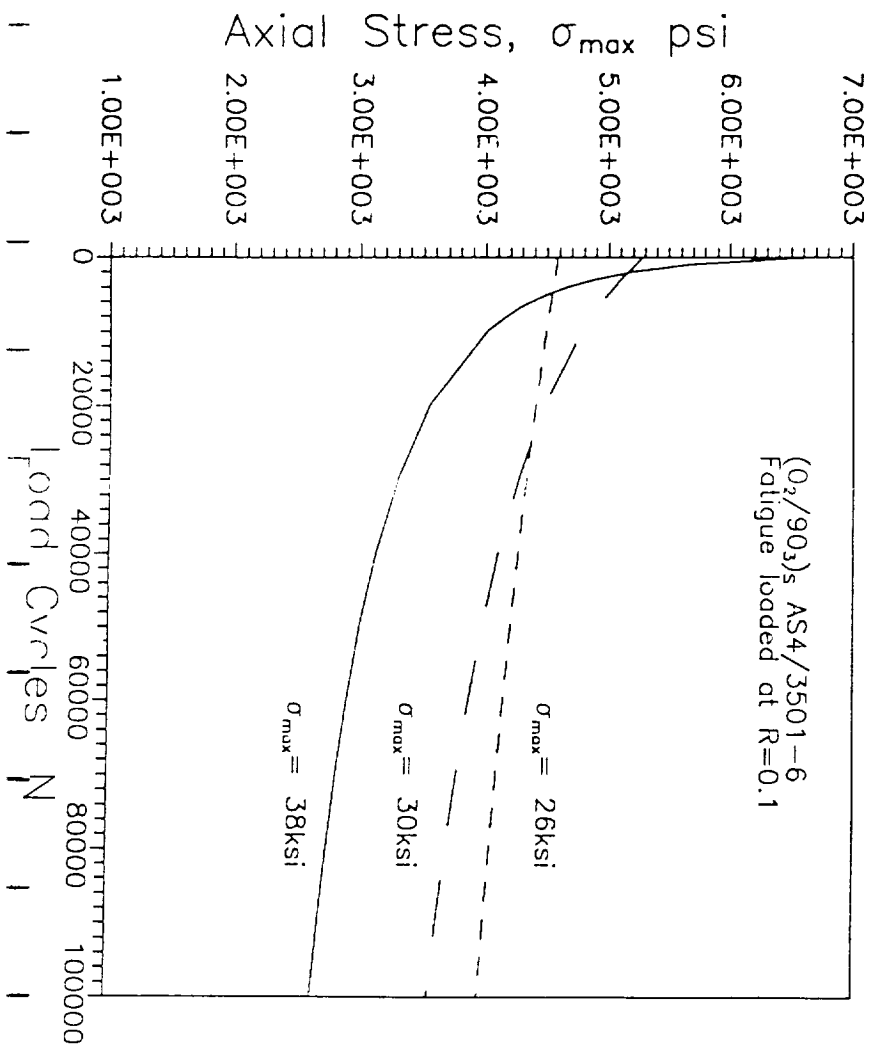


Handwritten notes:

1.0E-003
0.5E-003
0.0E+000

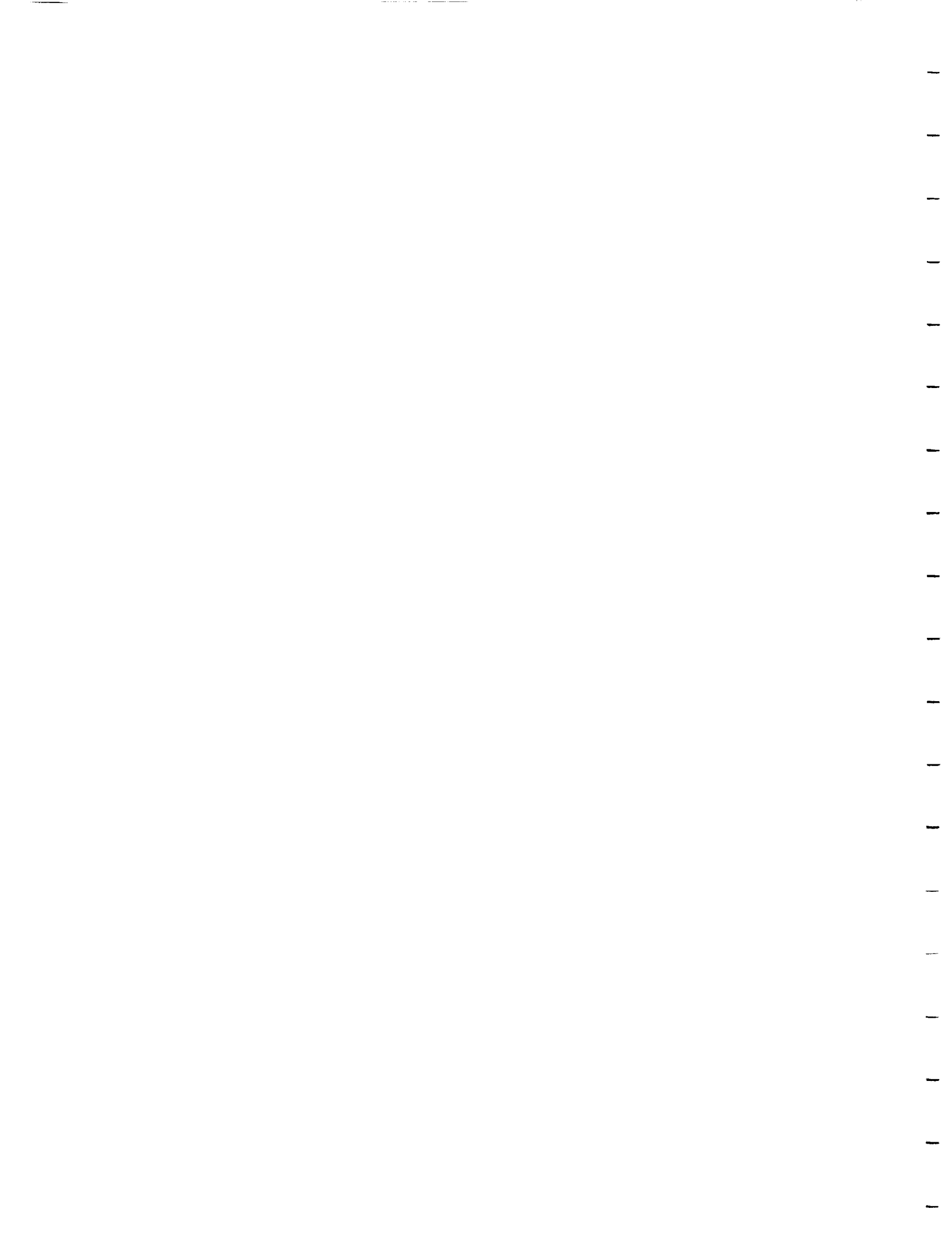
Load Cycles, N

ORIGINAL PAGE IS
OF POOR QUALITY

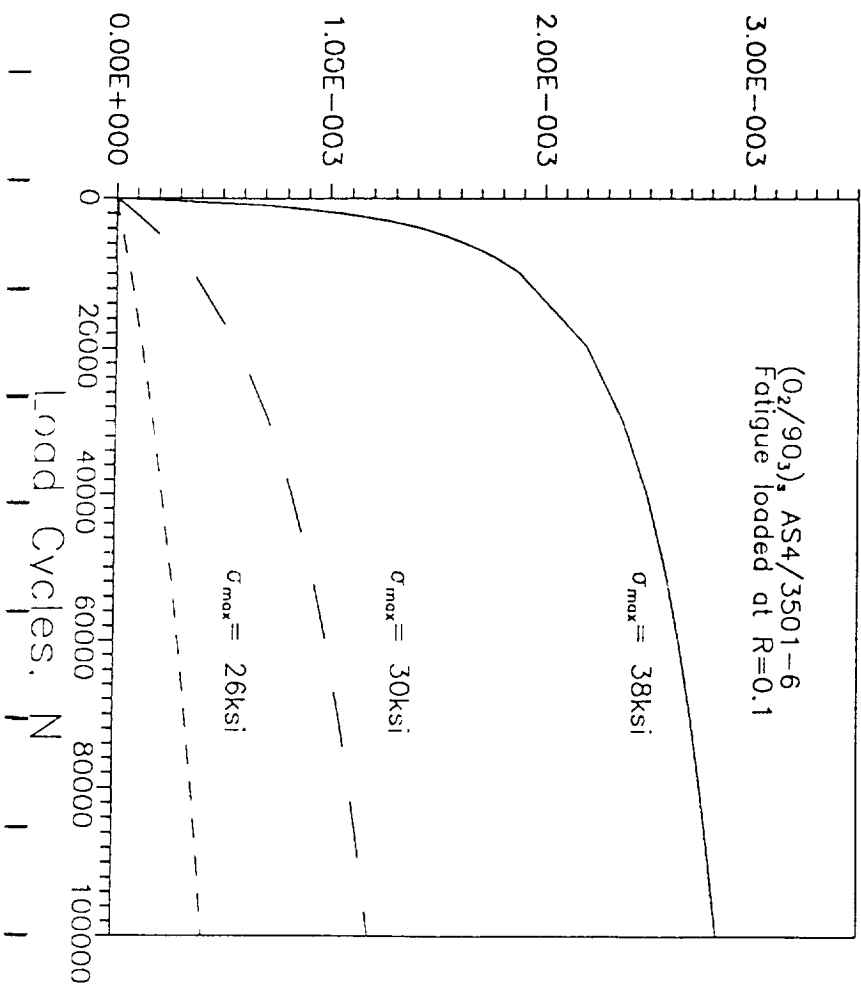


From: Barry J. Lee
 1.00E+003
 6.00E+003
 5.00E+003
 4.00E+003
 3.00E+003
 2.00E+003
 1.00E+003
 0
 Load Cycles N

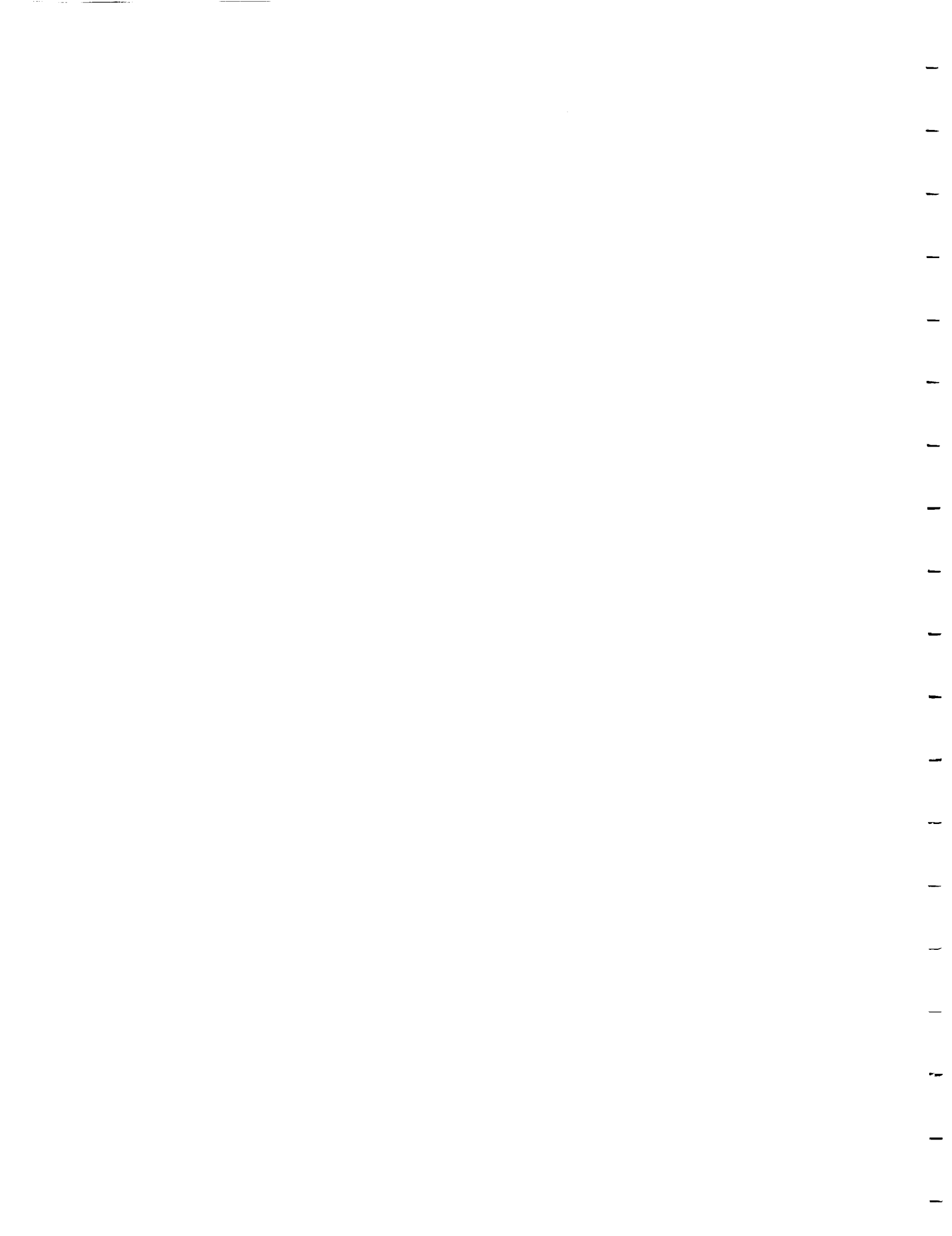
ORIGINAL PAGE IS
 OF POOR QUALITY



Damage Variable, α^M_{22}



ORIGINAL PAGE IS
OF POOR QUALITY



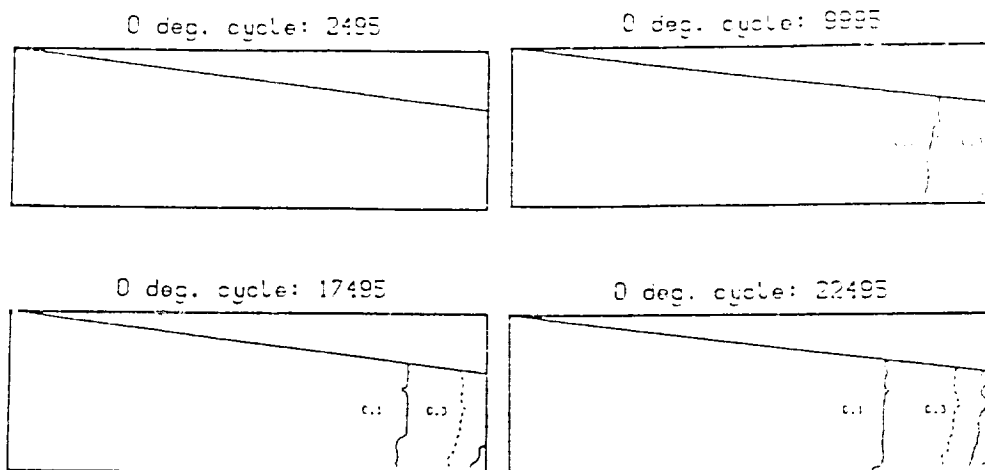


Fig. 1. The accumulation of matrix cracks in the 0° plies during various points in the loading history.

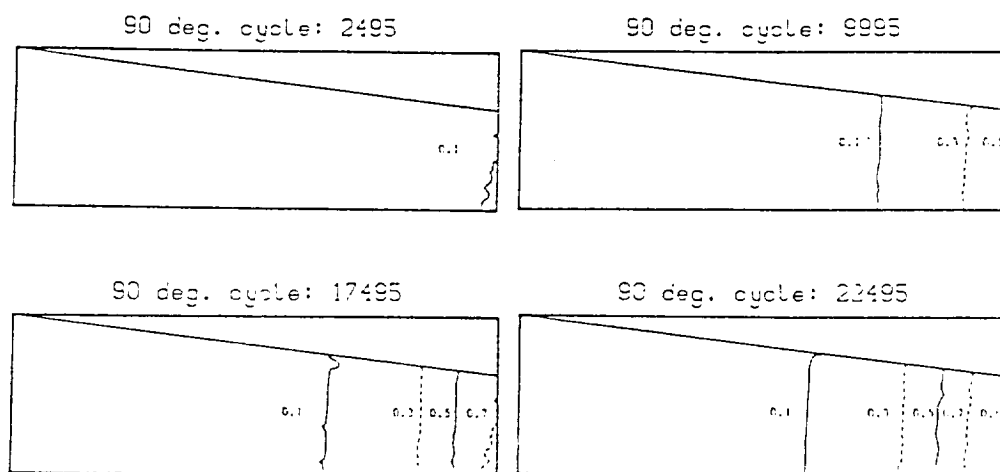


Fig. 2. The accumulation of matrix cracks in the 90° plies during various points in the loading history.

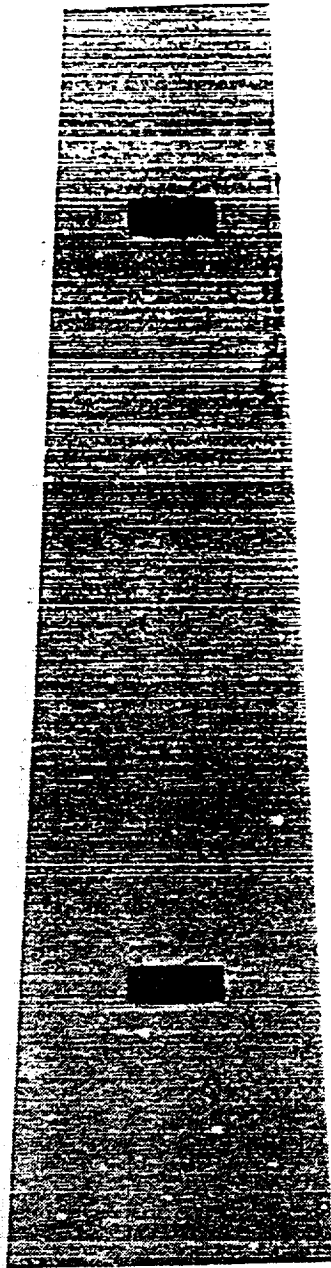
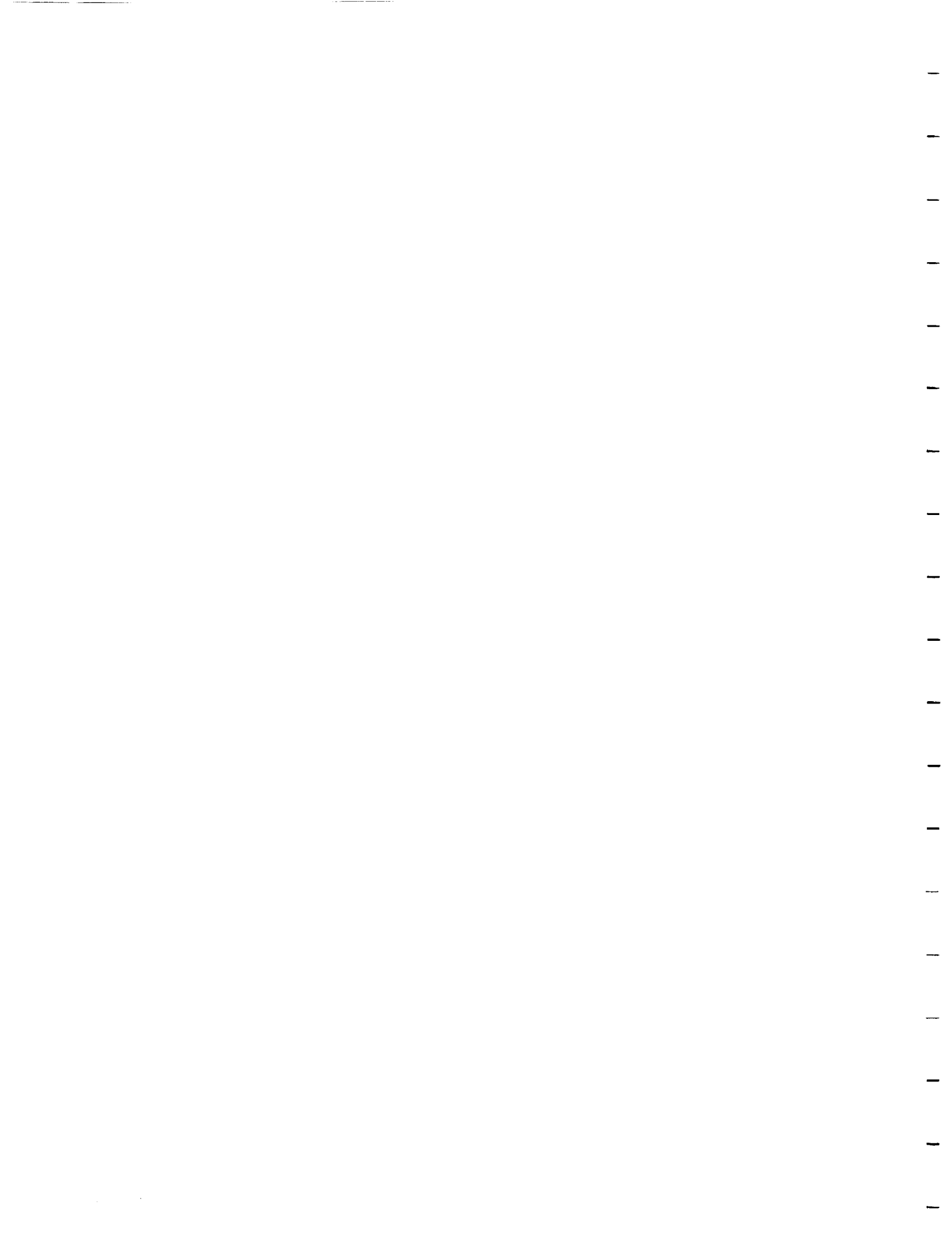


Fig. 3. X-ray radiograph of a $[0/90_2]$; AS4/3502 tapered beam specimen showing the development of transverse matrix cracks.



APPENDIX D



Damage Prediction in Laminated Composites
with Continuum Damage Mechanics

David C. Lo*
David H. Allen**
and
Kevin D. Buie†

Abstract

A finite element model is developed for laminated composite plates experiencing fatigue load induced microstructural damage. Continuum damage mechanics based constitutive relationships, in which the formation of damage with a laminated composite plate is modeled with strain-like internal state variables, are utilized to obtain the weak form of the equilibrium equation. A damage evolutionary relationship for matrix cracking is incorporated into the model to provide the capability to examine the response history of laminated plate structures. Finally, this model is implemented into a finite element computer code and is used to predict the response of a simple laminated plate structure loaded in fatigue.

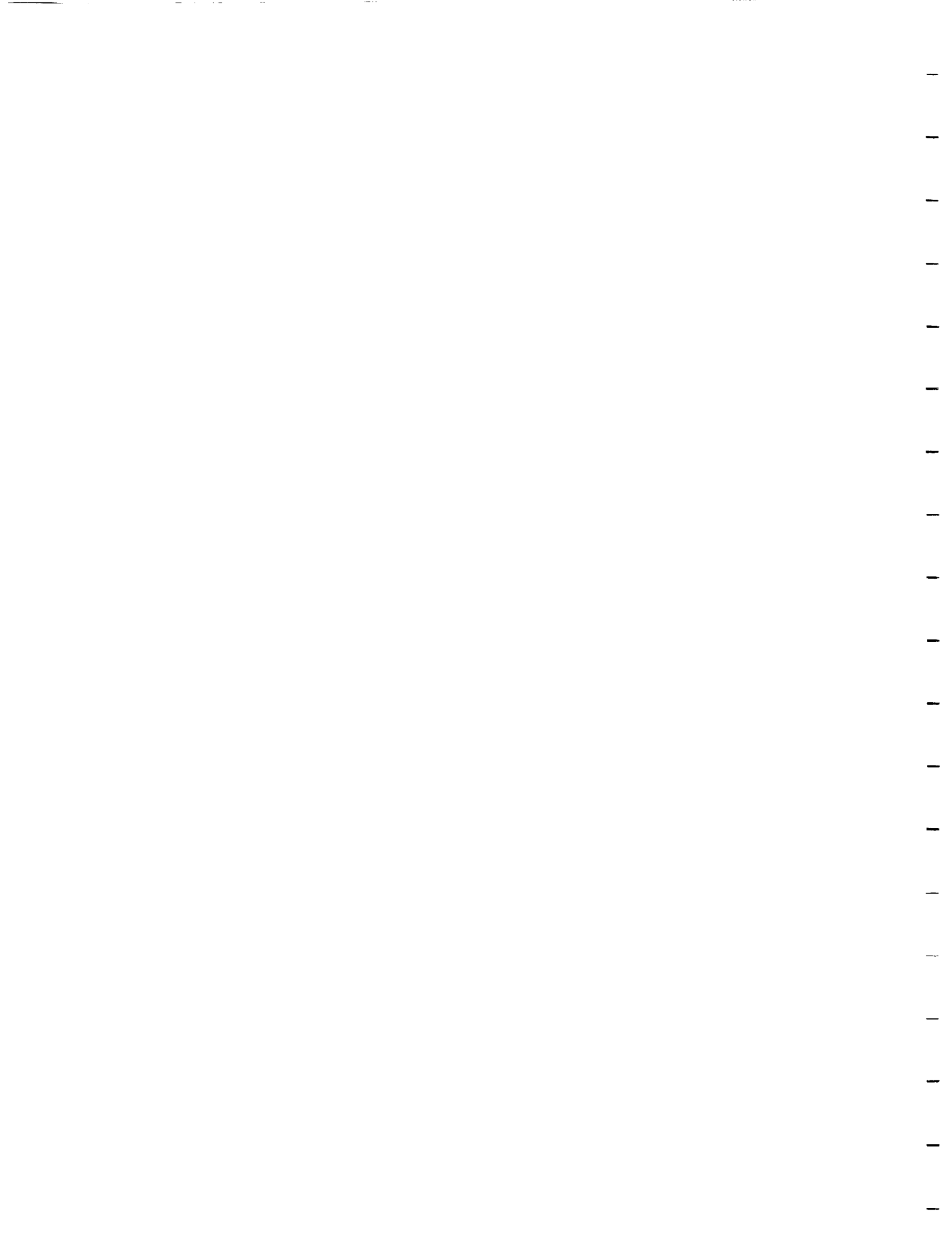
Introduction

The increasing use of laminated composite structures for engineering applications has lead to an increase in the number and types of methods introduced to analyze the mechanical response of this type of structure. Some theories incorporate the use of finite elements while others result in strictly closed form solutions. One of the earliest theories introduced for the analysis of laminated plates is known as the laminated plate theory. This theory is a modification of the classical plate theory that is based upon a set of assumptions known as Kirchhoff's hypothesis. This theory is the simplest available; however, the out-of-plane components of strain in the plate are neglected.

* Research Assistant, Aerospace Engineering Dept., Texas A&M University, College Station, TX 77843

** Professor, Aerospace Engineering Dept., Texas A&M University, College Station, TX 77843

† Rockwell Shuttle Operations Co., 600 Gemini, Houston, TX 77058

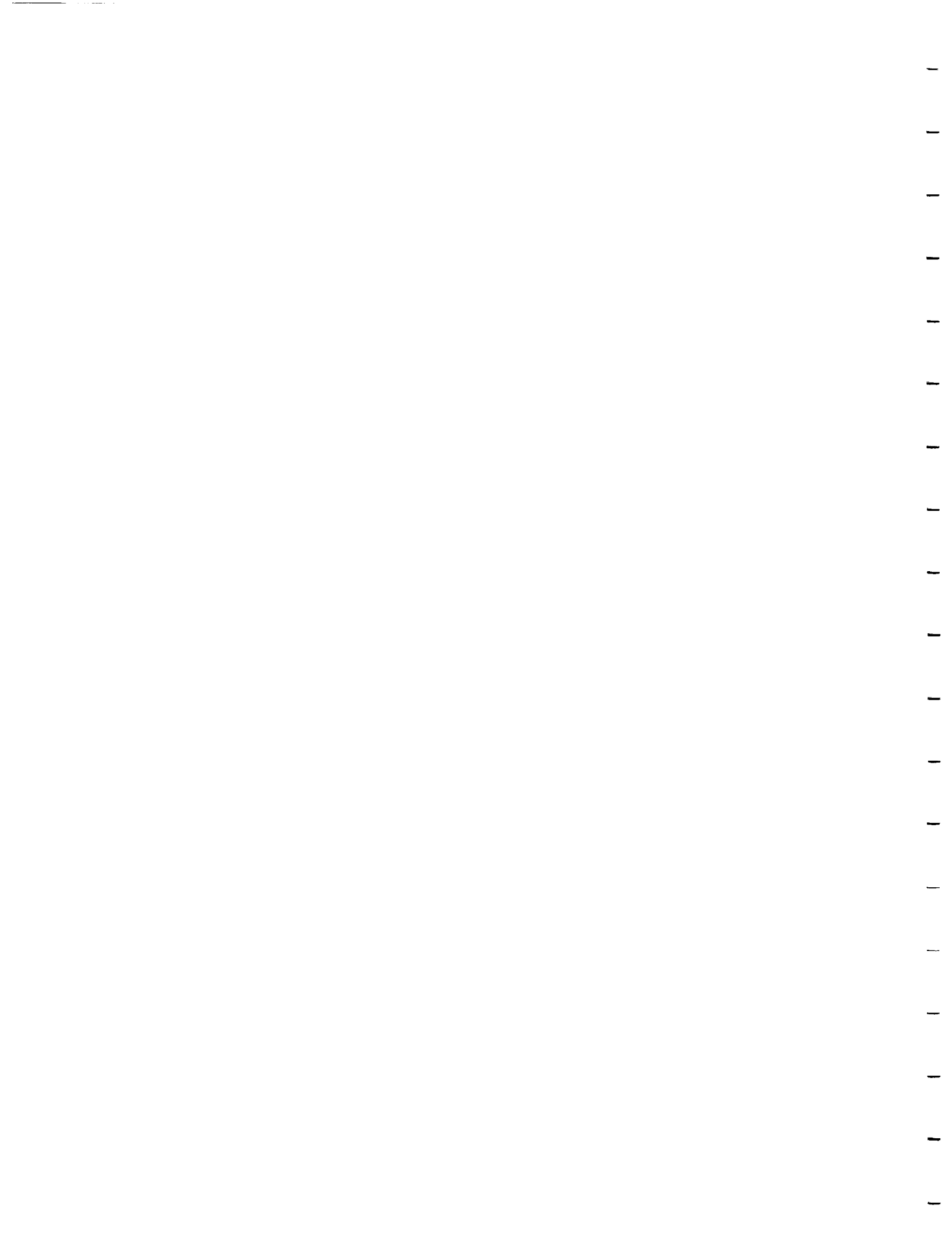


This is due to the assumption that a line normal to the mid-plane prior to deformation will remain normal to the mid-plane after deformation. Many higher-order laminated plate theories have been introduced in attempts to account for the transverse components of strain. One of the simplest higher-order laminated plate theories is known as the shear deformable theory (Reissner 1945, Mindlin 1951). The classical laminated plate theory is in fact a special case of the shear deformable theory.

To this point, very little work has been performed on laminated plate theories that account for the damage formation within the laminate and the effect it has on the material response (Reddy 1987, 1990). Damage within a laminate first appears in the form of matrix cracks and for some cases can be the only type of damage to form. At the intersection of these matrix cracks with those in the adjacent plies, interply delaminations are initiated. Edge delaminations can also be found along the free edges. These phenomena in turn contribute to the formation of fiber matrix debonds and fiber fractures which lead to catastrophic failure of the laminated composite. Experimental evidence indicates that the formation of matrix cracks and interply delaminations have a significant effect on the material properties of graphite/epoxy laminates (Norvell 1985, Georgiou 1986, Groves, et al. 1987). While other damage types affect the ultimate life of continuous fiber laminated composites, the formation of matrix cracks and interply delamination affect those properties that dictate the ultimate failure of the component. Thus, at the present time, it may be sufficient to consider only matrix cracking and interply delamination in the formulation of a laminated composite plate damage model.

New theories have been introduced in attempts to more accurately predict the response of laminated composites subjected to various loading conditions. One approach is based upon fracture mechanics; changes to the material behavior are characterized through alteration in local boundaries. Three dimensional finite elements are used to simulate observed matrix cracking patterns (Reddy, et al. 1987) and delamination formation (Murthy and Chamis 1985, 1986). Since each crack is modeled separately, a large number of elements is necessary to construct an accurate finite element mesh. Models of this magnitude will require a large amount of CPU time on a powerful computer, resulting in a very expensive solution to the problem.

It is submitted that a more cost effective method for obtaining accurate predictions to the response of laminated composites is needed. One possibility is to use continuum damage mechanics. In this approach, the averaged effects of each type of damage in a small representative volume element are considered rather than individual flaws. Thus, the boundary value problem is reduced to a simply connected domain with nonlinear material behavior and the number of finite elements is reduced to a manageable level. One of the



authors (Allen, et al. 1987a,b,c) has proposed one such continuum damage mechanics model and has produced accurate predictions to experimentally measured stiffness losses in graphite/epoxy laminated composites using the model. This model uses a set of second order tensor valued internal state variables to represent the matrix cracks and delaminations within the laminate. The incorporation of this theory into a finite element model will allow for the use of two dimensional elements in the modeling of a laminated composite plate. This will make it possible to model a laminated composite plate containing a large amount of damage with considerably fewer elements than those used by the previously discussed models. In this paper, the development of the finite element model will be presented. The accumulation of matrix cracking in a laminated composite plate is then examined with this finite element model.

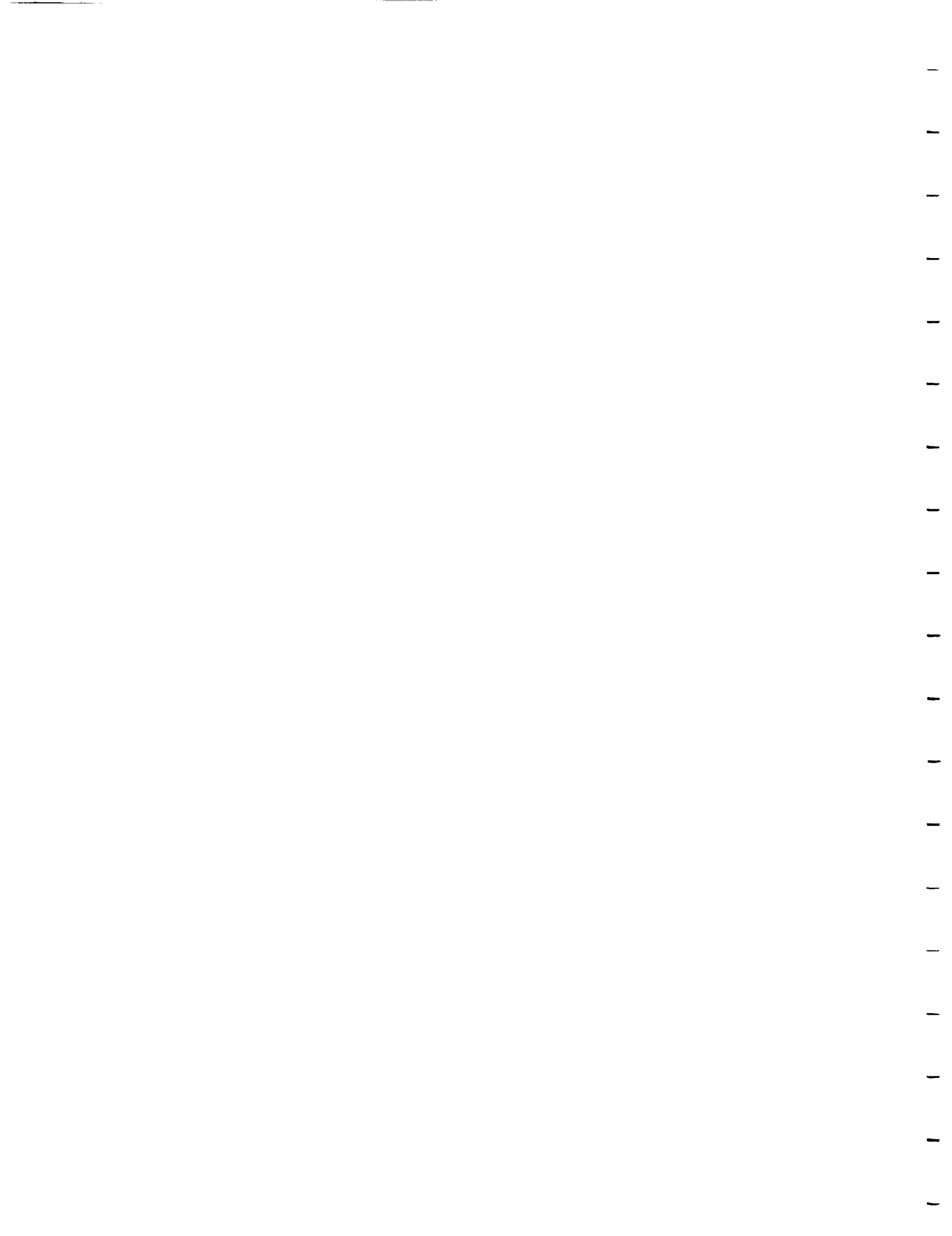
Field Problem Formulation

The formulation of the governing differential equation for a laminated composite plate with damage follows the same procedure as that used for an undamaged laminated composite plate (Agarwal and Broutman 1981). Damage in the composite plate is reflected through modified constitutive and displacement equations. The details of these equations as well as the development of the damage model can be found in several publications (Allen, et al. 1987a,b,c, 1988). Therefore, only those portions of the damage model necessary for the problem formulation will be considered herein. The effects of the matrix cracks are introduced into the ply constitutive equations through a modification of the thermodynamic constraints placed on the field problem. Specifically, the Helmholtz free energy is modified to contain the mechanical effects of matrix crack formation. This form of the Helmholtz free energy is then used to obtain the constitutive relation for an orthotropic material. Symmetry constraints are then applied to obtain the following constitutive relation:

$$\{\sigma_L\} = [Q]\{\varepsilon_L - \alpha_L^m\} \quad (1)$$

where $\{\sigma_L\}$ are the locally averaged components of stress, $[Q]$ is the transformed anisotropic stiffness matrix for the ply, $\{\varepsilon_L\}$ are the locally averaged components of strain, and $\{\alpha_L^m\}$ are the components of the internal state variable for matrix cracking in terms of laminate coordinates. They are defined to be the matrix crack surface displacements averaged over a local volume (Allen, et al. 1987a).

The presence of interply delamination in the laminate introduces jump discontinuities in the displacements and rotations of the normal line to the midplane. Since the normal to the midplane prior to deformation does not remain normal to the deformed surface of the midplane after deformation, it is no longer valid to neglect the out-of-plane shear strains in the problem formulation. In fact, it is through these out-of-plane shear strain terms that the



effects of the interply delaminations are introduced into the damage model development. The displacement equations are thus assumed to be of the following form (Allen, et al. 1987c):

$$u(x, y, z) = u^o(x, y) - z[\beta^o + H(z - z_i)\beta_i^D] + H(z - z_i)u_i^D, \quad (2)$$

$$v(x, y, z) = v^o(x, y) - z[\eta^o + H(z - z_i)\eta_i^D] + H(z - z_i)v_i^D, \quad (3)$$

$$w(x, y, z) = w^o(x, y) - H(z - z_i)w_i^D. \quad (4)$$

where u^o , v^o , and w^o are the undamaged midplane displacements; β^o and η^o are the undamaged ply rotations; u_i^D , v_i^D , and w_i^D are the ply jump displacements due to delamination; β_i^D and η_i^D are the ply jump rotations due to delaminations. The internal state variables corresponding to the delaminations are defined as the values of these jump rotations averaged over all the delamination surfaces. Finally, $H(z - z_i)$ is the Heavyside step function. The displacement equations are averaged over a local area to produce locally averaged displacements that are used in the laminate formulation.

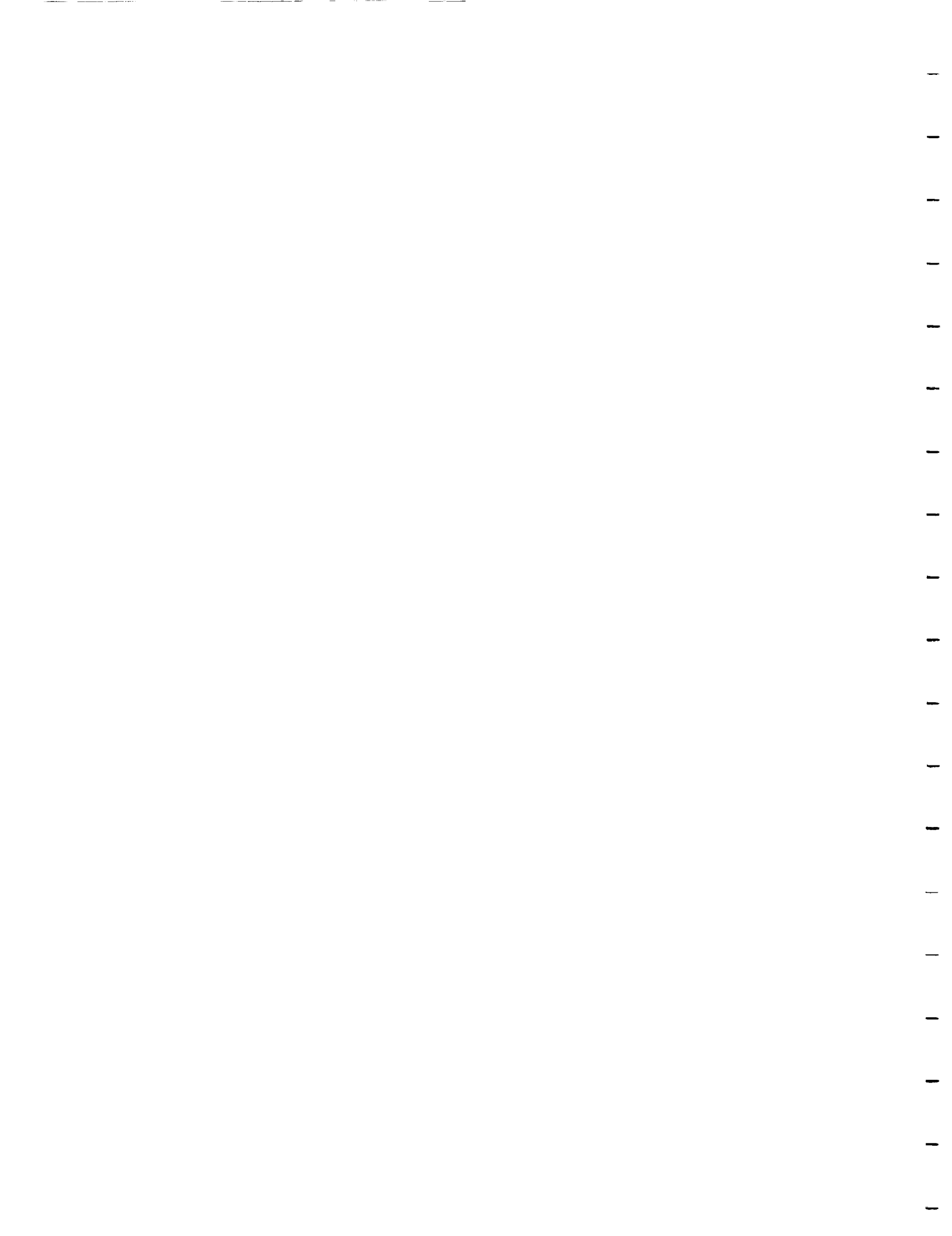
The laminate constitution is then obtained by integrating the ply constitutive equations through the thickness. The ply constitution is assumed to be anisotropic since the jump discontinuities in the displacements resulting from delamination produce local anisotropic responses. That is, the local out-of-plane shear strains, γ_{Lyx} and γ_{Lxz} , resulting from delamination will contribute to the resultants. The laminate equations for the force and moment resultants are,

$$\{N\} = [A]\{\epsilon_L^o\} + [B]\{\kappa_L\} + \{f^M\} + \{f^D\}, \quad (5)$$

$$\{M\} = [B]\{\epsilon_L^o\} + [D]\{\kappa_L\} + \{g^M\} + \{g^D\}, \quad (6)$$

where $[A]$, $[B]$, and $[C]$ are the laminate extensional stiffness matrix, coupling stiffness matrix, and bending stiffness matrix, respectively. $\{f^M\}$ and $\{f^D\}$ are "damage induced forces" resulting from the matrix cracks and delaminations. Their application to an undamage laminate will produce an equivalent amount of strain to those caused by the matrix crack and delamination damage surface kinematics. $\{g^M\}$ and $\{g^D\}$ corresponds to the "damage induced moments." These "damage induced forces and moments" are determined from the corresponding internal state variables (Allen, et al. 1988). The laminate equations (5) and (6) are substituted into the plate equilibrium equations to yield the governing differential equations for the plate deformations. The governing equation for the out-of-plane deformation is (Buie 1988),

$$\begin{aligned} p_z = & D_{11} \frac{\partial^4 w^o}{\partial x^4} + 4D_{16} \frac{\partial^4 w^o}{\partial x^3 \partial y} + 2(D_{12} + 2D_{66}) \frac{\partial^4 w^o}{\partial x^2 \partial y^2} \\ & + 4D_{26} \frac{\partial^4 w^o}{\partial x \partial y^3} + D_{22} \frac{\partial^4 w^o}{\partial y^4} - \frac{\partial^2}{\partial x^2} (g_1^M + g_1^D) \\ & - \frac{\partial^2}{\partial y^2} (g_2^M + g_2^D) - 2 \frac{\partial^2}{\partial x \partial y} (g_3^M + g_3^D). \end{aligned} \quad (7)$$



The in-plane governing equations are of similar form. The governing differential equations are then integrated against a test function in the variational formulation of the laminated plate equilibrium equations.

Finite Element Discretization

In the current formulation, it is assumed that a total of five degrees of freedom exist at each node. The components of deformation at a node consist of two in-plane displacements, one out-of-plane displacement, and two out-of-plane rotations. The following displacement fields are assumed to represent the components of deformation within the element:

$$u_L^o = \sum_{j=1}^m \Psi_j^e u_j^e, \quad (8)$$

$$v_L^o = \sum_{j=1}^m \Psi_j^e v_j^e, \quad (9)$$

$$w_L^o = \sum_{i=1}^p \Phi_i^e \delta_i^e, \quad (10)$$

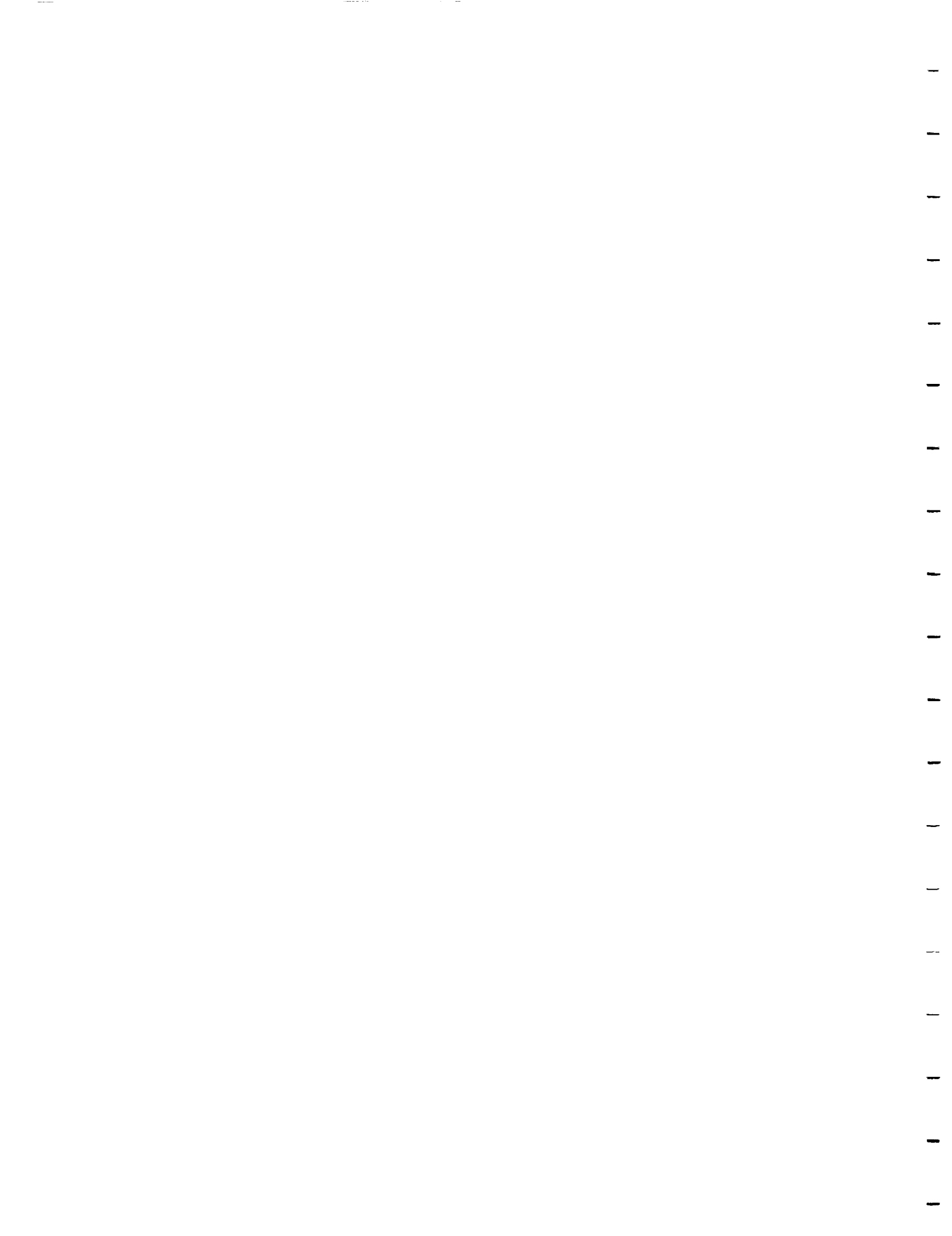
where $\{\delta_i^e\}$ are the out-of-plane displacement and rotational components, Ψ_j^e and Φ_i^e represent the shape functions for the element, m is the number of nodes the element contains and p is three times the number of nodes. Substituting the aforementioned displacement fields into the weak formulation of the plate equilibrium equations will result in the following elemental stiffness and force matrices (Buie 1988),

$$\begin{bmatrix} K^{11} & K^{12} & 0 \\ K^{21} & K^{22} & 0 \\ 0 & 0 & K^{33} \end{bmatrix} \begin{Bmatrix} u \\ v \\ \delta \end{Bmatrix} = \begin{Bmatrix} F_A^1 \\ F_A^2 \\ F_A^3 \end{Bmatrix} + \begin{Bmatrix} F_M^1 \\ F_M^2 \\ F_M^3 \end{Bmatrix} + \begin{Bmatrix} F_D^1 \\ F_D^2 \\ F_D^3 \end{Bmatrix}, \quad (11)$$

where $[K]$ is the elemental stiffness matrix, $\{F_A\}$ is the applied force matrix, and $\{F_M\}$ and $\{F_D\}$ are the "damage induced" force matrices resulting from matrix cracking and delamination, respectively. For the model developed in the present work, a three node triangular element with five degrees of freedom per node is selected. This element is formed by combining the constant strain triangular element and a nonconforming plate bending element (Buie 1988).

Internal State Variable Growth Law

The values of the internal state variable used to represent the effects of matrix cracking and delamination are found through the damage evolution laws. These evolution laws describe the rate at which the internal state variables are changing and are functions only of the current state at each material



point. The damage state, as described by the damage variables, can be found at any point in the loading history by integrating the damage evolutionary laws. The authors have recently developed one such relationship for the internal state variable representing mode I matrix cracking under fatigue loading conditions (Lo, et al. 1990). The rate of change of this internal state variable during fatigue loading is expressed by

$$d\alpha_{22} = \frac{d\alpha_{22}}{dS} k G^n dN \quad (12)$$

where $\frac{d\alpha_{22}}{dS}$ describes the change in the internal state variable for a given change in the crack surface area, k and n are material parameters. G is the strain energy release rate for the damaged ply, and N is the number of load cycles. Because the evolutionary relationship is dependent only on ply level quantities, its application is not restricted to a particular laminate stacking sequence. The interactions with the adjacent plies and damage sites are implicitly reflected in the calculations through the laminate averaging process. Equation (12) can therefore be used to model both the transverse matrix cracks and axial splits in crossply laminates subjected to tensile loading conditions. The formulation of the delamination evolutionary relationship is currently in progress. It will be incorporated into the model once it becomes available.

Model Application

A finite element code has been developed based on the above formulation. The implementation of the damage evolutionary relationship shown in equation (12) requires that the solution algorithm be repeated for every load cycle. During each cycle, the ply stresses are calculated and used to determine the increment of change in the matrix crack internal state variable for each ply. The updated damage state is then used in the calculation of the laminate and ply response at the next load cycle.

The response of a laminated tapered beam subjected to uniaxial fatigue loading conditions has been examined. This beam has a $[0/90_2]$ stacking sequence and possesses the material properties of continuously reinforced AS4/3502 Graphite/Epoxy. Its length is 17.78cm and the width is 4.50cm at the clamped end and tapered to 2.87cm at the end where the load is applied. The beam is loaded at a distributed load amplitude of $17.5 \times 10^3 \text{ N/m}$ and $R = 0.1$. Since the beam is symmetric about its length, it is sufficient to model half of the beam with a mesh containing 28 elements, 24 nodes, and 120 degrees of freedom. The development of matrix cracks, during the loading history, in the 0° and 90° plies as represented by the internal state variables is shown in Figs. 1 and 2, respectively. For clarity, the damage levels in each ply are normalized by the largest value of the internal state variable within that ply at the end of 22495 load cycles. The predicted results indicate that the matrix cracks first occur in the 90° plies at the narrow end and progress



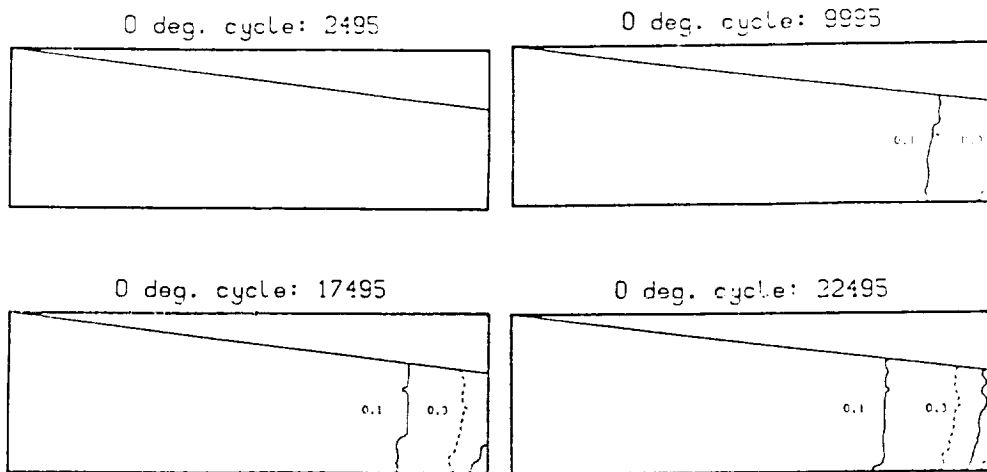


Fig. 1. The accumulation of matrix cracks in the 0° plies during various points in the loading history.

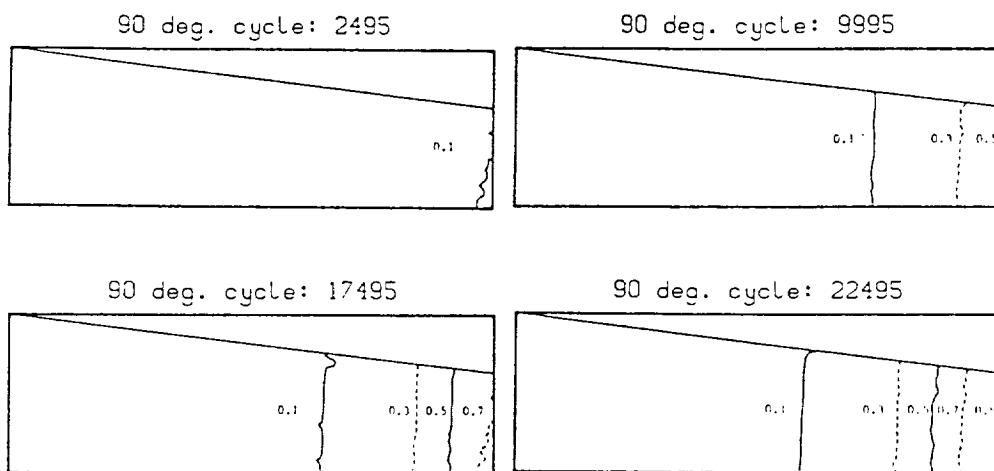
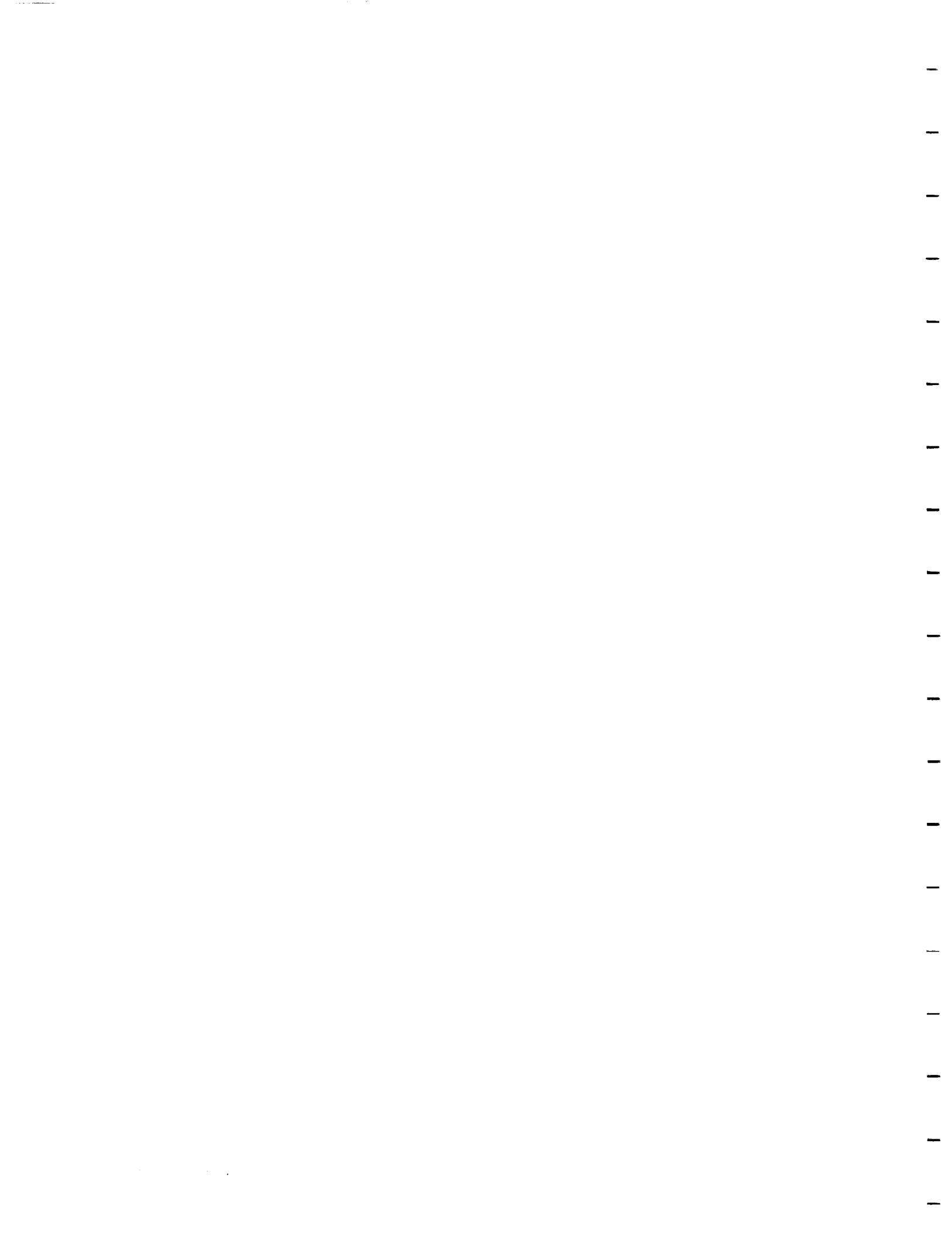


Fig. 2. The accumulation of matrix cracks in the 90° plies during various points in the loading history.



toward the wider end as loading continued. Axial splits in the 0° plies do not develop until after the appearance of the transverse matrix cracks in the 90° plies. Thus, the transverse matrix cracks serve as the driving mechanisms for the axial splits. As the transverse matrix cracks accumulate, loads carried by the 90° plies are transferred to the 0° plies. Depending on the amplitude of the fatigue load, more than half of the load initially carried by the undamaged 90° plies can be transferred to the 0° plies (Lo, et al. 1990). The additional loads coupled with the stress concentrations caused by the transverse matrix cracks create suitable conditions for the growth of axial splits. The results also show that the progression of transverse matrix cracks along the length of the tapered beam decelerates near the midway point. The stresses in the region beyond the midway point are most likely to be insufficient in sustaining additional damage. Instead, the intensity of matrix damage increases at the narrow end during the latter portion of the loading history. This process will continue until the matrix cracks have either reached the saturation level or when the laminate fails. The model predictions are qualitatively supported by the experimental result shown in Fig. 3.

Summary and Conclusion

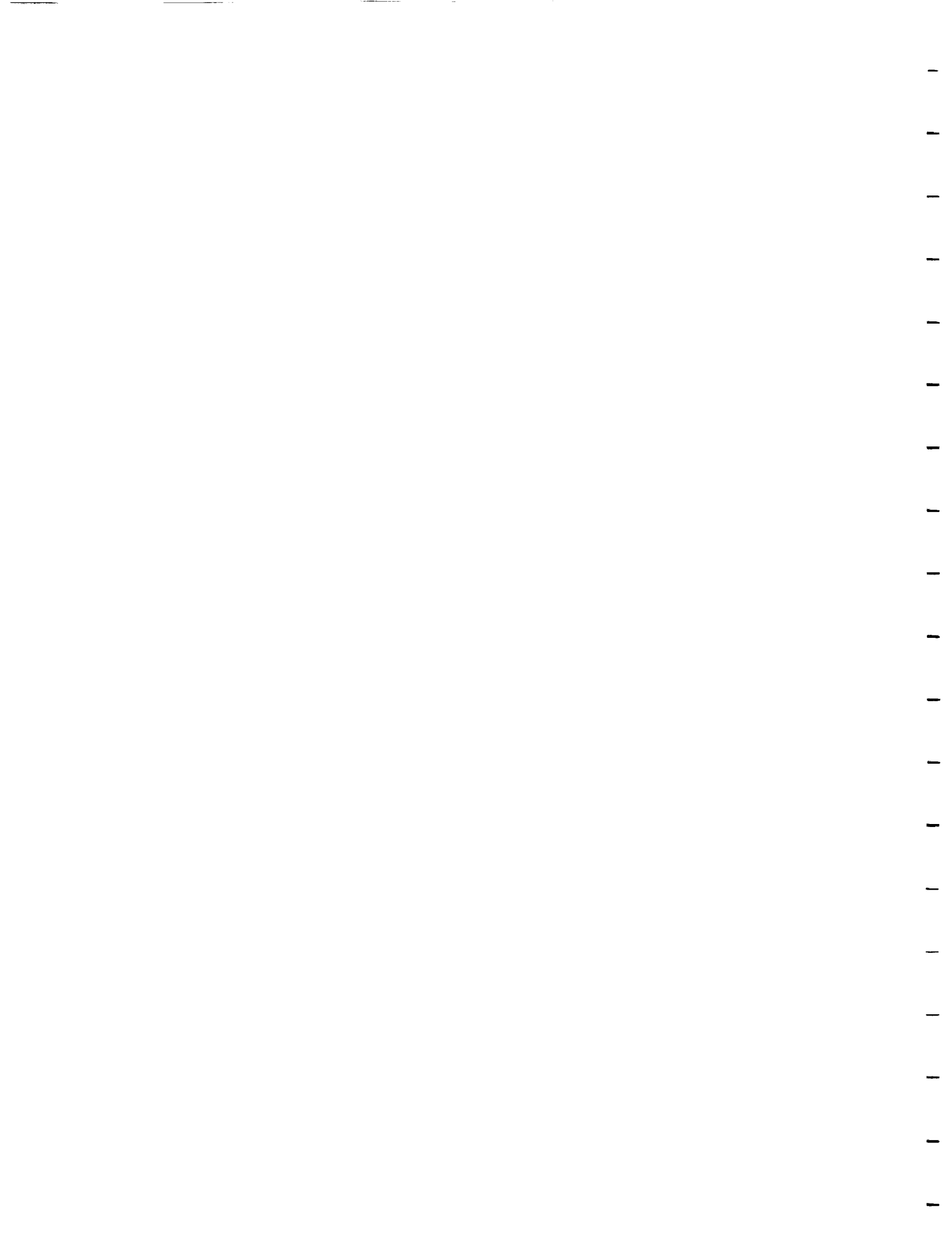
The authors have implemented a continuum damage mechanics model for laminated composite plates into a finite element computer code. The representation of matrix damage by second ordered tensor valued internal state variables and the utilization of modified laminate equations in the formulation has enabled the modeling of laminated composite plates with two dimensional rather than three dimensional finite elements. The reduction in the computational requirements of this model over that of the three dimensional finite element analysis has made the analysis of composite plate structures subjected to complex loading histories a feasible task. The accumulation of matrix cracks in a tapered laminated composite beam loaded in fatigue is examined. The results reflect the damage induced load redistribution among the plies. Since this transfer of load influences the characteristic of damage accumulation and the eventual failure of the laminate, this model can assist in the determination of a laminated composite plate component's structural integrity.

Acknowledgment

The support of this work by NASA Langley Research Center under grant nos. NGT-50262 and NAG-1-979 are gratefully acknowledged.

References

- Agarwal, B.D. and Broutman, L.J., 1981, *Analysis and Performance of Fiber Composites*, John Wiley & Sons, Inc., New York.
- Allen, D.H., Groves, S.E., and Harris, C.E., 1987a. "A Thermomechanical Constitutive Theory for Elastic Composites with Distributed Damage-Part I: Theoretical Development," *Int. J. Solids Struct.*, 23 (9), pp.1301-1318.



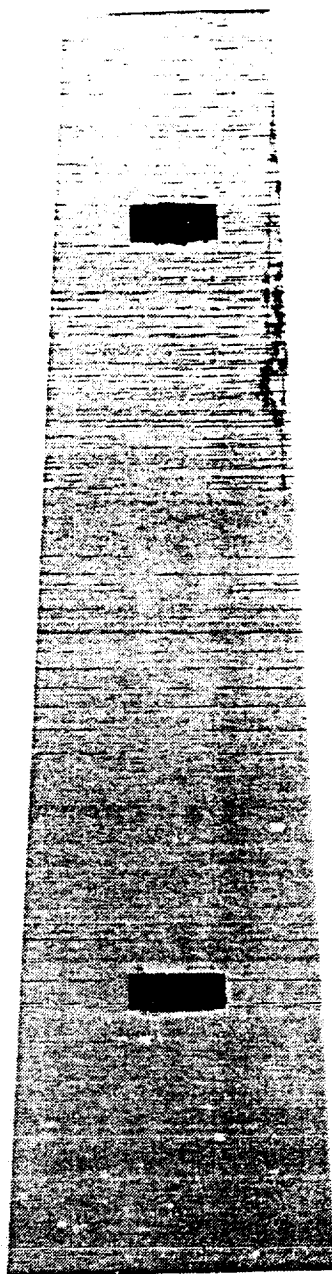


Fig. 3. X-ray radiograph of a $[0/90_2]$, AS4/3502 tapered beam specimen showing the development of transverse matrix cracks.



- Allen, D.H., Groves, S.E., and Harris, C.E., 1987b, "A Thermomechanical Constitutive Theory for Elastic Composites with Distributed Damage—Part II: Application to Matrix Cracking in Laminated Composites," *Int. J. Solids Struct.*, 23 (9), pp.1319-1338.
- Allen, D.H., Groves, S.E., and Harris, C.E., 1987c, "A Cumulative Damage Model for Continuous Fiber Composite Laminates with Matrix Cracking and Interply Delamination," Texas A&M Univ. Mechanics and Materials Center, Report No. MM-5023-87-2.
- Allen, D.H., Nottorf, E.W., and Harris, C.E., 1988, "Effect of Microstructural Damage on Ply Stresses in Laminated Composites," *Recent Advances in the Macro- and Micro-Mechanics of Composite Materials Structures*, ASME AD-Vol.13, pp.135-145.
- Buie, K.D., 1988, "A Finite Element Model for Laminated Composite Plates with Matrix Cracks and Delaminations," M.S.Thesis, Texas A&M Univ.
- Georgiou, I.T., 1986, "Initiation Mechanisms and Fatigue Growth of Internal Delaminations in Graphite/Epoxy Cross-Ply Laminates," M.S.Thesis, Texas A&M Univ.
- Groves, S.E., Harris, C.E., Highsmith, A.L., Allen, D.H., and Norvell, R.G., 1987, "An Experimental and Analytical Treatment of the Mechanics of Damage in Laminated Composites," *Exp. Mech.*, 27 (1), pp.73-79.
- Lo, D.C., Allen, D.H., and Harris, C.E., 1990, "A Continuum Model for Damage Evolution in Laminated Composites," to appear in the proceedings of the IUTAM Symposium on Inelastic Deformation of Composite Materials, Troy, New York, 1990.
- Mindlin, R.D., 1951, "Influence of Rotatory Inertia and Shear on Flexural Motions of Isotropic Elastic Plates," *J. Appl. Mech.*, 18 (1), pp.31-38.
- Murthy, P.L.N. and Chamis, C.C., 1985, "Interlaminar Fracture Toughness: Three-Dimensional Finite-Element Modeling for End-Notch and Mixed-Mode Flexure," NASA-TM-87138.
- Murthy, P.L.N. and Chamis, C.C., 1986, "Composite Interlaminar Fracture Toughness: 3-D Finite Element Modeling for Mixed Mode I, II, III Fracture," NASA-TM-88872.
- Norvell, R.G., 1985, "An Investigation of Damage Accumulation in Graphite/Epoxy Laminates," M.S.Thesis, Texas A&M University.
- Reddy, E.S., Wang, A.S.D., and Zhou, Y., 1987, "Simulation of Matrix Cracks in Composite Laminates Containing a Small Hole," *Damage Mechanics in Composites, Proc. ASME 1987 Winter Meeting*, 12, pp.83-91.
- Reddy, J.N., 1987, "Generalization of Two-Dimensional Theories of Laminated Composite Plates," *Commun. Appl. Numer. Meth.*, 3, pp.173-180.
- Reddy, J.N., 1990, "On the generalization of Displacement-Based laminate Theories," to appear in *Appl. Mech. Rev.*
- Reissner, E., 1945, "The Effect of Transverse Shear Deformation on the Bending of Elastic Plates," *J. Appl. Mech.*, 12, A-69-A-77.

1. **Introduction**
 2. **Background**
 3. **Methodology**
 4. **Results**
 5. **Discussion**
 6. **Conclusion**
 7. **References**
 8. **Appendix**
 9. **Figure 1**
 10. **Figure 2**
 11. **Figure 3**
 12. **Figure 4**
 13. **Figure 5**
 14. **Figure 6**
 15. **Figure 7**
 16. **Figure 8**
 17. **Figure 9**
 18. **Figure 10**
 19. **Figure 11**
 20. **Figure 12**
 21. **Figure 13**
 22. **Figure 14**
 23. **Figure 15**
 24. **Figure 16**
 25. **Figure 17**
 26. **Figure 18**
 27. **Figure 19**
 28. **Figure 20**
 29. **Figure 21**
 30. **Figure 22**
 31. **Figure 23**
 32. **Figure 24**
 33. **Figure 25**
 34. **Figure 26**
 35. **Figure 27**
 36. **Figure 28**
 37. **Figure 29**
 38. **Figure 30**
 39. **Figure 31**
 40. **Figure 32**
 41. **Figure 33**
 42. **Figure 34**
 43. **Figure 35**
 44. **Figure 36**
 45. **Figure 37**
 46. **Figure 38**
 47. **Figure 39**
 48. **Figure 40**
 49. **Figure 41**
 50. **Figure 42**
 51. **Figure 43**
 52. **Figure 44**
 53. **Figure 45**
 54. **Figure 46**
 55. **Figure 47**
 56. **Figure 48**
 57. **Figure 49**
 58. **Figure 50**
 59. **Figure 51**
 60. **Figure 52**
 61. **Figure 53**
 62. **Figure 54**
 63. **Figure 55**
 64. **Figure 56**
 65. **Figure 57**
 66. **Figure 58**
 67. **Figure 59**
 68. **Figure 60**
 69. **Figure 61**
 70. **Figure 62**
 71. **Figure 63**
 72. **Figure 64**
 73. **Figure 65**
 74. **Figure 66**
 75. **Figure 67**
 76. **Figure 68**
 77. **Figure 69**
 78. **Figure 70**
 79. **Figure 71**
 80. **Figure 72**
 81. **Figure 73**
 82. **Figure 74**
 83. **Figure 75**
 84. **Figure 76**
 85. **Figure 77**
 86. **Figure 78**
 87. **Figure 79**
 88. **Figure 80**
 89. **Figure 81**
 90. **Figure 82**
 91. **Figure 83**
 92. **Figure 84**
 93. **Figure 85**
 94. **Figure 86**
 95. **Figure 87**
 96. **Figure 88**
 97. **Figure 89**
 98. **Figure 90**
 99. **Figure 91**
 100. **Figure 92**
 101. **Figure 93**
 102. **Figure 94**
 103. **Figure 95**
 104. **Figure 96**
 105. **Figure 97**
 106. **Figure 98**
 107. **Figure 99**
 108. **Figure 100**
 109. **Figure 101**
 110. **Figure 102**
 111. **Figure 103**
 112. **Figure 104**
 113. **Figure 105**
 114. **Figure 106**
 115. **Figure 107**
 116. **Figure 108**
 117. **Figure 109**
 118. **Figure 110**
 119. **Figure 111**
 120. **Figure 112**
 121. **Figure 113**
 122. **Figure 114**
 123. **Figure 115**
 124. **Figure 116**
 125. **Figure 117**
 126. **Figure 118**
 127. **Figure 119**
 128. **Figure 120**
 129. **Figure 121**
 130. **Figure 122**
 131. **Figure 123**
 132. **Figure 124**
 133. **Figure 125**
 134. **Figure 126**
 135. **Figure 127**
 136. **Figure 128**
 137. **Figure 129**
 138. **Figure 130**
 139. **Figure 131**
 140. **Figure 132**
 141. **Figure 133**
 142. **Figure 134**
 143. **Figure 135**
 144. **Figure 136**
 145. **Figure 137**
 146. **Figure 138**
 147. **Figure 139**
 148. **Figure 140**
 149. **Figure 141**
 150. **Figure 142**
 151. **Figure 143**
 152. **Figure 144**
 153. **Figure 145**
 154. **Figure 146**
 155. **Figure 147**
 156. **Figure 148**
 157. **Figure 149**
 158. **Figure 150**
 159. **Figure 151**
 160. **Figure 152**
 161. **Figure 153**
 162. **Figure 154**
 163. **Figure 155**
 164. **Figure 156**
 165. **Figure 157**
 166. **Figure 158**
 167. **Figure 159**
 168. **Figure 160**
 169. **Figure 161**
 170. **Figure 162**
 171. **Figure 163**
 172. **Figure 164**
 173. **Figure 165**
 174. **Figure 166**
 175. **Figure 167**
 176. **Figure 168**
 177. **Figure 169**
 178. **Figure 170**
 179. **Figure 171**
 180. **Figure 172**
 181. **Figure 173**
 182. **Figure 174**
 183. **Figure 175**
 184. **Figure 176**
 185. **Figure 177**
 186. **Figure 178**
 187. **Figure 179**
 188. **Figure 180**
 189. **Figure 181**
 190. **Figure 182**
 191. **Figure 183**
 192. **Figure 184**
 193. **Figure 185**
 194. **Figure 186**
 195. **Figure 187**
 196. **Figure 188**
 197. **Figure 189**
 198. **Figure 190**
 199. **Figure 191**
 200. **Figure 192**
 201. **Figure 193**
 202. **Figure 194**
 203. **Figure 195**
 204. **Figure 196**
 205. **Figure 197**
 206. **Figure 198**
 207. **Figure 199**
 208. **Figure 200**
 209. **Figure 201**
 210. **Figure 202**
 211. **Figure 203**
 212. **Figure 204**
 213. **Figure 205**
 214. **Figure 206**
 215. **Figure 207**
 216. **Figure 208**
 217. **Figure 209**

